The University of Southern Mississippi
The Aquila Digital Community

Dissertations

Spring 5-2010

Synthesis, Characterization, and Deuterium Labeling of Polyamides Studied by Nuclear Magnetic Resonance Spectroscopy

Christopher Allen Lange
University of Southern Mississippi

Follow this and additional works at: https://aquila.usm.edu/dissertations

 Part of the Materials Chemistry Commons, and the Polymer Chemistry Commons

Recommended Citation

Lange, Christopher Allen, "Synthesis, Characterization, and Deuterium Labeling of Polyamides Studied by Nuclear Magnetic Resonance Spectroscopy" (2010). *Dissertations*. 933.
https://aquila.usm.edu/dissertations/933

This Dissertation is brought to you for free and open access by The Aquila Digital Community. It has been accepted for inclusion in Dissertations by an authorized administrator of The Aquila Digital Community. For more information, please contact Joshua.Cromwell@usm.edu.

The University of Southern Mississippi

SYNTHESIS, CHARACTERIZATION, AND DEUTERIUM LABELING OF POLYAMIDES STUDIED BY NUCLEAR MAGNETIC RESONANCE SPECTROSCOPY

by

Christopher Allen Lange

Abstract of a Dissertation
Submitted to the Graduate School
of The University of Southern Mississippi
in Partial Fulfillment of the Requirements
for the Degree of Doctor of Philosophy

May 2010

ABSTRACT

SYNTHESIS, CHARACTERIZATION, AND DEUTERIUM LABELING OF POLYAMIDES STUDIED BY NUCLEAR MAGNETIC RESONANCE SPECTROSCOPY

by Christopher Allen Lange

May 2010

The synthesis, characterization, and deuterium labeling of polyamides of polyamides have been investigated. In Chapter II, selective deuterium labeling of various polyamides was demonstrated via a facile method which does not require organic solvent or catalyst. Quantitative solution-state NMR analysis showed deuterium incorporation at the carbon alpha to the carbonyl ranged from 20-75%. Incorporation in ε-caprolactam increased with repeated treatments. Isotopic shift effects for the deuterated materials were additive for all sites within experimental error.

In Chapter III, the effect of stoichiometric imbalances on the polymerization of poly(dodecamethylene terephthalamide)was investigated. Molecular weight was varied by polymerizing the monomer salt with excess diaminododecane, terephthalic acid, or benzoic acid. End groups were identified and number average molecular weights were calculated by NMR analysis. Intrinsic viscosity measurements correlated well with NMR measurements and were used to calculate the Mark-Houwink constants of $K=55.8*10^{-5}$ dL/g and $\alpha = 0.81$.

Eutectic melting behavior of PA-10,T-6,T and PA-12,T-6,T copolymers are described in Chapter IV. Nuclear magnetic resonance spectra showed that comonomer sequences were distributed statistically to give random copolymers. Melt pressed film behavior, NMR, DSC, and WAXD analysis agree that PA-6,T monomer units do not co-crystallize with PA-10,T or PA-12,T monomer units, and do not form isomorphic structures in the copolymers studied. Instead, a eutectic melting point at 30 wt-% PA-6,T is observed for both copolymers. Compared to PA-10,T comonomer, PA-12,T comonomer has a greater effect on disrupting the crystallization of PA-6,T homo-segments above the eutectic point.

Chapter V describes the synthesis of a new family of compounds which form hydrogen-bonded supramolecular assemblies. As-synthesized materials did not assemble into supramolecular polymers until after they had been melted and cooled. Thermal treatment and solvent precipitation produced differently organized structures and extents of crystallinity. Crystallization diminished polymer-like behavior. Chiral centers played an important role in ordered domain behavior. Compounds containing urea linkages, or copolymers of compounds containing amide linkages formed glassy materials. Macroscopic assembly was demonstrated by fiber formation.

COPYRIGHT BY

CHRISTOPHER ALLEN LANGE

2010

I dedicate this work to my family.

ACKNOWLEDGEMENTS

I gratefully acknowledge Dr. Lon Mathias for encouraging me to earn my degree and teaching me how to learn, Dr. William Jarrett for providing expertise in NMR spectroscopy and keeping us safe, Ted Novitsky and Eylem Tarkin-Tas for significant contributions to my research and understanding, Huseyin Tas and Ethem Kaya for great friendship in the laboratory and abroad, and the rest of the department for making the experience enjoyable.

TABLE OF CONTENTS

LIST OF ILLUSTRATIONS

Figure

LIST OF TABLES

Table

LIST OF EQUATIONS

Equation

CHAPTER I

INTRODUCTION

Carbon-13 nuclear magnetic resonance (NMR) spectroscopy is a powerful tool for investigating a material's structure and organization at the molecular level. In Chapter II, quantitative solution-state NMR analysis was used to examine a novel method for deuterium labeling polyamides and ε-caprolactam. Routine solution-state NMR spectroscopy was used in Chapter III to probe the effect of stoichiometric imbalances on the molecular weight of semi-aromatic polyamides with potential commercial significance. In Chapter IV, monomer sequence distribution and eutectic melting behavior of semi-aromatic copolymers were investigated by solution-state NMR analysis. The effect of structure, stereo configuration, and thermal history on the behavior of hydrogen-bonded supramolecular polymers was explored using variable temperature solid-state NMR spectroscopy in Chapter V.

The resonant frequency (chemical shift) of carbon nuclei depend on the local chemical and electro-magnetic environment. NMR spectra exhibit peaks for each unique environment that is observed. From a characterization standpoint, experimental conditions determine, to a large extent, the degree of sensitivity at which different carbon nuclei can be distinguished. Furthermore, the magnitude of each peak is sensitive to experimental conditions and is not necessarily representative of the actual abundance in the sample.

Transfer of polarization from one nucleus to another is known as the Nuclear Overhauser Effect (NOE).[1,2] This is a through space effect in that

transfer will occur for proximal nuclei in three dimensional space regardless of bond connectivity. Routine acquisitions in solution-state ^{13}C NMR spectroscopy rely on continuous transfer of proton polarization to carbon nuclei in order to enhance the signal to noise ratio. Thus, carbon nuclei near an abundant source of protons will have artificially high signal strength relative to carbon nuclei with no nearby protons. The magnitude of each peak would not necessarily correspond to its abundance in the sample.

Peak shapes and intensities can also be distorted by differences in relaxation times. Data acquisition requires magnetization to be flipped transverse to the applied field. Signal strength is maximized when the magnetization resides exactly in the plane of the detector. This can be achieved by applying a calibrated radio frequency pulse to a fully equilibrated magnetization vector. The spin-lattice relaxation time (T_1) is related to the rate at which the perturbed magnetization vector realigns with the applied field. The amount of time allotted for this process to occur is specified in the pulse sequence as “recycle delay”. Each carbon atom in a sample may have a different T_1 time, but each carbon atom is only given the length of the recycle delay to reorient its magnetization. Magnetization vectors for carbons with T_1 times sufficiently short relative to the recycle delay will be precisely aligned every scan. However, the alignments of magnetization vectors for carbons with T_1 times longer than the recycle delay are less certain. Consequently, the magnitudes of corresponding peaks may not accurately represent their abundance in the sample.

Quantitative NMR experiments are designed to minimize inaccuracies caused by T_1 and NOE. Spin lattice relaxation times for each unique carbon are measured in a preliminary experiment. Then, a recycle delay appropriate for quantitative analysis is selected. A recycle delay five times longer than the maximum T_1 value yields data with up to 99% accuracy. Problems associated with NOE are minimized by gating the proton decoupler on only during the acquisition phase of the pulse sequence. This is known as gated decoupling. Both gated decoupling and long recycle delays will lengthen the time required to obtain spectra with sufficient signal to noise ratio for analysis.

Knowledge of polyamide end group functionality and concentrations is useful for understanding their polymerization process and properties. There are several challenges associated with NMR analysis of polyamide end groups. In traditional solvents such as *m*-cresol, formic acid, LiCl, and CH_3OH, analysis is difficult because the high solution viscosities result in broad peak widths and long T_1 times. Large peak widths can prevent unique resonances for end groups from becoming visible. Even in a good solvent, for high molecular weight polyamides, the preliminary analysis time required to measure the T_1s of end group carbons can take on the order of weeks due to their low concentration. Furthermore, end group chemical shifts are sensitive to pH and the concentration of acid and amine end groups themselves.[3]

However, developments by Mathias and others have overcome many of these problems. NMR analysis of polyamides in a mixed solvent system such as trifluoroethanol and $CDCl_3$ has allowed the observation of previously

undiscovered peaks due reduced viscosity and peak width.[4] The response of polyamide end group chemical shifts to changes in pH has been well documented.[3] End group quantitation is possible within a reasonable timeframe using the following assumption: an end group carbon atom has approximately the same NOE and T_1 as a similar main chain carbon atom. This was used to quantitate *cis* amide conformers, acid and amine end groups, cyclic unimers, and number average molecular weight of nylon 6,6.[3,5] The assumption was verified by comparing these data with results obtained by other characterization methods.

Solid-state NMR is used to analyze bulk materials without solvent. It is useful for studying the hydrogen bonding networks in supramolecular polymers and other ordered phenomena that are disrupted by the presence of solvent. Peak widths are typically greater in solid-state NMR spectra because solid matter is more constrained and motional averaging does not normally occur on the NMR timescale. Peak shapes can also reflect influences due to dipolar coupling, chemical shift anisotropy, irregular sample geometry, and voids. Magic angle spinning is a technique that involves fast rotation of samples about an axis oriented 54.74° to the applied field.[6] This is mainly used to minimize or remove chemical shift anisotropy. It may also cause artifacts known as spinning side bands. Quantitative data can be obtained on solid-state spectrometers using a Bloch decay or DEPTH pulse sequence.[7] Gated decoupling and long recycle delays are employed for reasons previously described. These techniques are employed throughout this dissertation to investigate polymer systems.

References

[1] Overhauser, A. W. *Physical Review* **1953**, 92, 411.

[2] Slichter, C. P. *Principles of Magnetic Resonance*. Springer. Berlin and New York, Third Editoin 651.

[3] Davis, R.D.; Steadman, S.J.; Jarrett, W.L.; Mathias, L.J. *Macromolecules* **2000**, 33, 7088.

[4] Steadman, S. J.; Mathias, L. J. *Polymer* **1997**, 38, 5297.

[5] Davis, R.D.; Jarrett, W.L.; Mathias, L.J. *Polymer* **2001**, 42, 2621.

[6] Schaefer, J.; Stejskal, E. O.; Buchdahl, R. *Macromolecules* **1977**, 10, 384.

[7] Cory, D. G.; Ritchey, W. M. *J. Magn. Reson.*, **1988**, 80, 128.

CHAPTER II

ENVIRONMENTALLY FRIENDLY ONE-POT SYNTHESIS AND ^{13}C NMR CHARACTERIZATION OF DEUTERIUM LABELED POLYAMIDES AND ε-CAPROLACTAM

Abstract

Polyamides were prepared with deuterium (20-50% incorporation) alpha to the carbonyl by dissolving monomers in deuterium oxide prior to polymerization. ε-Caprolactam was exchanged with deuterium (78% incorporation) at the same position without inducing polymerization. This is the first reported modification of such materials that does not require catalyst or organic solvent. High resolution quantitative NMR was used to examine deuterium induced effects on ^{13}C chemical shifts. Isotopic shifts were additive for both long range and compound interactions.

Introduction

Deuterium labeling has been utilized in a wide range of macromolecular investigations involving reaction mechanisms[1,2], hydrogen bonding[3,4], blend miscibility[5], thermal transitions[6], degredation[7], chain dynamics[8,6], and structural elucidation.[9-12] Analytical techniques that use deuterium's unique properties include neutron scattering[13,14], forward recoil spectrometry[15], Raman[16], infrared[17], mass spectroscopy[7,18,19], and nuclear magnetic resonance (NMR) spectroscopy.[6,20-28]

Despite the wealth of information obtained from deuterium labeled polymers, their use is deterred by high costs and limited commercial availability.

In addition, the synthesis of such materials is burdened by a combination of complex synthetic strategies, catalytic contaminants, multiple purification steps, and extensive use of volatile organic solvents and strong acids or bases.[29-35] A recent publication concerning nylon-6 characterization stated: "[Obtaining] information about molecular dynamics usually employs the line-shape analysis of deuterium NMR spectra. The requirement of labeled materials, however, renders application of this technique impractical… where synthetic effort necessary to selectively label the molecules can be nearly daunting."[36]

Thus, there is a need for generic deuterium labeling pathways that circumvent these shortcomings. Reported herein is a surprisingly facile, one-step method for preparing polyamides deuterated alpha to the carbonyl using only heavy water and their respective monomers. To the best of our knowledge, this is the first reported preparation of carbon-deuterium (C-D) labeled polyamides not requiring catalyst or organic solvent.

The feasibility of this method for labeling lactam monomers such as ε-caprolactam and lauryl lactam was also investigated. Currently, the simplest published procedure for preparing selectively deuterated caprolactam requires deuterium oxide (D_2O), potassium carbonate, and ethyl ether.[7] Here, similar products are generated in the absence of the later two chemicals, but at the expense of increased time.

The NMR chemical shift of a carbon atom changes when a proton is substituted by a deuterium. The difference in chemical shift is referred to as isotopic shift. Isotopic shift effects across a single bond are well understood.

However, no theories are available that accurately describe or predict isotopic shifts over multiple bonds.[37,38] Therefore, as part of this study raw data for multiple bond isotopic shifts and compound isotopic shifts (more than one deuterium exchangeable site) are presented and correlated.

Experimental

Materials

ε-Caprolactam, 6-aminocaproic acid, D_2O (99 atom % D), chloroform-d, 2,2,2-trifluoroethanol (TFE) and 1,1,1,3,3,3-hexafluoroisopropanol (HFIP) were purchased from Aldrich. Nylon 6,6 salt was donated by Solutia Inc. Nylon 6,9 salt and 11-aminoundecanoic acid were obtained from commercial sources. Lauryl lactam was donated by Evonik Degussa Corporation. All materials were used without purification.

Deuterated Polymer Synthesis

The generic procedure used for the preparation of deuterated polyamides is given below; specific information of each polymer is listed in Table 2.1. Deuterium oxide and monomer (lactam, amino acid, or salt) were added to a test tube and gently shaken for 15 minutes under dry nitrogen purge. A hot air gun was used to fully dissolve materials. (The monomer for **PA11-d** was the only one that did not fully dissolve and instead formed a cloudy white mixture.) The test tube was inserted into a preheated sand bath and held under nitrogen purge for 5 hours. Products were transparent and viscous in the molten state. Upon cooling, products crystallized into mechanically tough white or pale yellow solids. NMR spectra confirmed polymer formation. Yields were 75-85% for all

polymerizations based on weight of reactants and raw products and were not corrected for loss of molecular water or deuterium incorporation.

Table 2.1 Reactant quantities, times, and temperatures for polymerization of deuterated polyamides.

Compound	Reactants	Reaction Time (hours)	Reaction Temp-erature (°C)
PA11-d	11-aminoundecanoic acid (3.00 g, $1.49*10^{-2}$ mol), D_2O (3.0 mL, $1.5*10^{-1}$ mol)	5	230
PA6,9-d	salt of hexamethylene diamine and azelaic acid (5.02 g, $1.65*10^{-2}$ mol), D_2O (5.0 mL, $2.5*10^{-1}$ mol)	5	250
PA6,6-d	salt of hexamethylene diamine and adipic acid (2.01 g, $7.65*10^{-3}$ mol), D_2O (2.0 mL, $1.0*10^{-1}$ mol)	5	280
PA6*-d	**Cap-4-d** (0.90 g, $7.85*10^{-3}$ mol), 6-aminocaproic acid (0.08 g, $6.10*10^{-4}$ mol), D_2O (1.0 mL, $5.0*10^{-2}$ mol)	5	250
PA6-d	ε-caprolactam (1.82 g, $1.6*10^{-2}$ mol), 6-aminocaproic acid (0.17 g, $1.32*10^{-3}$ mol), D_2O (2.0 mL, $1.0*10^{-1}$ mol)	5	250

*ε-Caprolactam Modification **(Cap-d-[0-4])***

ε-Caprolactam (12.06 g, $1.07*10^{-1}$ mol), and D_2O (12.0 mL, $5.99*10^{-1}$mol) were added to a test tube and gently shaken for 15 minutes while purging with dry nitrogen through a rubber septum. After dissolution, the test tube was attached to a distillation unit and inserted into a sand bath preheated to 250 °C. Partial vacuum was applied for 30 minutes to remove water and prevent polymerization. After removing vacuum, the test tube was purged with dry nitrogen for 4.5 hours. ε-Caprolactam sublimed onto test tube walls and was periodically pushed down into the molten material with a spatula. The product was transparent and non-viscous in the molten state, and crystallized into a white, brittle solid upon cooling. After grinding into a powder with mortar and

pestle, an aliquot sufficient for NMR analysis was removed. The remaining product was reinserted into the test tube and the aforementioned experimental procedure was repeated with fresh D_2O for a total of four iterations. Products are designated according to how many times they were modified by this procedure: **Cap-0** (unreacted caprolactam), **Cap-1-d**, **Cap-2-d**, **Cap-3-d**, and **Cap-4-d** (modified 1-4 times). Quantitative ^{13}C NMR analysis confirmed deuterium incorporation and that conversion to polymer was limited to 2 mol-%. Yield for **Cap-4-d** was 70% based on weight of starting material and raw product and was not corrected for deuterium incorporation.

Lauryl Lactam Attempted Deuterium Modification

Lauryl lactam (2.0012 g, $1.0142*10^{-2}$ mol) and D_2O (2.0 mL, $1.0*10^{-1}$ mol) were added to a test tube and gently shaken for 1 hour while heated with hot air. Materials were observed to be immiscible up to 100 ℃ and remained phase separated when the test tube was inserted into a 250 ℃ sand bath. Deuterium oxide had boiled out of the test tube after approximately 15 minutes. The test tube remained in the sand bath for 5 hours while purging with dry nitrogen gas. Product was transparent and non-viscous in the molten state and crystallized into a white solid upon cooling. Quantitative ^{13}C NMR analysis showed no evidence of deuterium incorporation or conversion to polymer.

NMR Characterization

Polymer samples were ground into pellets and dissolved at 11 wt-% in a mixed solvent system of 30 wt-% chloroform-*d* and 70 wt-% TFE (**PA6-d**, **PA6*-d**, **PA6,6-d**) or HFIP (**PA11-d PA6,9-d**). Chloroform-*d* was used as a deuterium

lock and reference peak (77.23 ppm). ε-Caprolactam samples were ground into a powder and dissolved at 20 wt-% into DMSO-d_6 which also served as a reference peak (39.51 ppm). Lauryl lactam samples were ground into a powder and dissolved at 20 wt-% into a mixed solvent system consisting of 30 wt-% chloroform-d and 70 wt-% hexafluoroisopropanol.

Quantitative solution ^{13}C spectra were collected on a Varian ^{UNITY}INOVA NMR spectrometer operating at a frequency of 125.7 MHz. Recycle delays were ~5 times greater than the longest T_1 time of the slowest relaxing peak. All spectra were recorded at 25 ℃ with gated decoupling. Data were zero filled up to 512k points prior to application of Fourier transformation. No line broadening was applied to the FID (unfiltered line shapes are presented) to ensure ample resolution. Baselines were corrected by fitting to a 10^{th} order polynomial.

Results and Discussion

Deuterium Exchange

The NMR spectra in Figure 2.1 clearly shows ε-caprolactam was selectively deuterated alpha to the carbonyl using the mild, inexpensive procedure described here, with peak assignments based on previous work by Borgen.[39] **Cap-0** shows a typical spectrum of unmodified ε-caprolactam with six singlet peaks at 23.03 ($\mathbf{3}_{\alpha 0}$), 29.85 ($\mathbf{5}_{H}$), 30.04 ($4_{\alpha 0}$), 36.43 ($\mathbf{2}_{\alpha 0}$), 41.49 ($\mathbf{6}_{\alpha 0H}$), and 177.05 ($\mathbf{1}_{\alpha 0H}$) ppm. **Cap-1-d** is ε-caprolactam that has gone through one cycle of the deuterium modification procedure. The NMR spectrum of **Cap-1-d** shows additional peaks including a triplet ($\mathbf{2}_{\alpha 1}$) centered at 36.08 ppm representing ε-caprolactam molecules with a single deuterium atom at carbon **2**.

Cap-2-d (ε-caprolactam that has been modified twice) shows a quintet ($\mathbf{2}_{\alpha 2}$) centered at 35.73 ppm, indicating two deuterium atoms at carbon **2**. After three and four modifications (**Cap-3-d** and **Cap-4-d**), the intensity of $\mathbf{2}_{\alpha 1}$ and $\mathbf{2}_{\alpha 2}$ increase, while the intensity of $\mathbf{2}_{\alpha 0}$ diminishes. Thus, from the NMR data it is evident that total deuterium incorporation increases with repeated treatments. Although the abundance of $\mathbf{2}_{\alpha 0}$, $\mathbf{2}_{\alpha 1}$, and $\mathbf{2}_{\alpha 2}$ are a direct measure of deuterium incorporation, they are not the best peaks for quantitative calculations. Instead, carbon **3** peaks were used due to the base-line resolution of substituted and un-substituted peaks. Deuterium incorporations based on integrated areas of carbon **3** peaks are listed in Table 2.2.

The NMR spectra of lauryl lactam were identical before and after the attempted deuterium exchange procedure. Unlike ε-caprolactam, lauryl lactam did not dissolve in D_2O, preventing deuterium exchange at any position.

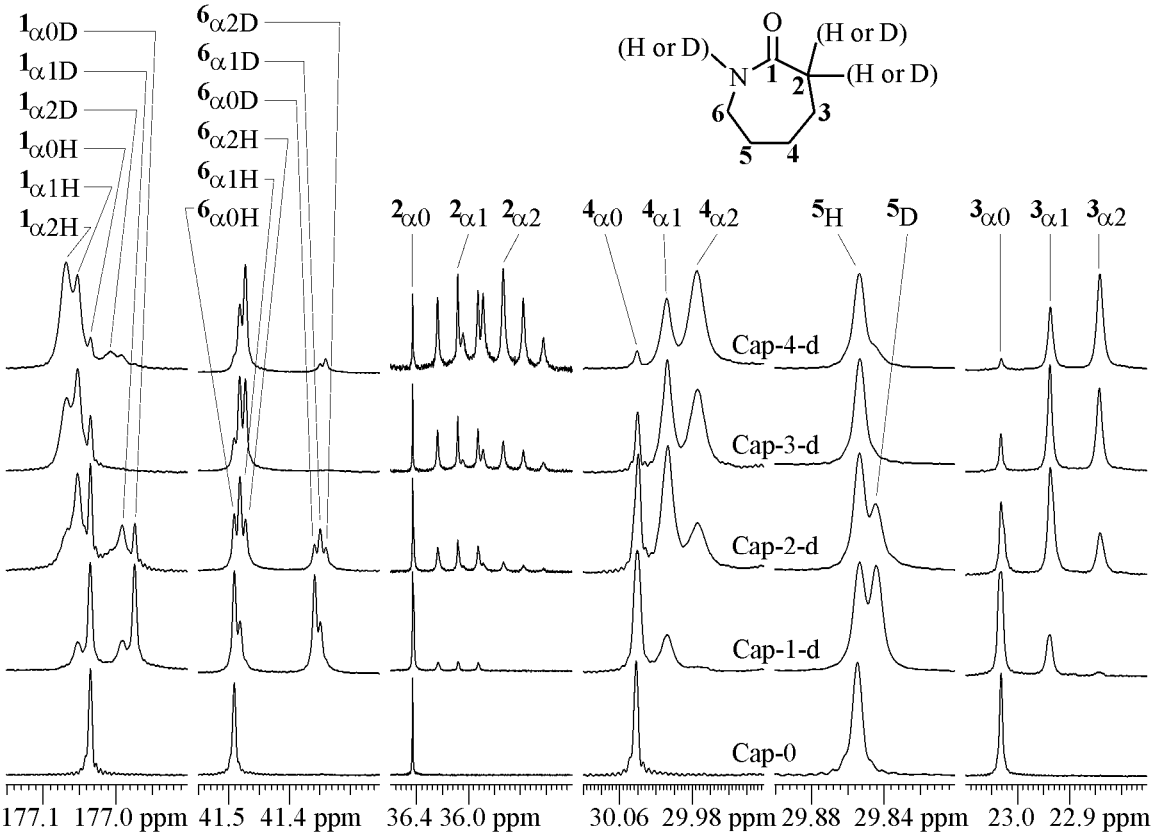

Figure 2.1 Quantitative ^{13}C NMR spectra of ε-caprolactam after 0, 1, 2, 3, and 4 (from bottom to top) deuterium exchange reactions. Horizontal scale has been broken and expanded for each region to enhance detail. Vertical scales have been maximized for each region of each spectrum and are not necessarily consistent. Subscripts on peak assignments denote the number of deuterium atoms at the alpha position **2** and/or whether the nitrogen is bonded to hydrogen (H) or deuterium (D).

Table 2.2 Incorporation of deuterium alpha to the carbonyl in ε-caprolactam and polyamides calculated by integrated areas of carbon **3** unless otherwise noted. Values are reported in mol-%.

Product	CD_0	CD_1	CD_2	Total
PA11-d	65	30	4	20
PA6,9-d	47	40	13	33
PA6,6-d	25[a]	44[a]	31[a]	53[a]
PA6*-d	14	23	63	75
PA6-d	43	41	17	37
Cap-4-d	6	33	61	78
Cap-3-d	12	43	45	66
Cap-2-d	28	47	25	48
Cap-1-d	64	31	6	21
Cap-0	100	0	0	0
Lauryl Lactam	100	0	0	0

[a]Calculation based on peak **1**.

All polymers synthesized in this study were selectively deuterated alpha to the carbonyl, as confirmed by NMR analysis (Figure 2.2). Although broader peak widths are observed in the polymer spectra, the behavior of carbons **2** and **3** is nearly identical to that of ε-caprolactam-*d* described above. Deuterium incorporation for the polymers was calculated based on integrated areas of carbon **3** peaks (Table 2.2) except for **PA6,6-d**; here, the number of bonds between exchangeable sites is shorter in **PA6,6-d** than for other polymers in this study. Consequently, additional interactions are detected at carbon **3**, requiring the quantitation of deuterium incorporation be measured using carbon **1**.

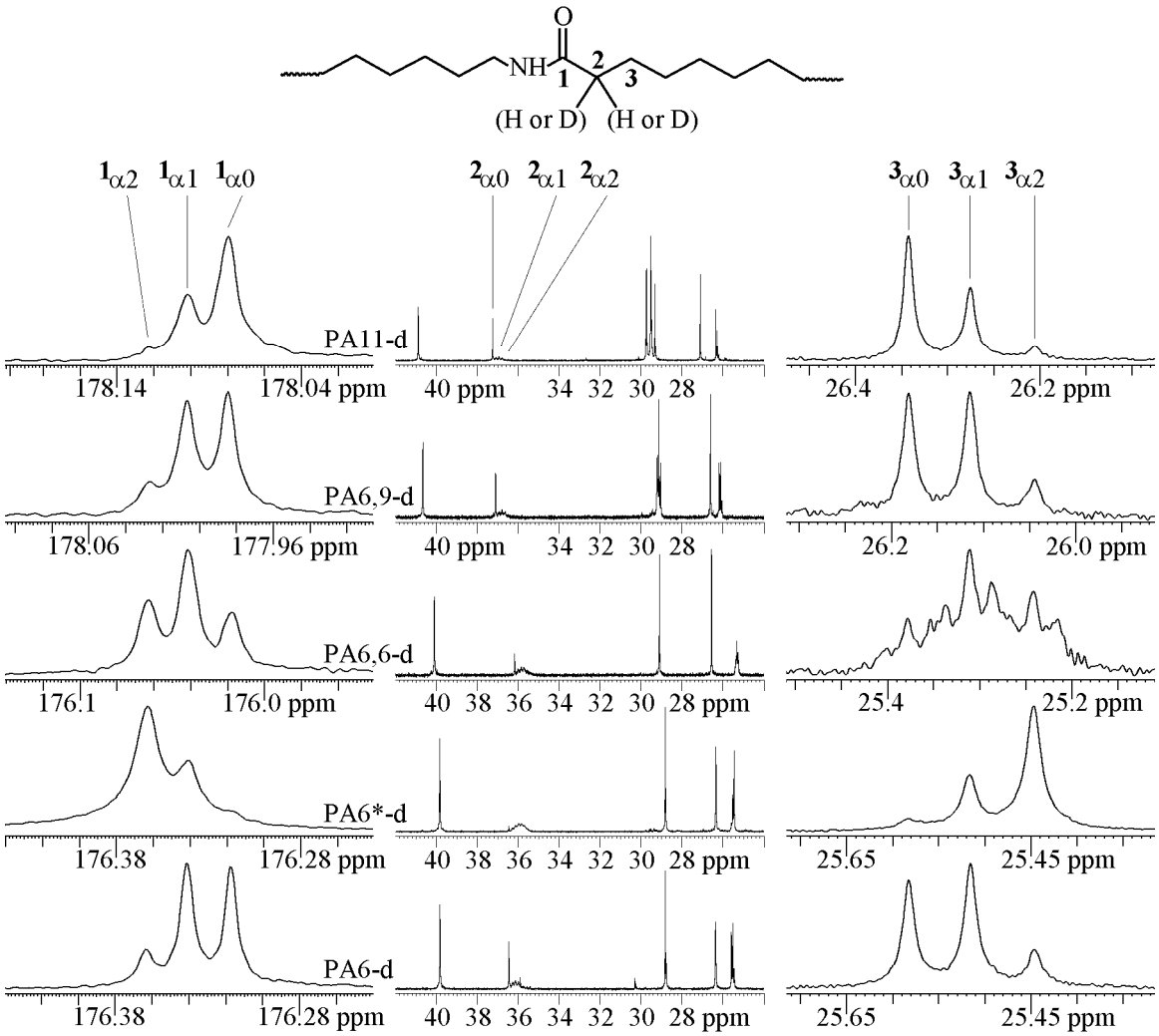

Figure 2.2 From bottom to top: Quantitative ^{13}C solution NMR spectra of products **PA6-d**, **PA6*-d**, **PA6,6-d**, **PA6,9-d**, and **PA11-d**. Horizontal scales are centered on carbon **1** in left spectra, fixed at the aliphatic region in middle spectra, and centered on carbon **3** in right spectra. Vertical scales have been maximized for each region of each spectrum and are not necessarily consistent.

Levels of incorporation of deuterium alpha to the carbonyl ranged from 20-75% (Table 2.2). For **PA11-d**, 11-aminoundecanoic acid did not fully dissolve in D_2O prior to polymerization, thus causing the polymer to have the lowest deuterium incorporation. In contrast, **PA6*-d** had the highest deuterium

incorporation because the water-soluble monomer (**Cap-4-d**) was exchanged with deuterium four times prior to polymerization.

Interestingly, a similar method reported in 1965 assumed that the deuterium located at the nitrogen position in ε-caprolactam would not further react during polymerization.[40] Anomalous peaks in the infrared spectrum of the resulting polymer were attributed to differences in fine crystalline structure between N-D nylon 6 and N-H nylon 6. However, based on the new spectroscopic evidence given here, an alternative conclusion is proposed: the previously described polymer was partially deuterated at the carbon alpha to the carbonyl rather than just at the nitrogen, which caused the observed spectral differences.

Additional experiments were conducted to gain insight into the practicality of this deuterium exchange method. Using methods similar to those described in the experimental section, ε-caprolactam was refluxed in D_2O for 6 hours and then heated to 250 °C for 1 hour with no deuterium exchange alpha to the carbonyl occurring. Hence, for successful exchange to occur in ε-caprolactam, high temperatures and long reaction times (5 hours) must be used in combination. However, this is not true for the polymers. These were prepared using the method described in the experimental section, except the reaction time was limited to 1 hour. The resulting polymers were deuterated alpha to the carbonyl, perhaps due to a catalyzing effect of primary amines and carboxylic acids present in the monomers.

English and coworkers reported problematic “scrambling” of deuterated nylon 6,6 during melt equilibration.[41] Approximately one third of the deuterium atoms located alpha to the carbonyl transferred to the nitrogen position within 15 minutes at 300 °C. This was attributed to a keto-enol tautomeric exchange reaction, consistent with the deuterium incorporation process described here, which almost certainly occurs via a similar mechanism.

NMR Analysis of Isotopic Shifts

Isotopic shifts for ε-caprolactam are tabulated in Table 2.3 and presented visually in Figure 2.1. The chemical shift of carbon **5** is sensitive to substitution of the nitrogen site. Chemical shifts for carbons **1**, **2**, **3**, **4**, and **6** depend upon the number of deuterium atoms at carbon **2**. Chemical shifts for carbons **1** and **6** are also sensitive to N-D effects. Therefore, the isotopic shifts of carbons **1** and **6** are compound in that they are sensitive to deuterium exchange at two different sites. Isotopic shifts for carbons **1** and **6** induced by N-D effects alone are in agreement with values previously reported by Dintzner.[42]

For ε-caprolactam, there is no apparent correlation between degree of incorporation (0-49% deuterium) at the nitrogen atom and the number of treatments. In this case, uncontrolled absorption of atmospheric moisture during sample isolation and preparation for NMR analysis is responsible.

Isotopic shifts for polymers are tabulated in Table 2.3 and presented visually in Figure 2.2. Compound effects are observed but not fully resolved for carbon **3** in **PA6,6-d**. The isotopic shifts observed in this study were additive for all sites within experimental error.

Table 2.3 Deuterium Isotope Shifts (ppb) and *J* Coupling Constants (Hz) for ε-caprolactam and polyamides deuterated alpha to the carbonyl and/or at the nitrogen position (-upfield, +downfield). The number preceding delta refers to the number of bonds between deuterium and carbon. The first bold number designates the carbon for which an isotopic shift is reported. In parentheses, the site of deuteration and the number of deuterium atoms at that site are specified. Reported values are differences in chemical shift for deuterated versus undeuterated samples.

Designation	ε-Caprolactam	Nylon 6	Nylon 6,6	Nylon 6,9	Nylon 11
$^{1}\Delta$C**2**(C**2**D$_1$)	-347.5	-321.7	-311.2	-309.3	-310.2
$^{1}\Delta$C**2**(C**2**D$_2$)	-698.8	-626.2	A	A	A
$^{2}\Delta$C**1**(C**2**D$_1$)	19.0	22.0	21.0	20.0	21.0
$^{2}\Delta$C**1**(C**2**D$_2$)	38.0	44.5	43.0	41.0	43.0
$^{2}\Delta$C**3**(C**2**D$_1$)	-94.5	-66.8	B	-66.8	-66.8
$^{2}\Delta$C**3**(C**2**D$_2$)	-189.9	-134.6	B	-132.7	-135.5
$^{3}\Delta$C**4**(C**2**D$_1$)	-33.4	-25.8	A	B	B
$^{3}\Delta$C**4**(C**2**D$_2$)	-66.8	-51.6	A	B	B
$^{4}\Delta$C**6**(C**2**D$_1$)	-9.5	B	B	B	B
$^{4}\Delta$C**6**(C**2**D$_2$)	-19.1	B	B	B	B
$^{2}\Delta$C**1**(ND)	-61.0				
$^{2}\Delta$C**6**(ND)	-131.7				
$^{3}\Delta$C**2**(ND)	-8.6				
$^{3}\Delta$C**5**(ND)	-8.6				
$^{2}\Delta^{2}\Delta$C**1**(ND,C**2**D$_1$)	-43.0				
$^{2}\Delta^{2}\Delta$C**1**(ND,C**2**D$_2$)	-28.0				
$^{2}\Delta^{4}\Delta$C**6**(ND,C**2**D$_1$)	-142.2				
$^{2}\Delta^{4}\Delta$C**6**(ND,C**2**D$_2$)	-151.8				
J_{CD}	19.6	18.3	17.5	18.3	18.6

A) Measurement unobtainable due to noise.
B) Measurement unobtainable due to resolution.

Conclusions

Various polyamides and ε-caprolactam were deuterated alpha to the carbonyl by a method that is facile and does not require organic solvent or catalyst. For polymers, incorporations (20-75% deuterium) depend on monomer solubility in D_2O. Deuterium incorporation in ε-caprolactam increased with

repeated treatments. Isotopic shifts observed by high resolution quantitative ^{13}C NMR spectroscopy appear to be additive for all instances.

Acknowledgements

Thanks to Evonik Degussa Corporation for supplying materials, and Solutia Inc. for supplying materials and funding this research.

References

[1] D'Ulivo, A.; Mester, Z.; Sturgeon, R. E. *Spectrochimica Acta Part B* **2005**, 60, 423.

[2] Bauer, R.; Thomke, K. *J. Molecular Catalysis* **1993**, 79, 311.

[3] Liu, A.; Wang, J.; Lu, Z.; Yao, L.; Li, Y.; Yan, H. *ChemBioChem* **2008**, 9, 2860.

[4] Sosnicki, J. G.; Langaard, M.; Hansen, P. E. *J. Org. Chem* **2007**, 72, 4108.

[5] Galvin, M. E.; Heffner, S.; Winey, K. I. *Macromolecules* **1994**, 27, 3520.

[6] Hirschinger, J.; Miura, H.; Gardner, K. H.; English, A. D. *Macromolecules* **1990**, 23, 2153.

[7] Mitera, J.; Kubelka, V. *Org. Mass Spectrom.* **1971**, 5, 651.

[8] Huijun, L. *Polymer, (Article in Press)* **2009**.

[9] O'Leary, D. J.; Allis, D. G.; Hudson, B. S.; James, S.; Morgera, K. B.; Baldwin, J. E. *J. Am. Chem. Soc.* **2008**, 130, 13659.

[10] Reed, D. R.; Kass, S. R. *J. Am. Soc. Mass Spectrom.* **2001**, 12, 1163.

[11] Le, H. C.; Hintermann, T.; Wessels, T.; Gan, Z.; Seebach, D.; Ernst, R. *Helvetica Chimica Acta* **2001**, 84, 208.

[12] Schaeffer, P.; Ocampo, R.; Callot, H.; Albrecht, P. *Geochimica et Cosmochimica Acta* **1994**, 58, 4247.

[13] Ruegg, M. L.; Newstein, M. C.; Balsara, N. P.; Reynolds, B. J.; *Macromolecules* **2004**, 37, 1960.

[14] Reichart, G. C.; Register, R. A.; Graessley, W. W.; Krishnamoorti, R.; Lohse, D. J. *Macromolecules* **1995**, 28, 8862.

[15] Composto, R. J.; Kramer, E. J. *Polymer* **1990**, 31, 2320.

[16] Jordan, T.; Spiro, T. G. *J. Raman Spectroscopy* **1995**, 26, 867.

[17] Gericke, A.; Moore, D. J.; Erukulla, R. K.; Bittman, R.; Mendelsohn, R. *J. Mol. Structure* **1996**, 379, 227.

[18] Souza, B. M.; Palma, M. S. *Biochimica et Biophysica Acta* **2008**, 1778, 2797.

[19] Man, P.; Montagner, C.; Vernier, G.; Dublet, B.; Chenal, A.; Forest, E.; Forge, V. *J. Mol. Biol.* **2007**, 368, 464.

[20] Callaghan, P. T.; Samulski, E. T. *Macromolecules* **2003**, 36, 724.

[21] O'Connor, R. D.; Blum, F. D.; Ginsburg, E.; Miller, R. D. *Macromolecules* **1998**, 31, 4852.

[22] Shi, J. F.; Inglefield, P. T.; Jones, A. A.; Meadows, M. D. *Macromolecules* **1996**, 29, 605.

[23] Pace, M. D.; Brown, I. M. *Macromolecules* **1994**, 27, 1879.

[24] Merritt, M. E.; Goetz, J. M.; Whitney, D.; Chang, C. P.; Heux, L.; Halary, J. L.; Schaefer, J. *Macromolecules* **1998**, 31, 1214.

[25] Abe, A.; Hiejima, T.; Takeda, T.; Nakafuka, C. *Polymer* **2003**, 44, 3117.

[26] Zeng, E.; Jacob, K. I.; Polk, M. B. *Polymer* **2002**, 43, 2169.

[27] Botev, M.; Neffati, R.; Rault, J. *Polymer* **1999**, 40, 5227.

[28] Garin, N.; Hirschinger, J.; Beaume, F.; Laupretre, F. *Polymer* **2000**, 41, 4281.

[29] Williams, J. C.; McDermott, A. E. *J. Phys. Chem. B* **1998**, 102, 6248.

[30] Nicholson, J. C.; Crist, B. *Macromolecules* **1989**, 22, 1704.

[31] Anastasiadis, A.; Separovic, F.; White, J. *Aust. J. Chem.* **2001**, 54, 747.

[32] Liang, M.; Blum, F. D. *Macromolecules* **1996**, 29, 7374.

[33] Erdogan, G.; Grotjahn, D. B. *J. Am. Chem. Soc.* **2009**, 131, 10354.

[34] Concellon, J. M.; Rodriguez-Solla, H.; Concellon, C. *Tetrahedron Lett.* **2004**, 45, 2129.

[35] Spletstoser, J. T.; White, J. M.; Georg, G. I. *Tetrahedron Lett.* **2004**, 45, 2787.

[36] Brus, J.; Urbanova, M.; Kelnar, I.; Kotek, J. *Macromolecules* **2006**, 39, 5400.

[37] Bolvig, S. Ph.D. Thesis. Deuterium Isotope Effects on 13C Chemical Shifts as a Tool to Determine Tautomerism and Structural Features in Intramolecular Hydrogen Bonded Systems. Roskilde University, Denmark, **1997**.

[38] Hansen, P. E.; Nicolaisen, F. M.; Schaumburg, K. *J. Am. Chem. Soc.* **1986**, 108, 625.

[39] Borgen, G.; Rise, F. *Magnetic Resonance in Chemistry* **1993**, 31, 51.

[40] Koshimo, A. *J. Appl. Polymer Sci.* **1965**, 9, 55.

[41] Angelo, R. J.; Miura, H.; Gardner, K. H.; Chase, D. B.; English, A. D. *Macromolecules* **1989**, 22, 117.

[42] Jarret, R. M.; Sin, N.; Dintzner, M. *Microchemical Journal* **1997**, 56, 19.

CHAPTER III

EFFECT OF STOICHIOMETRIC IMBALANCES ON THE MELT CONDENSATION POLYMERIZATION OF POLY(DODECAMETHYLENE TEREPHTHALAMIDE) STUDIED BY INTRINSIC VISCOSITY AND ^{13}C NMR SPECTROSCOPY

Abstract

Poly(dodecamethylene terephthalamide) (PA-12,T) was synthesized by melt condensation polymerization of 12,T salt with 0, 1, 3, 5, or 10 % molar excess of 1,12-diaminododecane (DA), terephthalic acid (TA), or benzoic acid (BA). Intrinsic viscosities (IV) (0.5 g/dL in 96% H_2SO_4 at 25 ℃) were measured to determine relative molecular weight differences. IV was highest for reactions containing 1 and 3 mol-% excess DA (1.36 and 1.31 dL/g, respectively), followed by the product of pure 1:1 salt (1.25 dL/g). For all concentrations of excess TA and BA, IV decreased progressively. Carbon-13 nuclear magnetic resonance (NMR) chemical shifts for DA, TA, and BA end groups were identified and their concentrations determined by comparison with the intensity of main chain polymer peaks. A log-log plot of IV versus number average molecular weight calculated from ^{13}C NMR data shows a linear trend with Mark-Houwink constants of $K=55.8*10^{-5}$ dL/g and $\alpha = 0.81$.

Introduction

Semi-aromatic polyterephthalamides (SAPT) are polymers formed from aliphatic diamines and terephthalic diacids. These materials possess thermal and mechanical properties superior to purely aliphatic polyamides while being

easier to process than wholly aromatic polyamides.[1] Symmetrical aromaticity in the SAPT backbone gives them higher melting and glass transition temperatures which are useful for automotive applications. For example, poly(hexamethylene terephtalamide) (PA-6T) has a melting temperature of 370 ℃ and a glass transition temperature of 125 ℃, as compared to 265 ℃ and 60 ℃ for PA-6,6 respectively. However, high melt viscosities and melting temperatures that approximate the degradation temperature make conventional melt processing of SAPT's difficult. Overcoming these obstacles has been the main focus of much patent literature.[2-13] Melting temperatures of SAPT's can be tuned by changing the chemical composition of monomers. For example, increasing the length of diamine from 6 to 12 carbons decreases the polymer melting temperature from ~375 ℃ to 295 ℃.

Controlling molecular weight during melt condensation polymerizations of SAPT's is crucial for obtaining desired mechanical properties and processability. For instance, materials below a critical molecular weight are brittle with poor mechanical properties. Increasing molecular weight above the critical value results in high melt viscosities that complicates processing. Control of molecular weight in this A-A B-B system is attained by adjusting the stoichiometry of reactants. Although perfect stoichiometric balance is theoretically most favorable for obtaining high molecular weight condensation polymers, there exists a practical discrepancy between relative concentrations of starting materials and finished products. Industrial practices and patents indicate that excess diamine[4] or terephthalic acid[6] need to be added to the diacid/diamine salt to generate

suitable products. This unbalanced stoichiometry achieves a product of desired molecular weight. Additionally, end capping is another technique used to limit the molecular weight during melt condensation polymerizations.[14] In SAPT literature, these are referred to as terminal blocking agents[9], viscosity stabilizers[2], and molecular weight stabilizers[6]. The most commonly used end capping agents for SAPT's are benzoic and acetic acid.

Adjusting stoichiometry is common practice in SAPT patent literature. Nevertheless, there remains a need to quantify these effects on molecular weight and end group functionality. Typically, single-point intrinsic viscosity (IV) measurements are used to determine relative molecular weight changes. However, since Mark-Houwink constants are not available for SAPT's, the impact of stoichiometric adjustments on the molecular weight of the products is unknown.

Our group has developed ^{13}C NMR spectroscopy as a tool for examining end groups as well as determining *cis* amide content and number average molecular weights of various aliphatic polyamides.[15,16] The present study uses ^{13}C NMR spectroscopy to determine end group concentrations and number average molecular weights of poly(dodecamethylene terephthalamide) (PA-12,T). Molecular weights were varied by adjusting the reaction stoichiometry of the melt condensation polymerization.

Experimental

Materials

Terephthalic acid, 1,12-diaminododecane, benzoic acid, hexafluoroisopropanol (HFIP), concentrated sulfuric acid (96%) and chloroform-*d* ($CDCl_{3)}$ were purchased from Aldrich Chemical Company. Benzoic acid and 1,12-diaminododecane were sublimed at 70 ℃ and dried at room temperature under vacuum before use. HFIP and $CDCl_3$ were dried with molecular sieves before use.

Synthesis

PA-12,T salt. Into a 2 L beaker, 1200 mL of deionized water, 40.1 grams (0.20 mol) of 1,12-diaminodecane, and 32.9 grams (0.198 mol) of terephthalic acid were added, and the slurry heated to a boil. Additional water was added and the mixture brought to boil to give a supersaturated clear salt solution (6.3 wt-%). The hot salt solution was then added to a 2 L beaker containing 800 mL of reagent alcohol and cooled to room temperature, followed by overnight cooling in a freezer at 0.5 ℃. The precipitate was filtered and washed with reagent alcohol, to give 68 g of the PA-12,T salt (95% yield). The product was recrystallized using a water/ethanol mixture and dried overnight at 80 ℃ under vacuum. The salt had a sharp melting point of 271.9 ℃ and an enthalpy of 428 J/g as observed by differential scanning calorimetry.

Melt condensation polymerization of polyamide (12,T). PA-12,T was synthesized using 0, 1, 3, 5, and 10 mol-% excess 1,12-diaminododecane (DA), terephthalic acid (TA), or benzoic acid (BA). The synthesis scheme of PA-12,T is

depicted in Figure 3.1. PA-12,T salt and excess reactant (DA, TA, or BA) were weighed and mixed with a mortar and pestle. The solid mixture was added to a test tube with approximately 50 wt-% water and mixed to create a slurry. Thirteen test tubes (with different stoichiometric imbalances) were loaded into a Parr reactor, which was then sealed and purged with nitrogen.

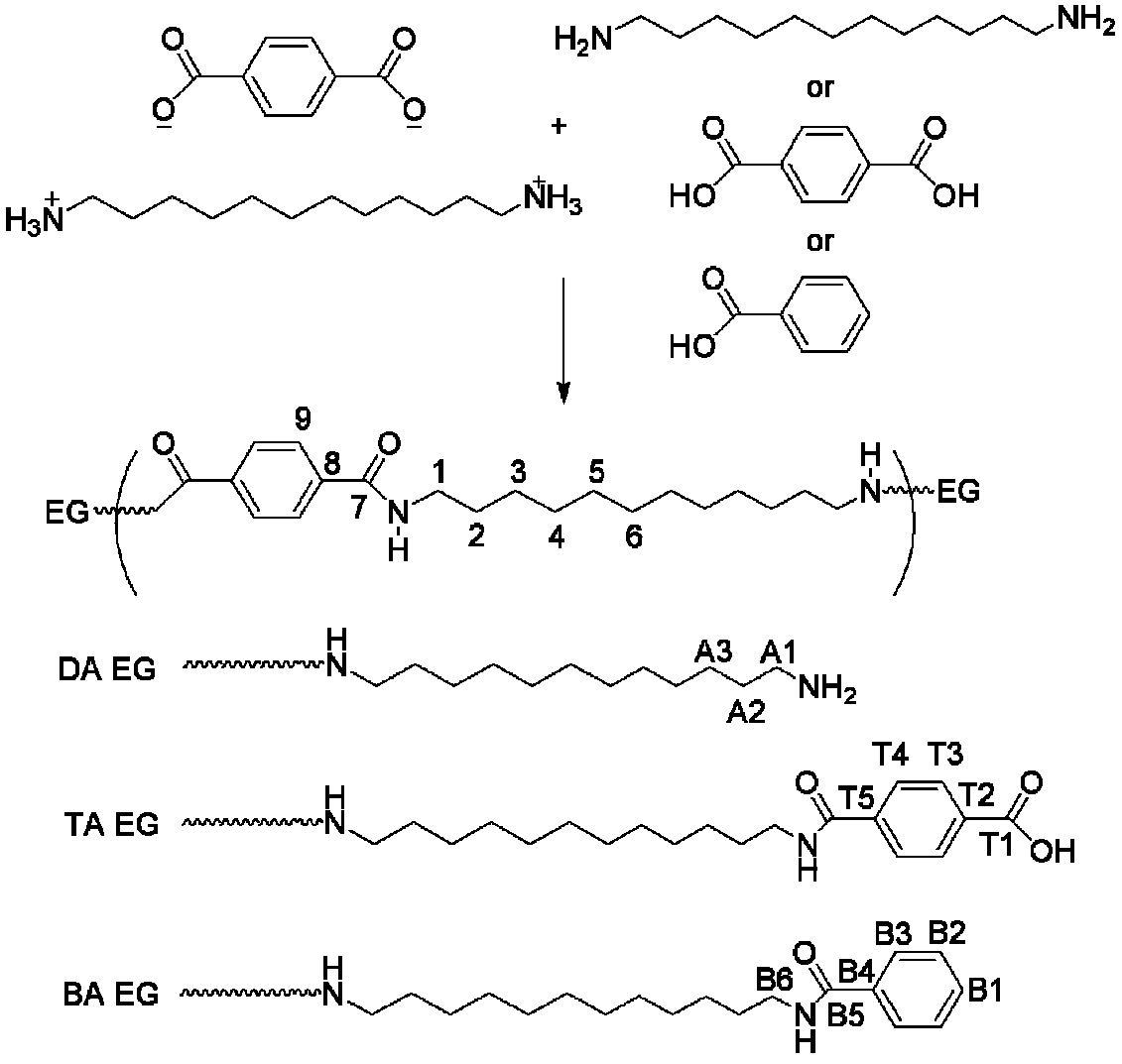

Figure 3.1. Synthesis of PA-12T with main chain and end group (EG) assignments for ^{13}C NMR spectra.

Temperature in the Parr reactor was monitored using a thermocouple located in one of the test tubes. Heater set points were programmed into the reactor controller. The reactor was surrounded by insulation to ensure precise heating control. Pressure was controlled manually with nitrogen and measured by a gauge on the reactor head. Temperature and pressure profiles of the melt condensation polymerization are plotted versus time in Figure 3.2. The reaction can be divided into three stages according to the pressure profile. In the first stage, pressure was maintained at 125 kPa with the heater set at 200 ℃. The temperature ramped up to a plateau at 126 ℃ as the water boiled. At approximately 110 minutes the temperature increased indicating that all the water had evaporated. In the second stage of the reaction, pressure was increased to 1724 kPa and the heater was set at 315 ℃. Here, the high pressure was used to minimize volatilization of monomer. After 145 minutes the temperature had reached 276 ℃, at which point the pressure valve was opened. At 180 minutes the reactor reached atmospheric pressure and 312 ℃. This marks the beginning of the reaction's third stage, with nitrogen gas purged through the reactor at zero gauge pressure and the heater turned off. Temperature decreased rapidly during the third stage. The DSC first heating of the resulting product showed a melting temperature of 295 ℃, confirming that the polymer was molten during polymerization.

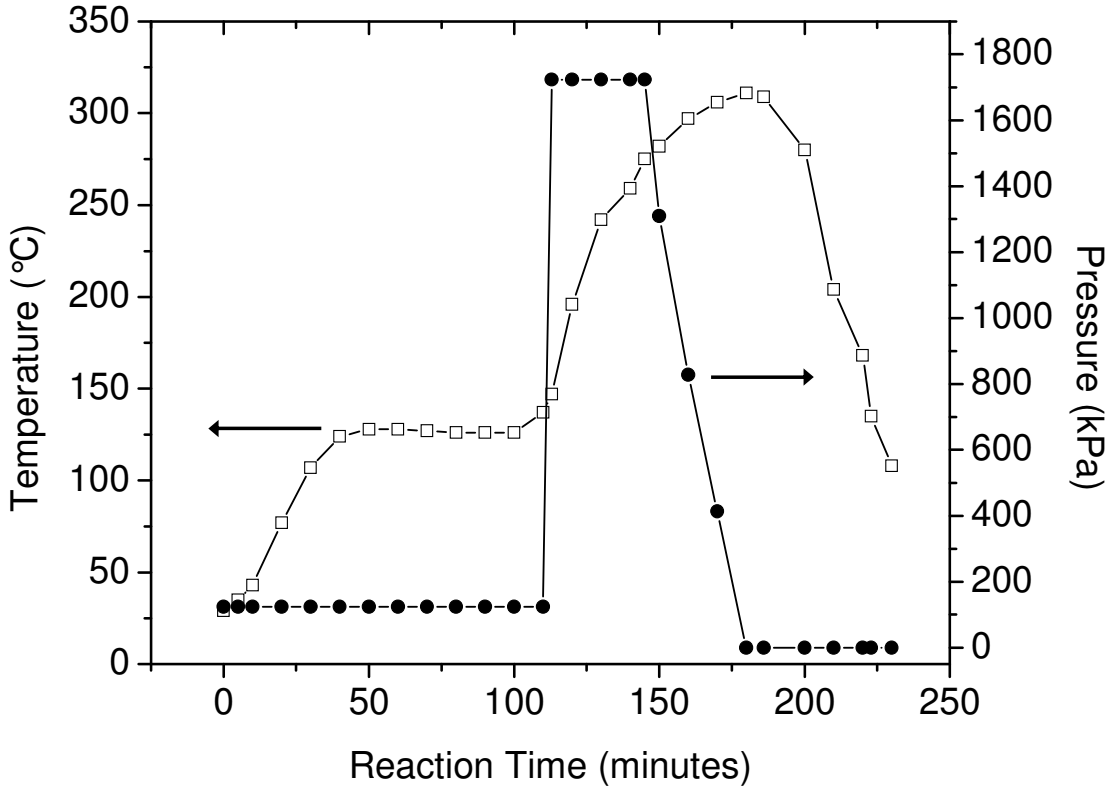

Figure 3.2. Temperature (□) and pressure (●) profiles of PA-12,T melt condensation polymerization.

Sample Preparation

Material plugs were immersed in liquid nitrogen for approximately 10 minutes, then ground using a Waring blender with stainless steel mixing jar. Resulting pellets were dried at 80 °C under vacuum for 24 hours and stored in a desiccator before characterization.

Characterization

High resolution ^{13}C NMR spectroscopy. Samples containing 10 wt-% polymer in a 3:1 volume ratio of HFIP to $CDCl_3$ were prepared by dissolving pellets in HFIP, followed by addition of $CDCl_3$. Solution-state ^{13}C NMR spectra were collected on a Varian ^{UNITY}INOVA NMR spectrometer operating at a

frequency of 125.7 MHz. Routine acquisitions were obtained using a 1.3 second acquisition time, a 45° pulse width of 2.9 µs, and a 1 second recycle delay. The number of accumulated transients ranged from 15,000 to 30,000, involving 12-24 hour collection times.

Viscometry. Solutions containing 0.5 g/dL of polymer in concentrated sulfuric acid were made to obtain a single point IV. The solutions were prepared by adding 0.25 grams of polymer and 25 mL of concentrated sulfuric acid into a 50 mL flask. After 12 hours of mixing using magnetic stirring, the solutions were diluted with an additional 25 mL of sulfuric acid, and stirring continued for another 12 hours. Any gelled material was removed by passing the samples through a funnel packed with glass wool. Measurements were obtained using a Cannon viscometer in a 25 ℃ controlled water bath. The viscometer was washed with sulfuric acid and a portion of the next sample to be tested before measurements were recorded. Flow times were an average of three measurements that agree within +/- 0.2 seconds. These were used to determine the specific and relative viscosities. Single point IVs were calculated using the Solomon and Ciuta relationship:[17]

$$[\eta] = [(2*(\eta_{sp} - \ln(\eta_{rel})]^{1/2})]/C$$

where η_{sp} is specific viscosity, η_{rel} is relative viscosity, and C is sample concentration.

Results and Discussion

Viscometry

Single-point IV measurements are shown in Figure 3.3. The melt condensation polymerization of pure salt yields PA-12,T polymer with an IV of 1.25 dL/g. Introduction of 1 and 3 mol-% excess DA into the reaction increases IV to 1.36 and 1.31 dL/g, respectively. However, adding excess DA beyond 3 mol-% yielded products with lower IVs. For example, 5 and 10 mol-% excess DA produced IVs of 1.08 and 0.70 dL/g respectively. The PA-12,T salt is in theory stoichiometrically balanced prior to the polymerization and should yield the highest IV. However, PA-12,T synthesized using 1 and 3% excess DA have higher IVs. The volatility of the monomers is significantly different. Adding excess 1,12-diaminododecane to the starting reactants compensates for this. In contrast, the presence of 1 and 3 mol-% excess TA decreases IV to 0.94 and 0.67 dL/g, respectively. Excess TA at any concentration contributes to the imbalance imposed by volatilization of DA, further decreasing IV. Despite their differences in functionality, BA and TA appear to reduce IV to a similar extent at all concentrations.

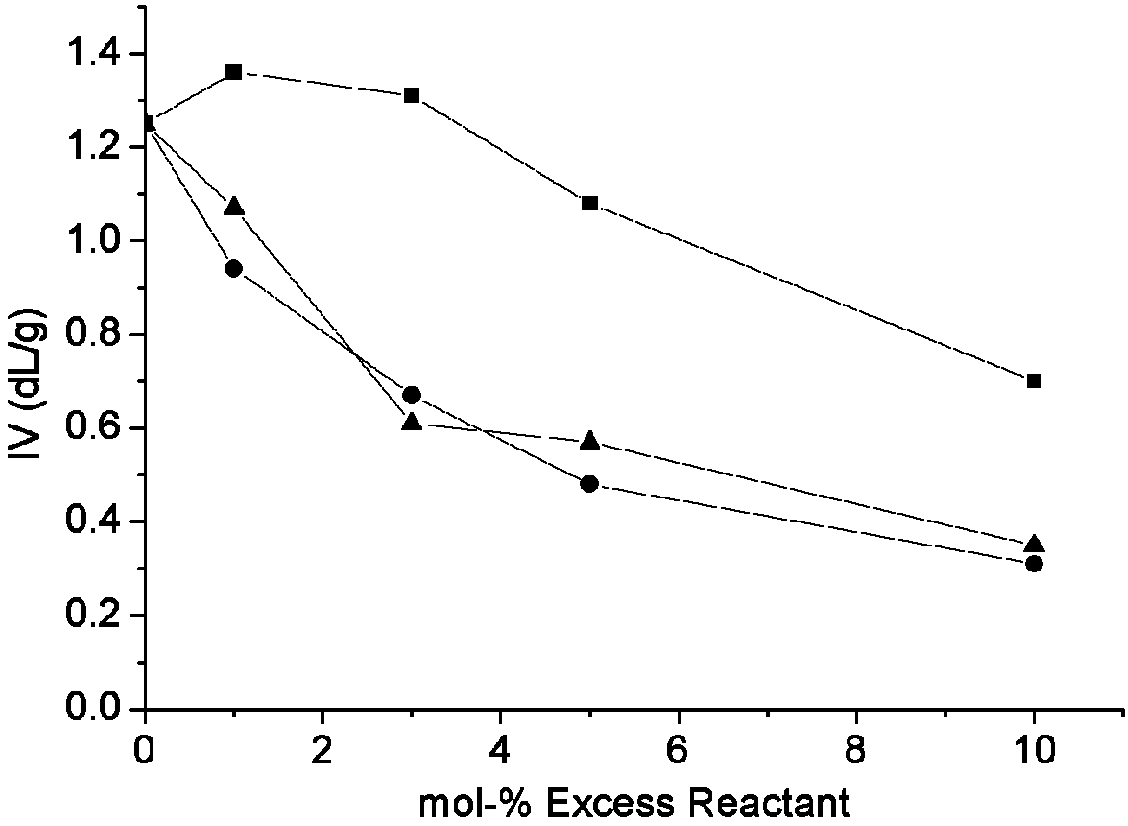

Figure 3.3. Single point intrinsic viscosities for products of PA-12,T salt polymerized with excess diaminododecane (■), terephthalic acid (●), or benzoic acid (▲).

High Resolution ^{13}C NMR Spectroscopy

Figures 3.4-3.6 show the full NMR spectrum of each polymer within each family. Backbone carbon atoms appear as intense peaks at expected chemical shifts. Assignments for repeat units and anticipated end groups are shown in Figure 3.1. Additionally, three sets of solvent peaks are present and labeled accordingly. The vertical scales for each spectrum have been adjusted to maximize the intensity of the tallest polymer peak without truncation. These spectra confirm the identity of each polymer main chain as poly(dodecamethylene terephthalamide).

Horizontal and vertical scales are expanded in Figures 3.7-3.15 to show end groups and other less populous peaks. Here the vertical scales in the aliphatic, aromatic and carbonyl regions have been normalized with respect to backbone carbon atoms **1**, **9**, and **7** respectively, in order to determine trends in the lesser peaks. Main chain carbon atoms appear as relatively broad, truncated peaks in these figures.

Figure 3.7 shows 3 peaks at 42.3 (**A1**), 27.8 (**A2**), and 26.2 (**A3**) ppm whose intensities are directly proportional to the concentration of excess DA present in starting materials. As excess DA increases from 0 to 10 mol-%, their relative intensities (measured as peak heights) increase from 0 to 5.3% as compared to main chain peak **1**. For all concentrations of excess TA, these resonances are not observed (Figure 3.10). This behavior confirms their assignment as the amine end groups **A1**, **A2**, and **A3**. Specific assignments are based on previous work for PA-6,6 and PA-12.[17]

Figure 3.11 shows 4 peaks at 127.6 (**T4**), 131.5 (**T3**), 132.6 (**T5**), and 139.3 (**T2**) ppm whose intensities are directly proportional to the concentration of excess TA present in starting materials. As excess TA increases from 0 to 10 mol-%, their peak intensities relative to main chain peak **9** increases from 1.5 to 10.7%, and are inversely proportional to excess DA (Figure 3.8). Additional peaks in the carbonyl region (Figures 3.9 and 3.12) follow similar trends, with intensities directly proportional to excess acid concentration and inversely proportional to excess diamine concentration. This behavior confirms their assignments as acid end groups. Chemical shifts for peaks **T2** and **T4** are within

1 ppm of those reported by Hall and others[18] using HFIP as an NMR solvent to observe end groups of other terephthalic acid containing polyamides. However, **T3** and **T5** differ from those reported by Hall by 1-3 ppm. Two possible reasons are: 1) spectra in this study were acquired using a mixed solvent system, and 2) the end group chemical shifts are sensitive to pH altered by changes in concentration of acid and amine end groups themselves.[15,18]

In Figure 3.14, the intensity of terephthalic end group peak **T3** increases from 1.47 to 5.16% relative to terephthalic main chain peak **9** as excess BA is increased from 0 to 10 mol-%. This is due to a corresponding decrease in the number average molecular weight with increasing monofunctional BA concentration. In addition to the terephthalic end group peaks, 4 new peaks appear in the aromatic region at 133.6 (**B1**), 132.8 (**B4**), 129.9 (**B3**), and 127.4 (**B2**) ppm, along with a new peak in the aliphatic region at 42.0 (**B6**) ppm (Figure 3.13), and in the carbonyl region at 173.2 ppm (Figure 3.15). The peak at 129.9 ppm increases from 0 to 5.61% as the concentration of BA increases from 0 to 10 mol-%. These peaks are assigned to benzamide end groups based on work previously reported by Hall and others[18] for systems with similar end groups.

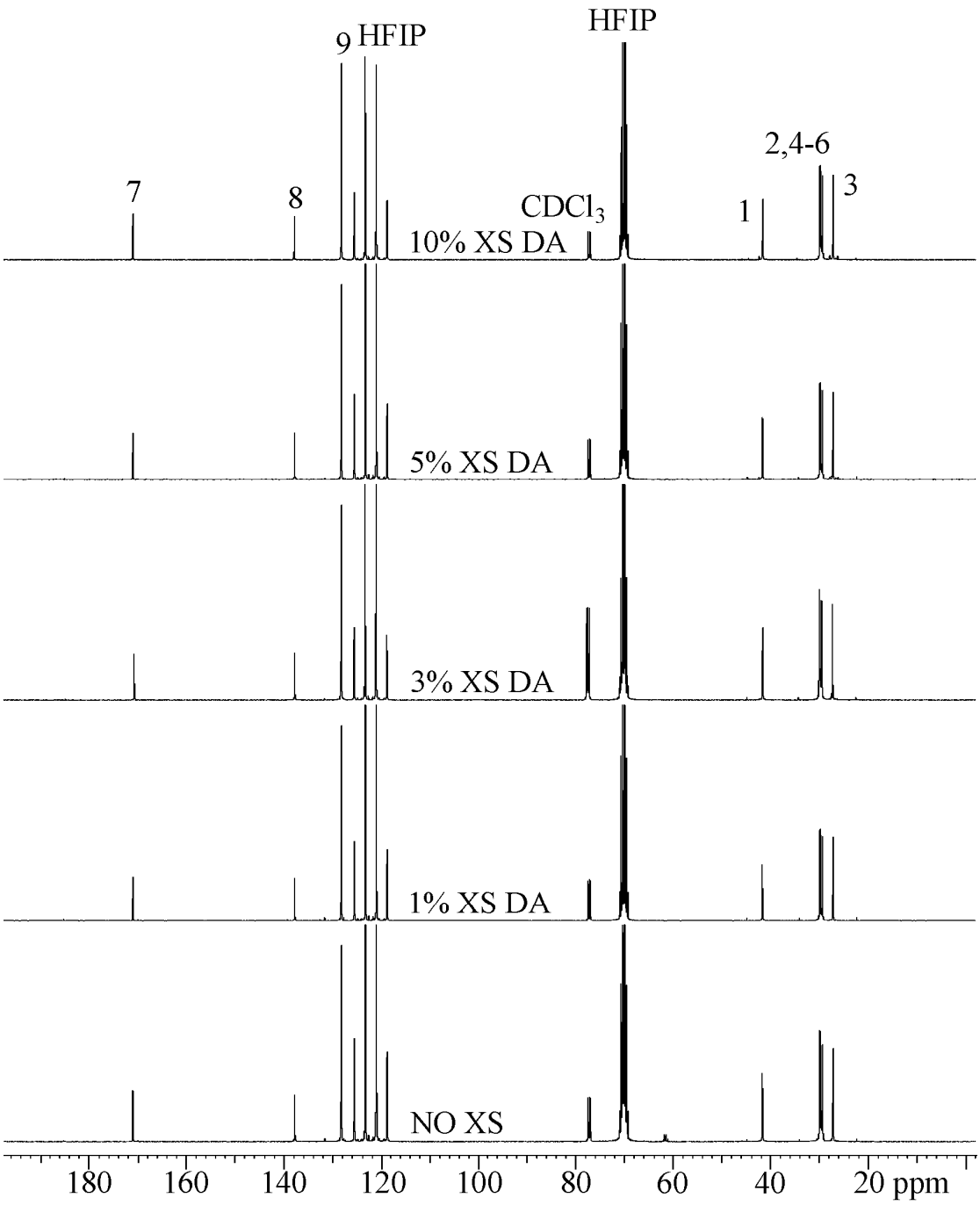

Figure 3.4. Solution ^{13}C NMR spectra of polymers synthesized from starting materials containing 0, 1, 3, 5, and 10 mol-% excess 1,12-diaminododecane (XS DA). Vertical scales for each spectrum have been adjusted to maximize polymer peak intensities without truncation.

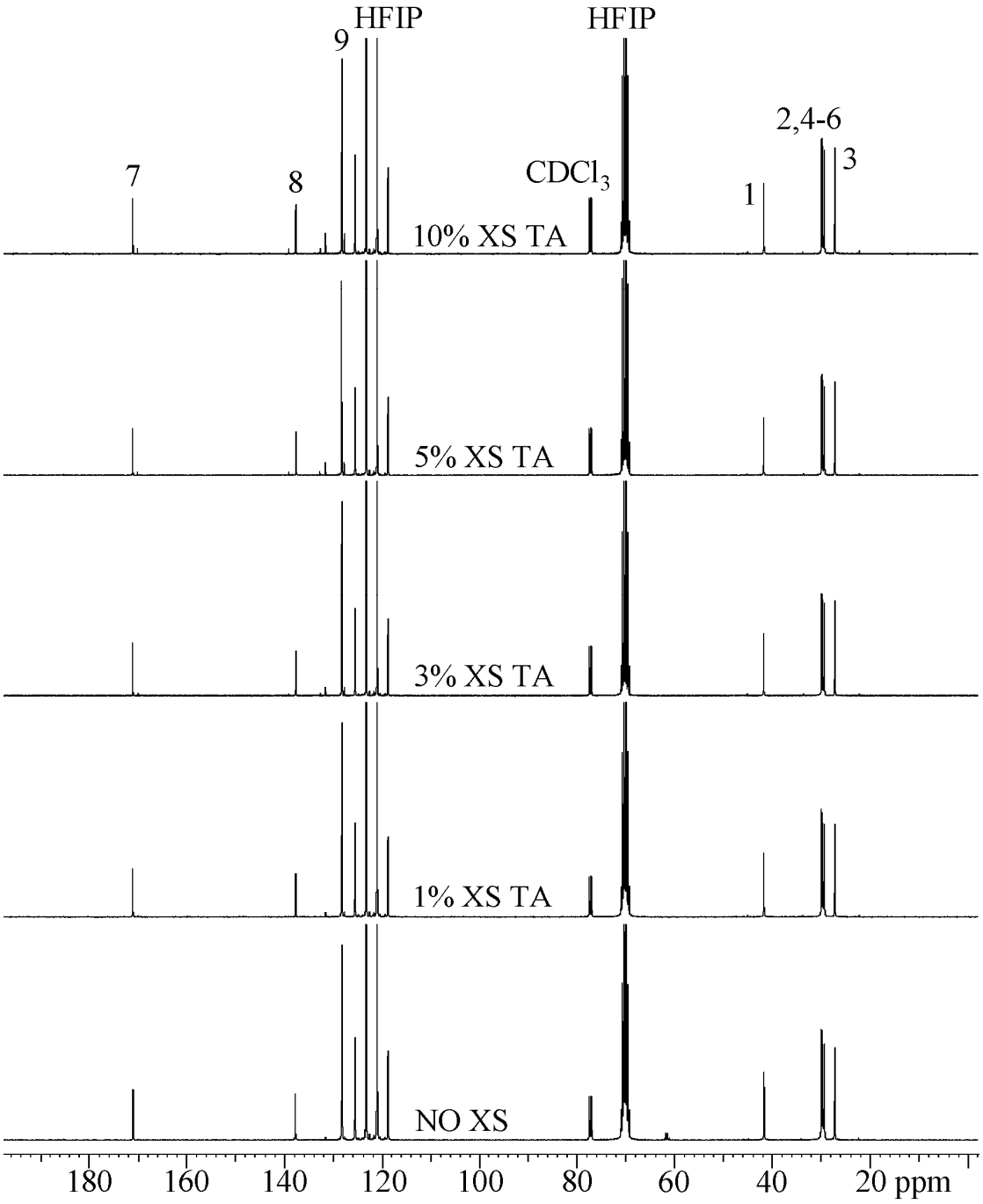

Figure 3.5. Solution ^{13}C NMR spectra of polymers synthesized from starting materials containing 0, 1, 3, 5, and 10 mol-% excess terephthalic acid (XS TA). Vertical scales for each spectrum have been adjusted to maximize polymer peak intensities without truncation.

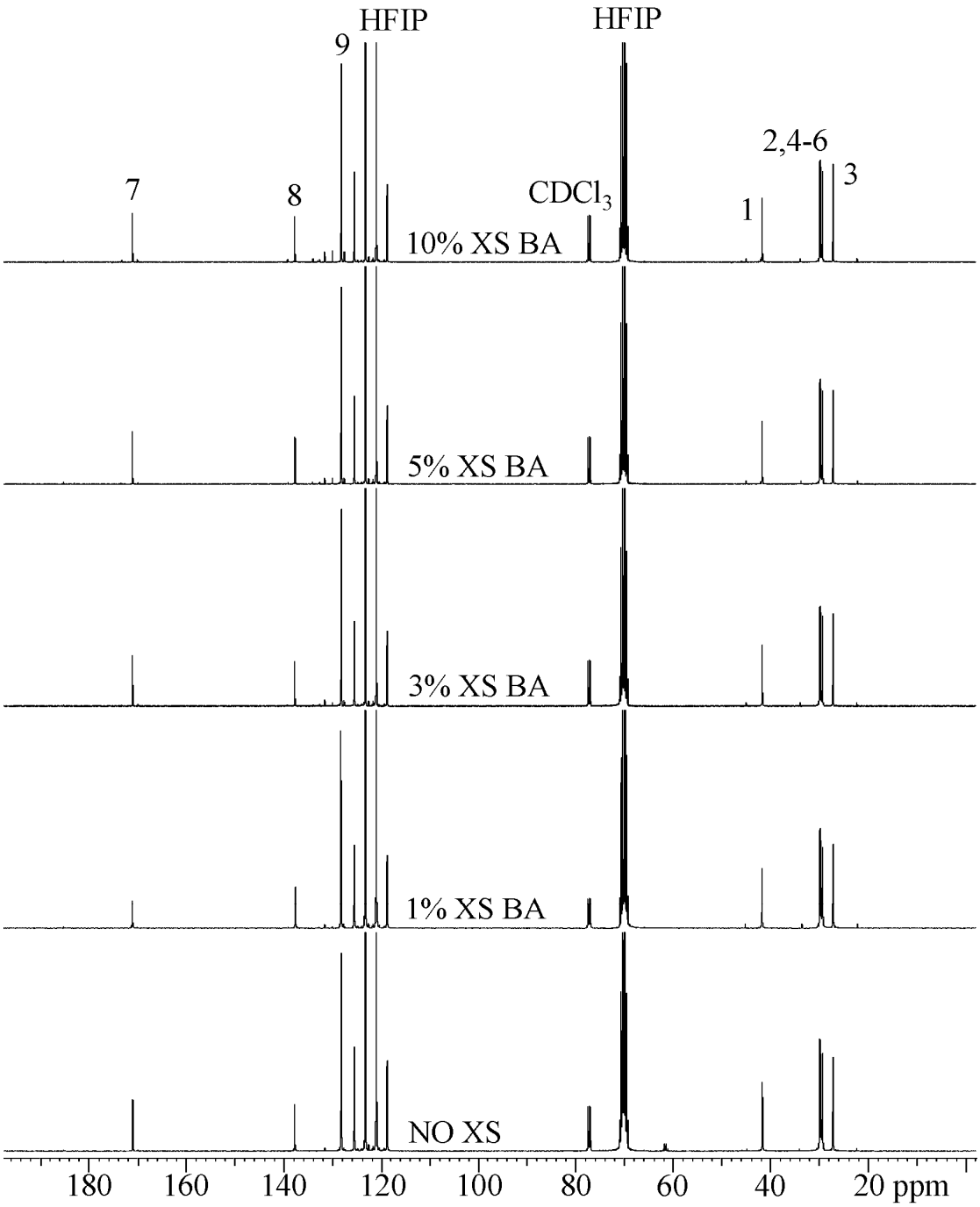

Figure 3.6. Solution ^{13}C NMR spectra of polymers synthesized from starting materials containing 0, 1, 3, 5, and 10 mol-% excess benzoic acid (XS BA). Vertical scales for each spectrum have been adjusted to maximize polymer peak intensities without truncation.

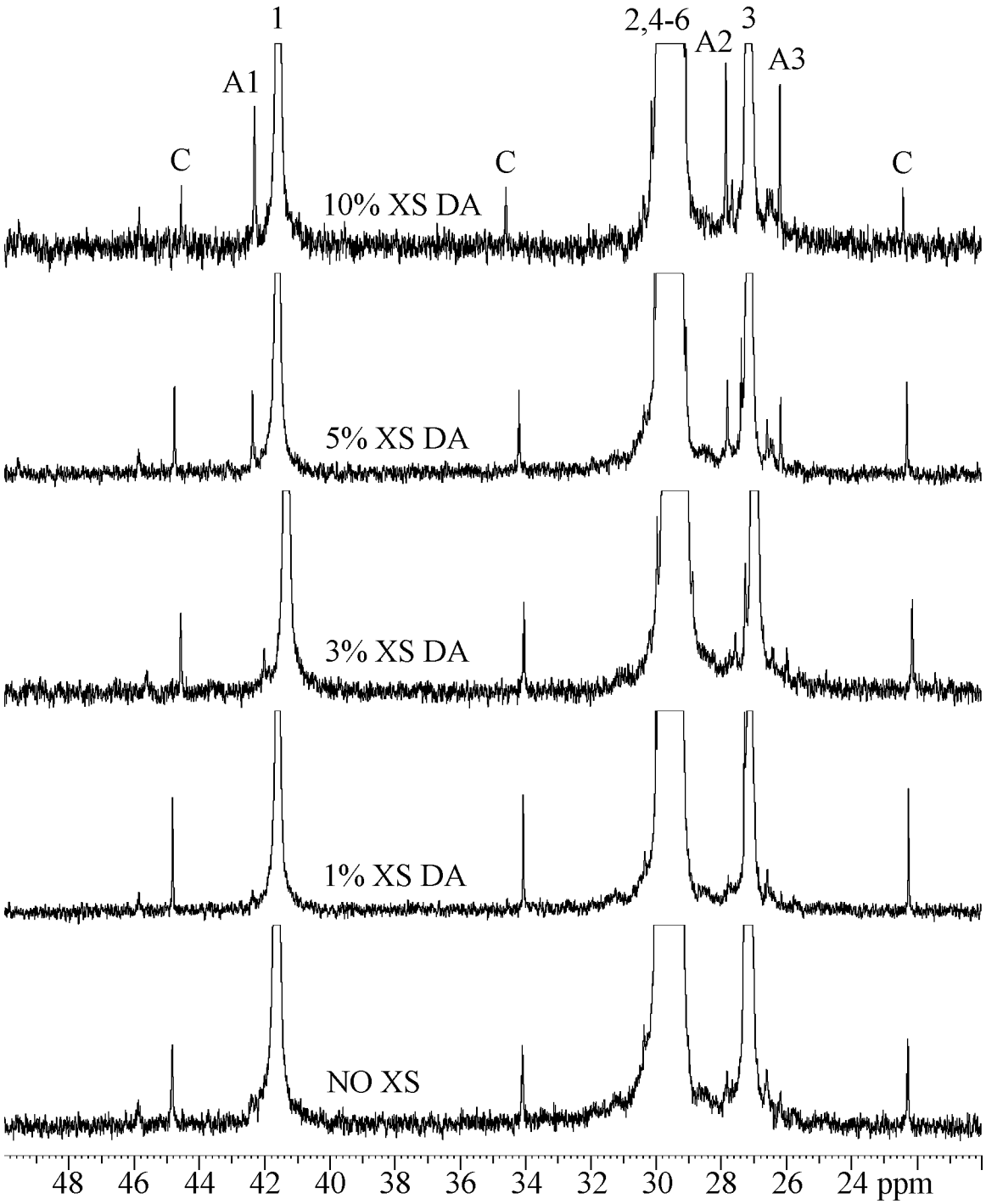

Figure 3.7. Aliphatic region of solution ^{13}C NMR spectra for polymers synthesized from starting materials containing 0, 1, 3, 5, and 10 mol-% excess diaminododecane (XS DA). Peak intensities are normalized with respect to backbone carbon **1**.

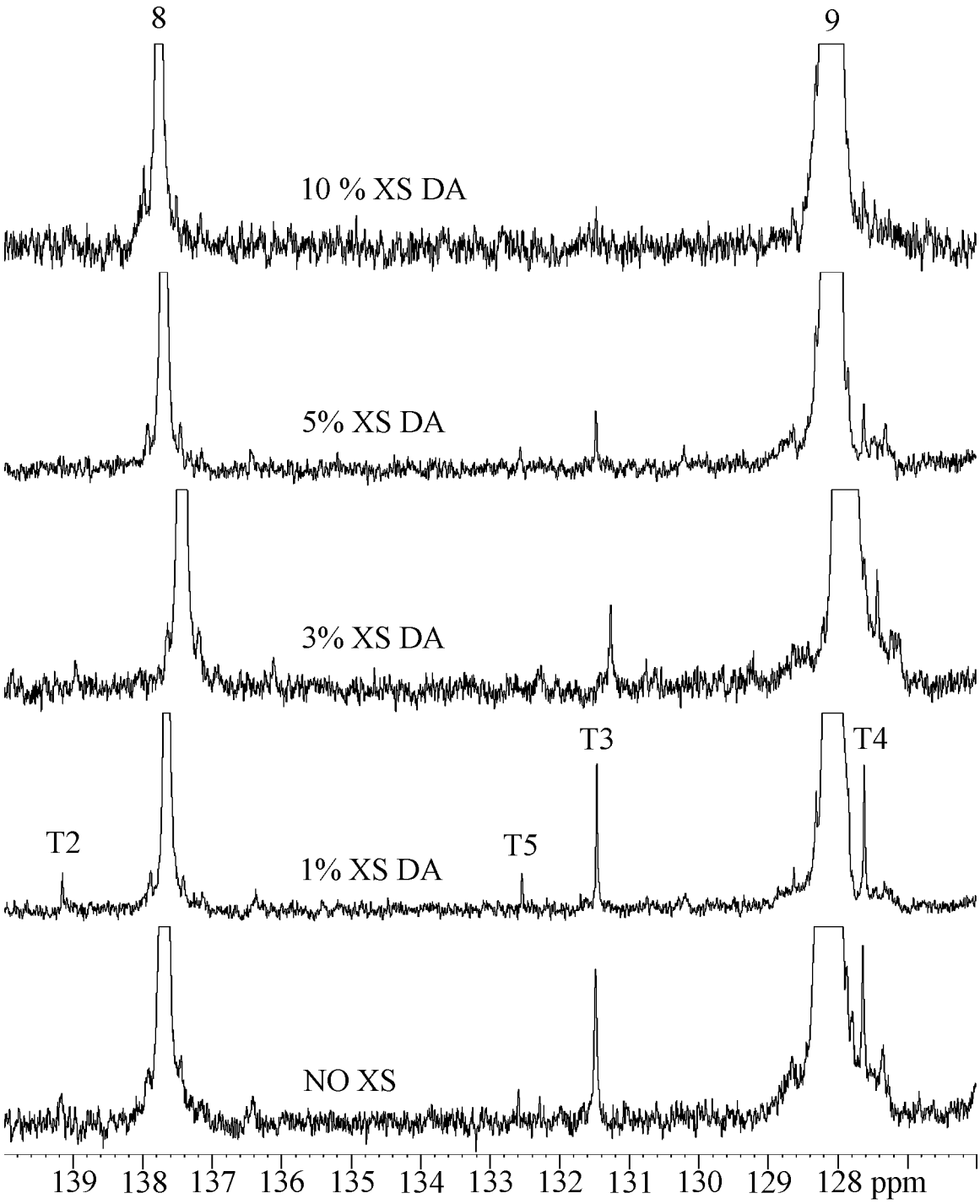

Figure 3.8. Aromatic region of solution ^{13}C NMR spectra for polymers synthesized from starting materials containing 0, 1, 3, 5, and 10 mol-% excess diaminododecane (XS DA). Peak intensities are normalized with respect to backbone carbon **9**.

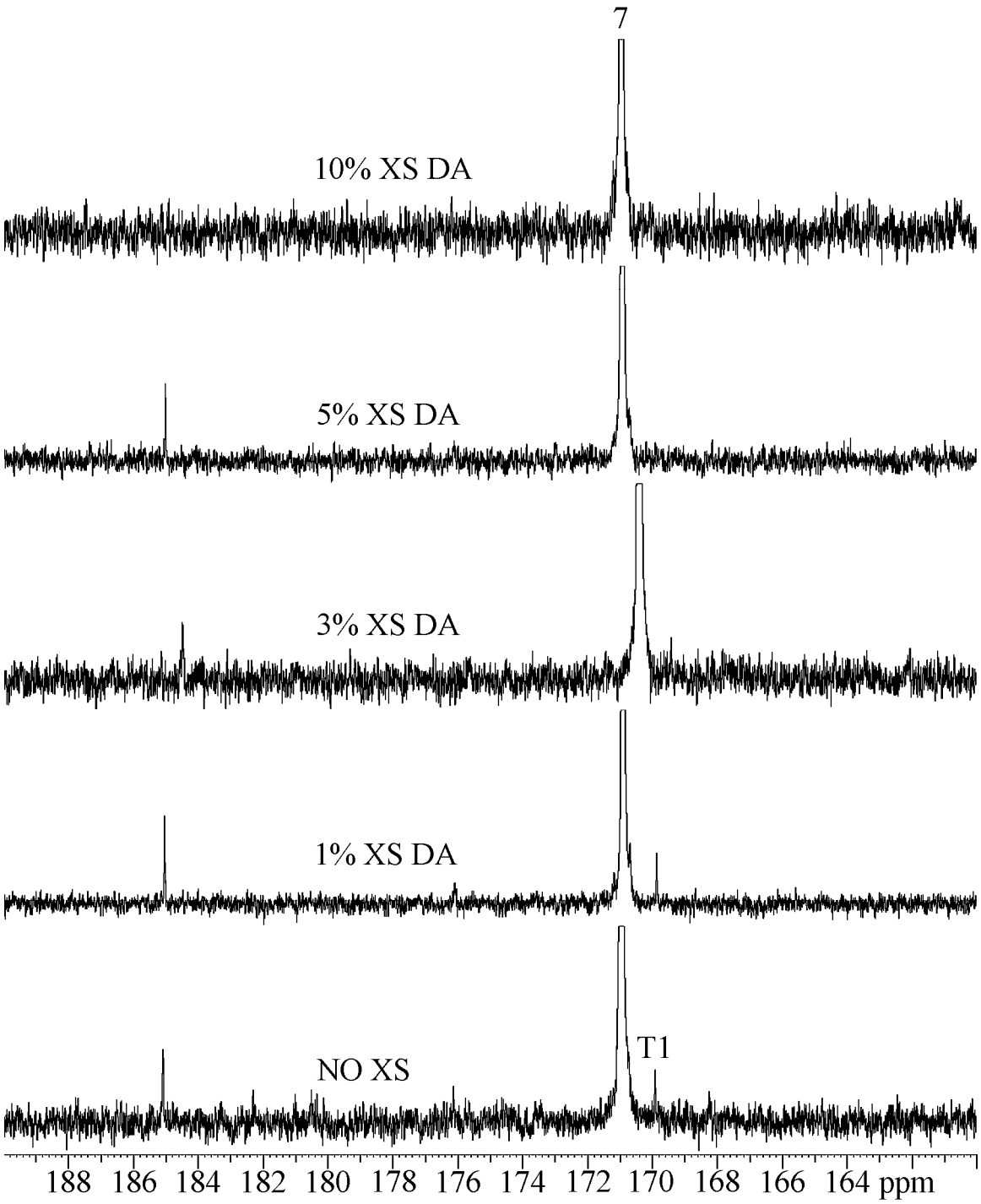

Figure 3.9. Carbonyl region of solution ^{13}C NMR spectra for polymers synthesized from starting materials containing 0, 1, 3, 5, and 10 mol-% excess diaminododecane (XS DA). Peak intensities are normalized with respect to backbone carbon **7**.

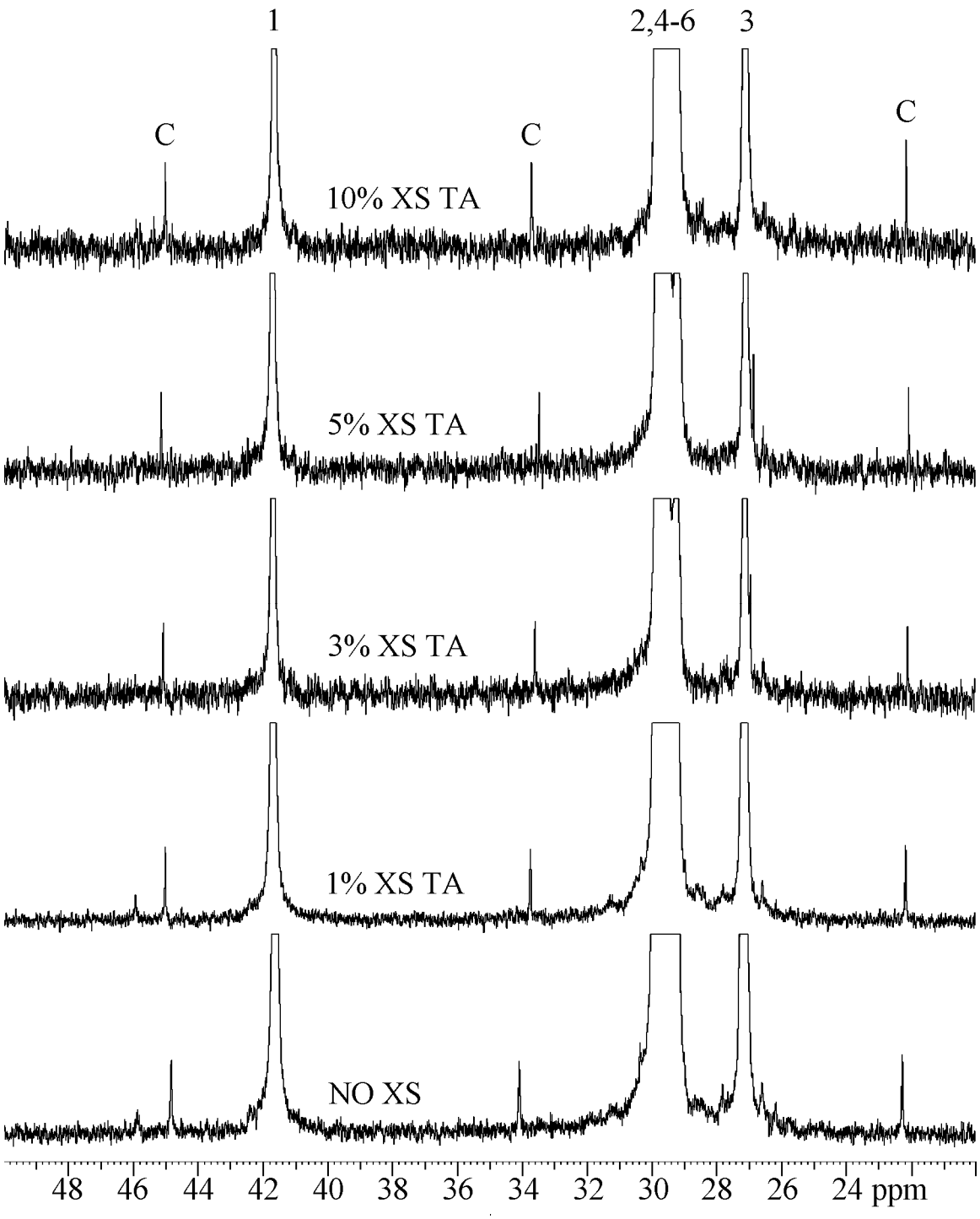

Figure 3.10. Aliphatic region of solution ^{13}C NMR spectra for polymers synthesized from starting materials containing 0, 1, 3, 5, and 10 mol-% excess terephthalic acid (XS TA). Peak intensities are normalized with respect to backbone carbon **1**.

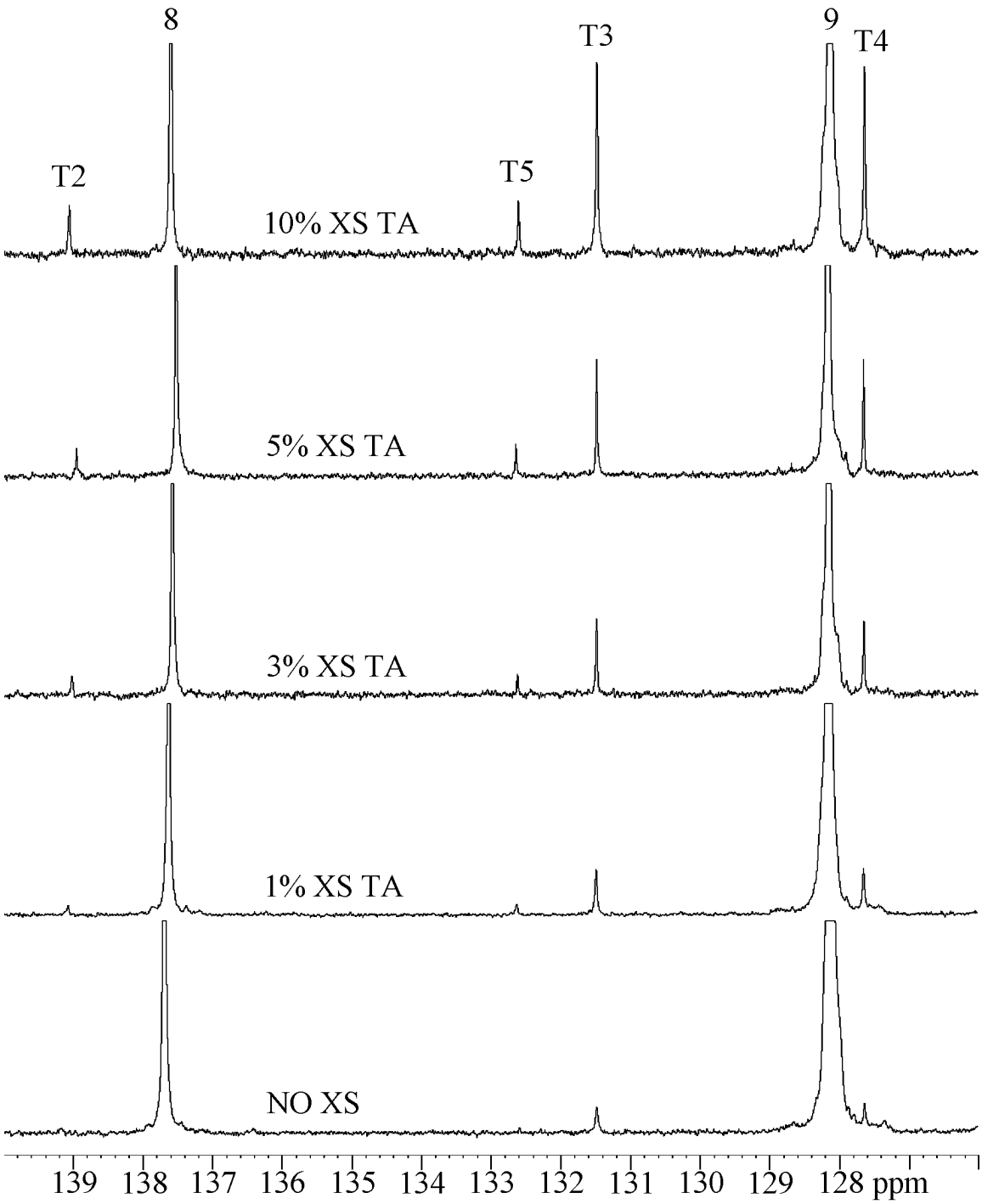

Figure 3.11. Aromatic region of solution ^{13}C NMR spectra for polymers synthesized from starting materials containing 0, 1, 3, 5, and 10 mol-% excess terephthalic acid (XS TA). Peak intensities are normalized with respect to backbone carbon **9**.

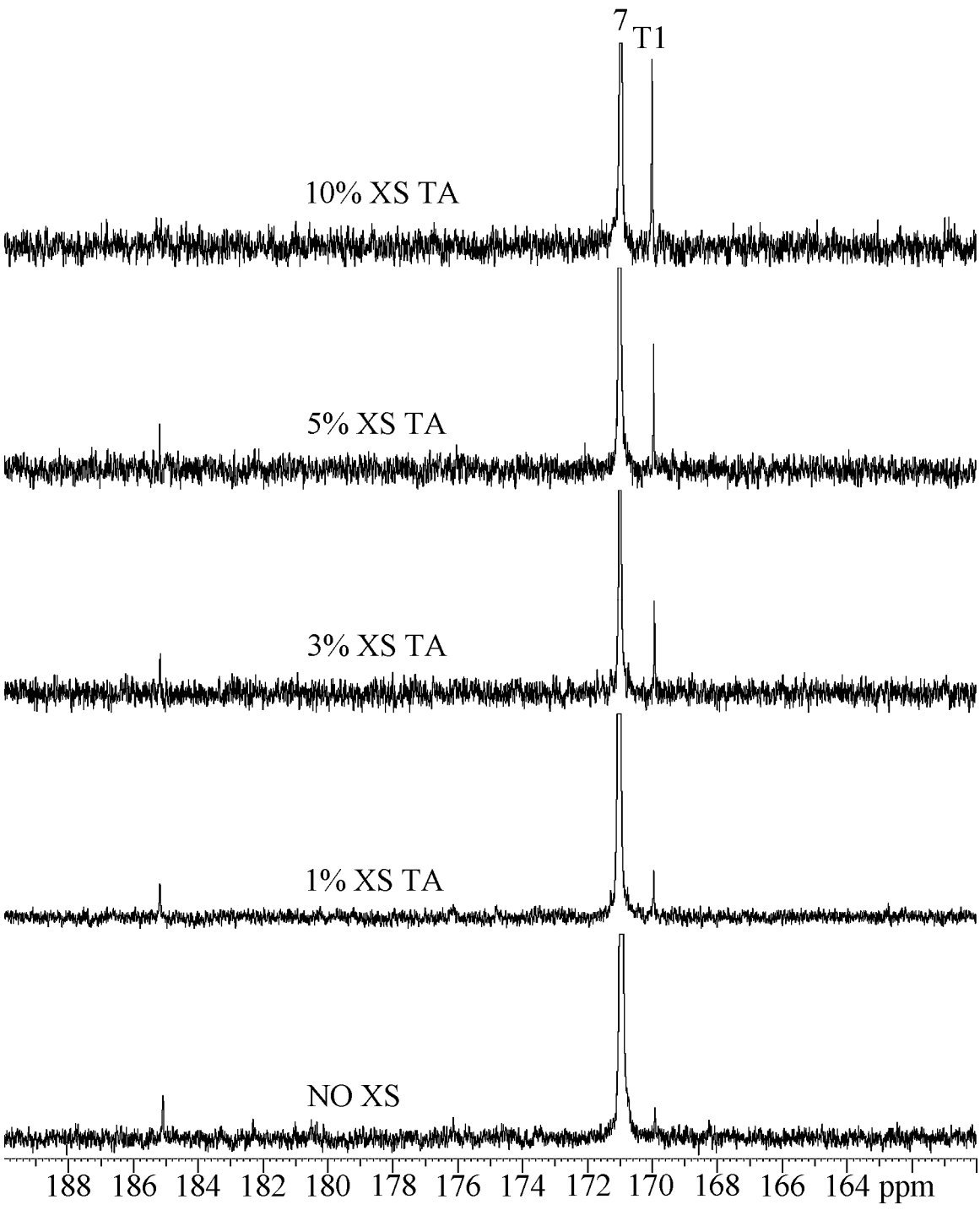

Figure 3.12. Carbonyl region of solution ^{13}C NMR spectra for polymers synthesized from starting materials containing 0, 1, 3, 5, and 10 mol-% excess terephthalic acid (XS TA). Peak intensities are normalized with respect to backbone carbon **7**.

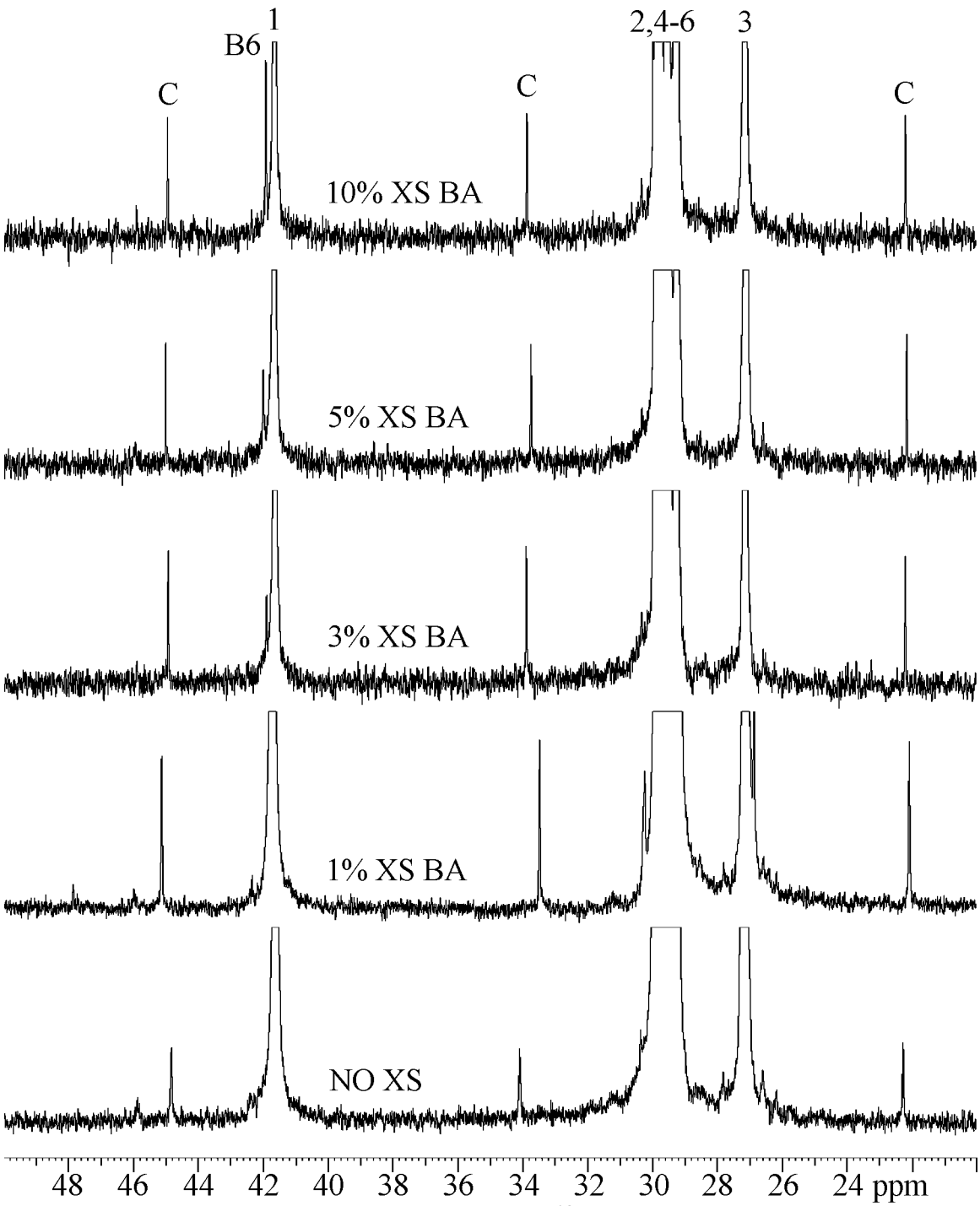

Figure 3.13. Aliphatic region of solution ^{13}C NMR spectra for polymers synthesized from starting materials containing 0, 1, 3, 5, and 10 mol-% excess 1,12-diaminododecane (XS BA). Peak intensities are normalized with respect to backbone carbon **1**.

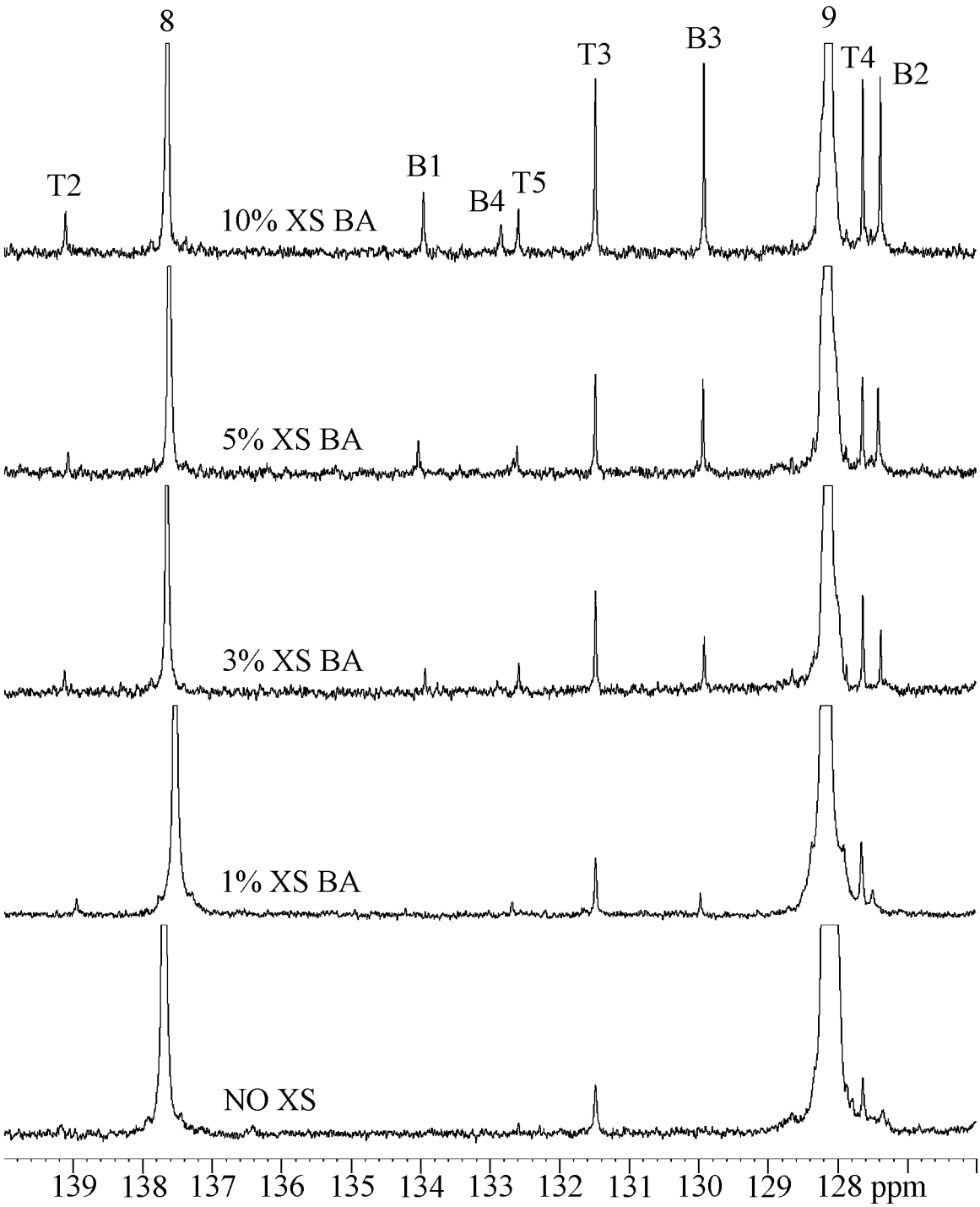

Figure 3.14. Aromatic region of solution ^{13}C NMR spectra for polymers synthesized from starting materials containing 0, 1, 3, 5, and 10 mol-% excess 1,12-diaminododecane (XS BA). Peak intensities are normalized with respect to backbone carbon **9**.

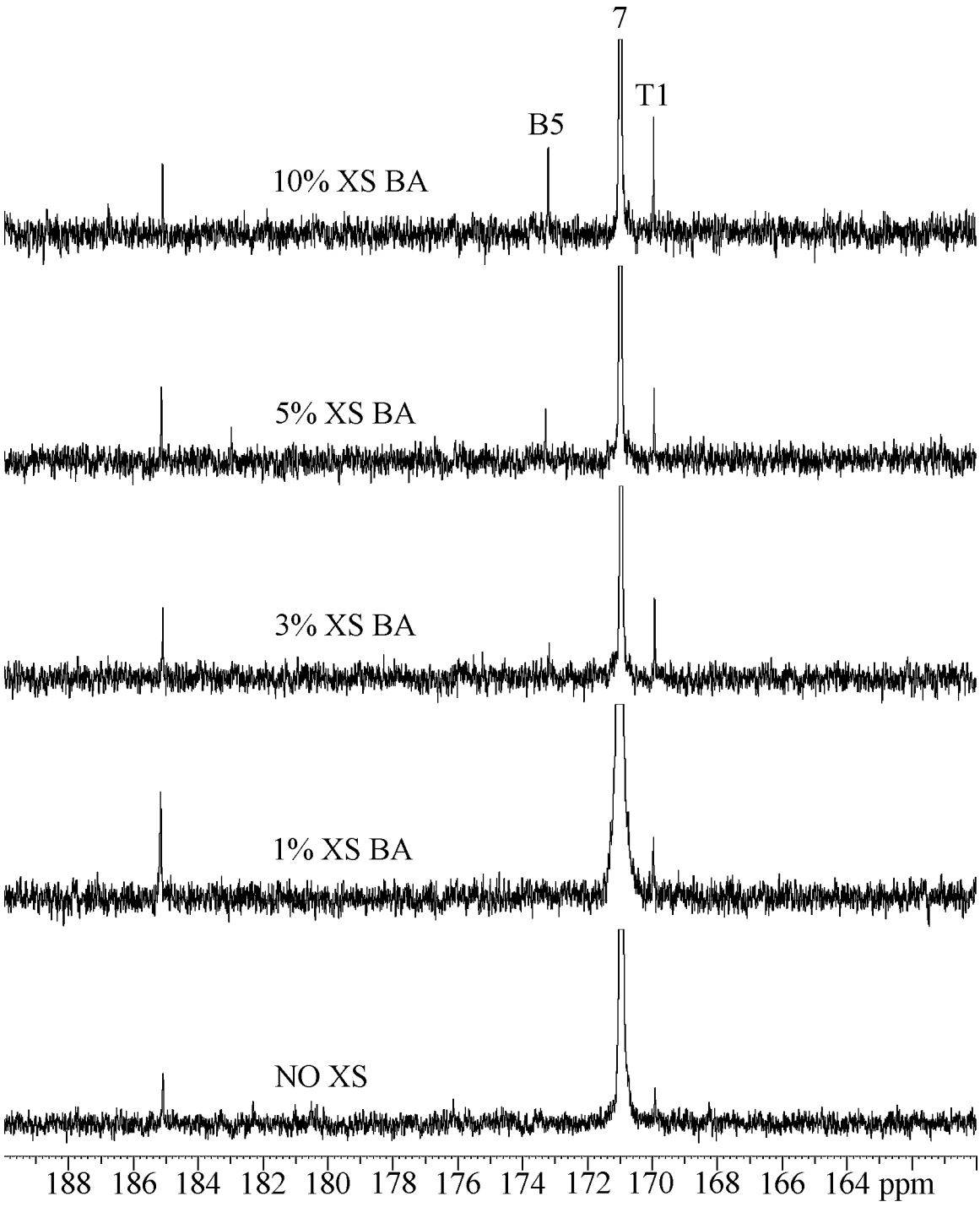

Figure 3.15. Carbonyl region of solution ^{13}C NMR spectra for polymers obtained from starting materials containing 0, 1, 3, 5, and 10 mol-% excess 1,12-diaminododecane (XS BA). Peak intensities are normalized with respect to backbone carbon **7**.

All samples analyzed by NMR spectroscopy exhibited three peaks of equal height at 44.9 (**C**), 33.9 (**C**), and 22.2 (**C**) ppm whose intensity fluctuated between 2.3 and 6.3% (average 3.9%). The only noticeable trend is that they are more pronounced for polymers containing excess BA (5.5% average intensity) as compared to those containing no excess (3.2% average intensity). However, the significance of this data is uncertain. These peaks are not consistent with NMR spectra of the monomers nor do they behave like end groups. They may indicate the presence of cyclical structures or *cis* amide repeat units. In addition figures 3.9, 3.12, and 3.15 show a peak at 185.2 ppm that also exhibits anomalous behavior. It is present in all spectra except for products formed using 10 mol-% excess diamine or diacid. Its identity is unconfirmed to date.

End Group Concentration and Molecular Weight

Previous studies have demonstrated that accurate end group and molecular weight calculations for nylon 6,6 could be made based on NMR data acquired in a similar solvent system[15] by comparing relative concentrations of end groups and repeat units even when NOE enhancement and short recycle delays were used during acquisition. The integrated areas and peak heights were both useful for calculating accurate molecular weights as long as comparisons were made between similar types of carbons. The present work is based on similar assumptions: Nuclear Overhauser effects and relaxation times of end groups and repeat units are approximately equal for similar carbons, and differences in relative peak heights of end groups and repeat units are influenced primarily by molecular weight. These assumptions reduce analysis time by

approximately one order of magnitude compared with rigorously quantitative conditions.

End group concentrations relative to the polymer main chain peaks were calculated by NMR analysis using the equation;

$$[EG] = I_{EG}/[(I_1/2 + I_9/4)/2]$$

where $I_{EG} = I_{A1}$ or $I_{T3}/2$ or $I_{B3}/2$.

Figure 3.16 shows the plot of total end group concentration [EG] and IV as a function of excess DA and TA. Note that the positive and negative x-axis values refer to the mol-% excess or deficiency of DA. For all samples, end group concentration is inversely proportional to IV. For example, the product synthesized with 10 mol-% excess TA has the lowest IV and the highest [EG]. As excess TA decreases from 10 to 0 mol-%, [EG] decreases and IV increases, with a similar trend observed as excess DA decreases from 10 to 3 mol-%. However, there is a large difference in IV and [EG] between samples containing 10 mol-% excess DA and TA. This deviates from traditional step-growth theory which assumes equivalent imbalances in either A-A or B-B monomer affects molecular weight equally.

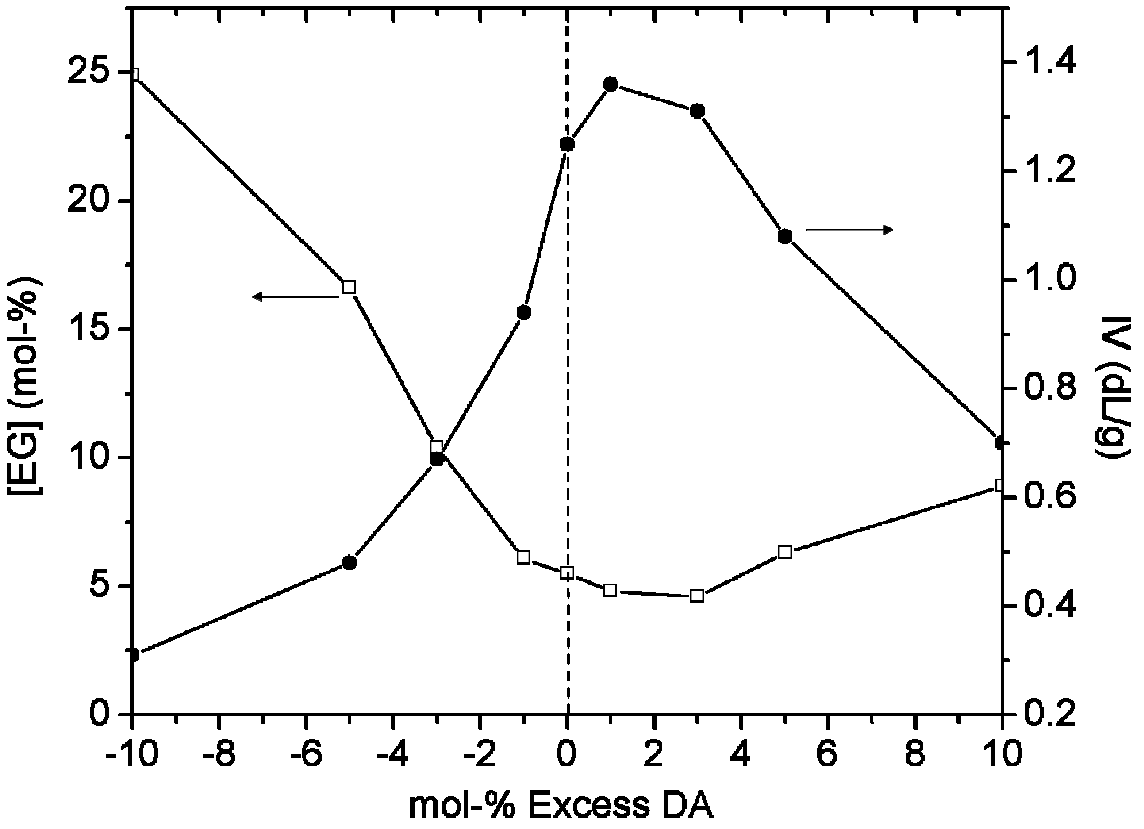

Figure 3.16. Total end group concentrations determined by ^{13}C NMR spectroscopy (□) and IV (●) of PA-12,T synthesized with excess DA (positive values) and excess TA (negative values of DA).

Figure 3.17 shows the concentration of amine and acid end groups as a function of excess DA and TA. Terephthalic acid end groups were observed in all samples, but no amine end groups were detected for polymers synthesized with excess TA, due to the higher volatility of the DA monomer. The majority of end groups are acid from 10 mol-% excess TA to 1 mol-% excess DA, while amine end groups predominate from 3 to 10 mol-% excess DA. These data suggest that although maximum molecular weight is achieved when the stoichiometry of the product is balanced, this is not necessarily the same as balancing the

stoichiometry of the initial reactants. Interpolation of Figure 3.17 reveals that for these polymerization conditions, product stoichiometry would be balanced with approximately 2.4 mol-% excess DA in the initial reactants.

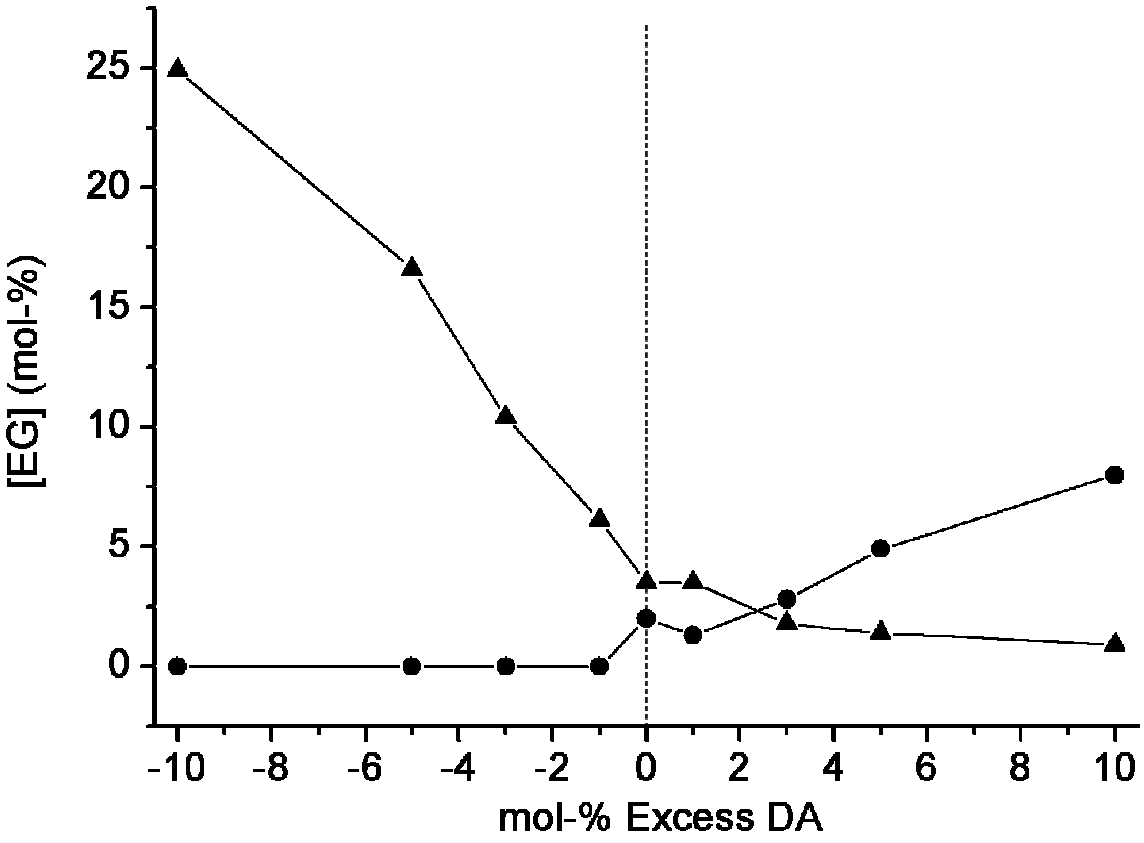

Figure 3.17. Acid (▲) and amine (●) end group concentrations of PA-12,T synthesized with excess DA (positive values) and TA (negative values).

Total end group concentrations and IV for PA-12,T synthesized with excess BA and TA are presented in Figure 3.18. Here, since no amine end groups were detected in polymers synthesized with excess BA or TA, the total end group concentration is the sum of terephthalic acid and benzamide end groups. The total end group concentration increased and IV decreased with increasing concentration of excess BA and TA. The magnitude of these effects

were identical on a molar basis despite their different functionality. The only difference observed between PA-12,T synthesized with excess BA and TA was end group functionality. An excess of 1 mol-% BA yielded polymer containing 71% acid and 29% benzamide end groups. A 10 mol-% excess BA, yielded 48% acid and 52% benzamide end groups. Differences in the reactivity and polarity of these end groups affect post polymerization processes, dyeability[5] and interactions with fillers in a composite.[19]

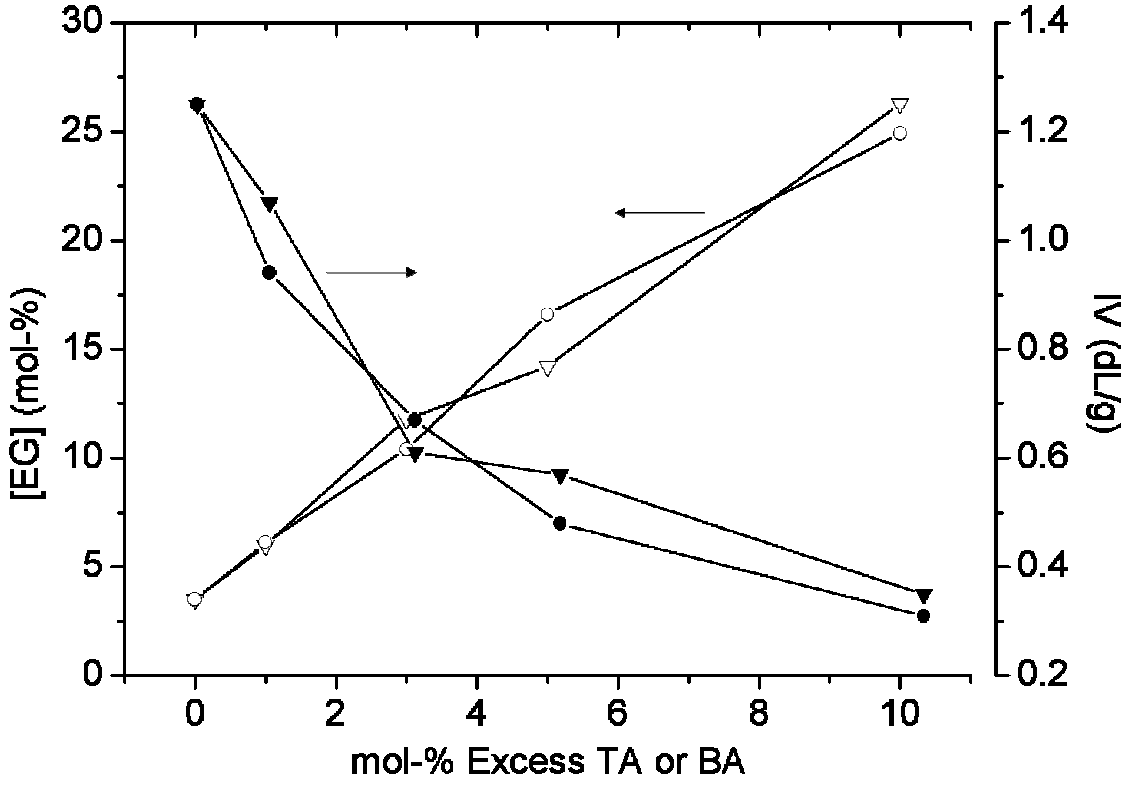

Figure 3.18. IV (solid) and total end group concentration (hollow) for PA-12,T synthesized with TA (●, ○) and BA (▼,▽).

Number average molecular weights (M_n) were calculated by multiplying the molecular weight of the repeat unit for PA-12,T (M_0 = 330.5 g/mol) by the average degree of polymerization (DP) using the equation:

$$M_n \text{ (g/mol)} = M_0[(I_1/2 + I_9/4)/2] / [(I_{A1} + I_{T3}/2 + I_{B3}/2)/2]$$

The degree of polymerization was calculated by NMR analysis as the ratio of average main chain repeat units to the sum of end group units. Here, I_1 and I_9 represent the intensity of amine and acid main chain peaks, respectively, while I_{A1}, I_{T3}, and I_{B3} respectively represent the intensity of amine, terephthalic acid, and benzoic acid end group peaks as assigned in Figure 3.1.

Figure 3.19 shows the plot of M_n versus excess reactant. The similar trends observed in Figures 3.3 and 3.19 clearly show strong agreement between IV measurements and M_n calculations based on NMR analysis. Both confirm that 1-3 mol-% excess DA yielded polymers with higher M_n and IV than the product of pure 12,T salt, with M_n and IV decreasing progressively above 3 mol-% excess DA and for all concentrations of excess BA and TA.

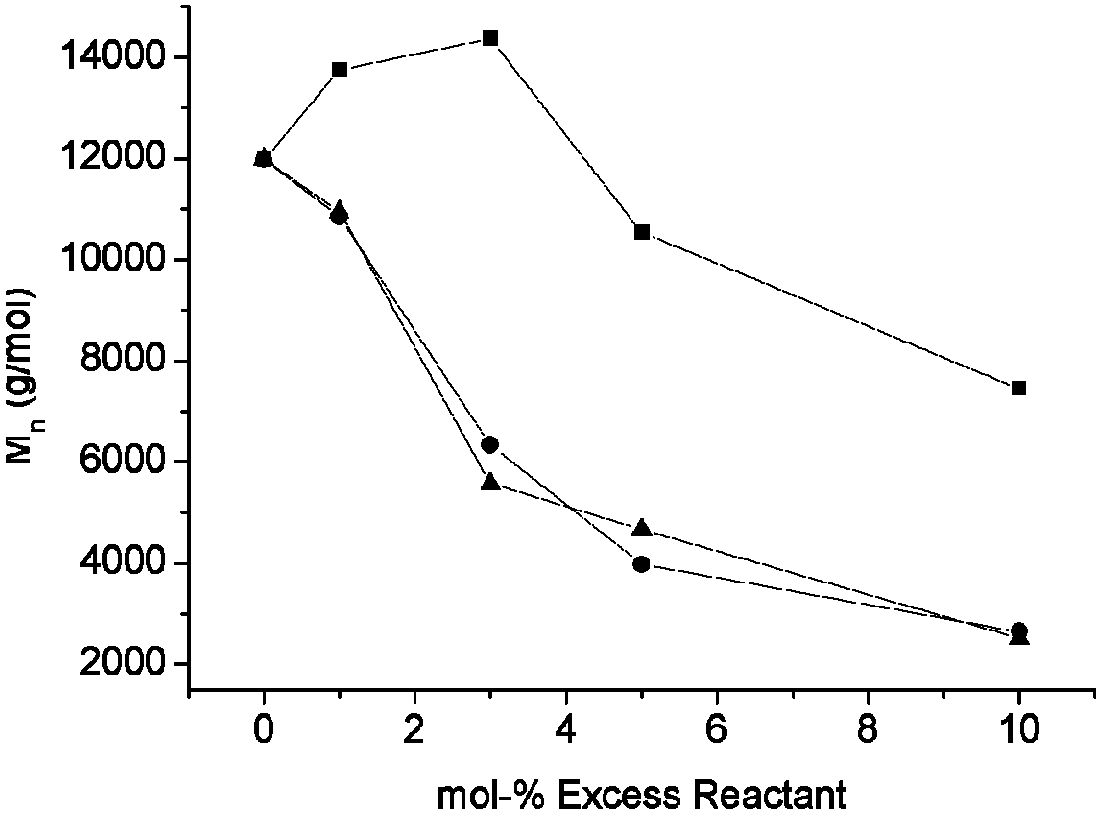

Figure 3.19. Number average molecular weight calculated by NMR analysis of PA-12T salt polymerized with 0, 1, 3, 5, and 10 mol-% excess 1,12-diaminododecane (■), terephthalic acid (●), or benzoic acid (▲).

Figure 3.20 shows a log-log pot of IV versus M_n with a linear trend for these polymers. A best fit line was used to calculate Mark-Houwink constants of $K=55.8*10^{-5}$ dL/g and a = 0.81. This indicates the polymers behave like flexible chains rather than rigid rods.[20] Sulfuric acid is not a theta solvent for these polymers; therefore plots are only shown over the molecular weight range where the Mark-Houwink relationship has been demonstrated to be accurate for each system.[21-23] IV of PA-12,T is 1-2 orders of magnitude less than poly(p-benzamide) and PA-6,I over the range of molecular weights studied. However, PA-12,T shows only a marginal increase in IV over completely aliphatic nylons of

comparable molecular weights. For example, at a M_n of 14,300 g/mol, PA-6,6 has an IV of 0.70 g/dL, PA-12,T has an IV of 1.30 g/dL, and poly(p-benzamide) has an IV of 185 g/dL.

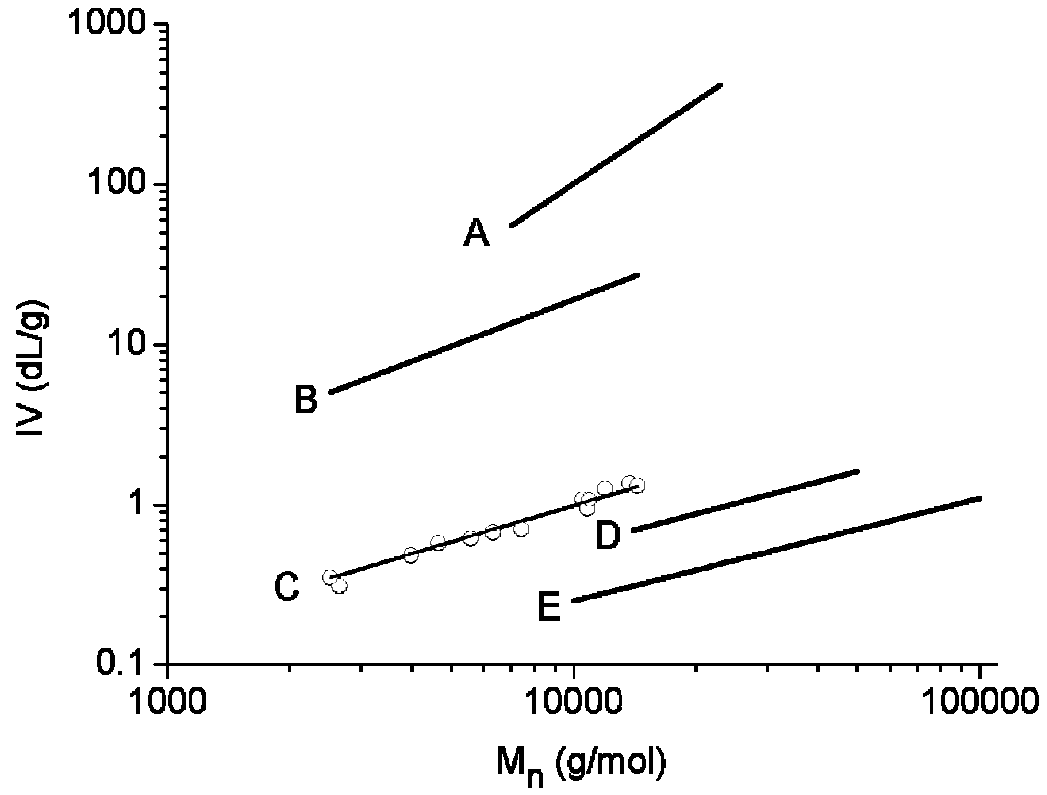

Figure 3.20. Log-Log plot of IV vs. Mn for: A) poly(p-benzamide) (96% sulfuric acid, 20°C)[21]; B) PA-6I (conc. sulfuric acid, 25°C)[22,23]; C) experimental data (○) and best fit curve for PA-12,T(conc. sulfuric acid, 25°C); D) PA-6,6 (96% sulfuric acid, 25°C)[23]; E) PA-12 (96% sulfuric acid, 25°C)[23].

Conclusions

Polyamide-12,T of varying molecular weight was synthesized by melt condensation polymerization of 12,T salt with 0-10 mol-% excess 1,12-diaminododecane, terephthalic acid, or benzoic acid. Intrinsic viscosity measurements were directly related with molecular weights calculated by NMR

analysis. Addition of 1 and 3 mol-% excess diamine increased the number average molecular weight of products compared to pure salt. Calculations predict that acid and amine polymer end groups would be at equal concentration with 2.4 mol-% excess DA added to the salt. Using these specific processing conditions, maximum molecular weight polymer would be obtained. On a molar basis, excess terephthalic acid and benzoic acid both decreased molecular weights to a similar degree. Molecular weights of all polymers calculated using ^{13}C NMR spectroscopy showed a linear trend on a log (Mn) - log (IV) plot with Mark-Houwink constants of $K=55.8*10^{-5}$ dL/g and $\alpha=0.81$. Since these values are based on the single-point IV measurements used to a great extent in semi-aromatic polymer patent literature, they are useful for evaluating data in existing literature and future investigations.

Acknowledgments

Theodore Novitsky synthesized all materials and performed IV measurements for this study. Dr. Scott Osborne, Dr. Steven Manning, Dr. Roger Ayotte and Solutia Nylon Plastics and Fibre division provided funding, access to their facilities, starting materials, and expertise throughout this project.

References

[1] Kohan, M.I. Nylon Plastics Handbook. Hanser Gardner Publications: Cincinnati, **1995**.

[2] Keen, W.E.; Kirkaldy, D. (Imperial Chemical Industries). G.B. Patent 3,642,710, Feb. 15, **1972**.

[3] Takeshi Sakahita, I.; Hashimoto, H.; Nakano, T. (Kuraray Co., Ltd.). U.S. Patent 4,607,073, Aug. 19, **1986**.

[4] Howard, Ng. (DuPont Canada, Inc.). U.S. Patent 6355769, Mar. 12, **2002**.

[5] Campbell, R.W. (Phillips Petroleum Company). U.S. Patent 3,843,611, October 22, **1974**.

[6] Rulkens, R.; Crombach R.C.B. (DSM). U.S. Patent 6,747,120, June 8, **2004**.

[7] Chapman, R.D.; Pickett, Jr, O.A.. (Monsanto Company). U.S. Patent 3,917,561, Nov. 4, **1975**.

[8] Tamura, K.; Oka, H.; Wantabe, K.; Matsunga, S. (Kuraray Co., Ltd.). U.S. Patent 6,156,869, Dec. 5, **2000**.

[9] Mok, S.L.; Pailagan, R.U. (E.I. Du Pont de Nemours and Company). U.S. Patent 5,378,800, Jan. 3, **1995**.

[10] Campbell, R.W. (Phillips Petroleum Company). U.S. Patent 3,839,296, Oct. 1, **1974**.

[11] Akkapeddi, M. K.; Cummings, M. F.; Dege, G. J. (Allied Signal). U.S. Patent 5,191,060, Mar. 2, **1993**.

[12] Cheng, P.P. (E.I. Du Pont de Nemours and Company). World Patent 2006/020845 A2, Feb. 23, **2006**.

[13] Oka, H.; Kashimura, T.; Yokota, S.;Hayashihara, H. (Kuraray Co., Ltd.). U.S. Patent 5,670,608, **1997**.

[14] Odian, G. Principles of Polymerization. John Wiley and Sons, Inc: New Jersey, **2004**; 4th edition, Chapter 2, pp 74-78.

[15] Davis, R.D.; Steadman, S.J.; Jarrett, W.L.; Mathias, L.J. *Macromolecules* **2000**, 33, 7088.

[16] Davis, R.D.; Jarrett, W.L.; Mathias, L.J. *Polymer* **2001**, 42, 2621.

[17] Solomon, O. F.; Ciuta, I.Z. *J. Appl. Polym. Sci.* **1962**, 6, 683.

[18] Singletary, S.; Bates, R. B.; Jacobsen, N.; Lee, A. K.; Lin, G.; Somogyi, A.; Streeter, M. J.; Hall, H. K. *Macromolecules* **2009**, 42, 2336-2343.

[19] Youngjae Yoo, D. R. Paul. *Polymer* **2008**, 17, 3795-3804.

[20] Arpin, M.; Strazielle, C. *Polymer* **1977**, 18, 591.

[21] Brandup, J.; Immergut, E.H. Polymer Handbook. John Wiley and Sons, Inc: New York, **1989**; 3rd edition, Section 7, pp 24-25.

[22] Cote, P.; Brisson, J. *Macromolecules* **1994**, 27, 7329-7338.

[23] Brisson, J.; Breault, B. *Macromolecules* **1991**, 24, 495-504.

CHAPTER IV

EUTECTIC MELTING BEHAVOIR OF PA-10,T-6,T AND PA-12,T-6,T COPOLYMERS

Abstract

Polyamides 10,T and 12,T were synthesized with 0-60 wt-% PA-6,T comonomer by melt condensation polymerization to form copolymers. Solution-state ^{13}C NMR analysis revealed that substituted aromatic peaks were sensitive comonomer sequence information. Distribution of comonomers was shown to be statistical. Molecular weights of the copolymers ranged from 12,000 to 27,000 g/mol and all produced tough melt-pressed films. NMR, DSC, and WAXD analysis agree that PA-6,T monomer units are not co-crystalline with PA-10,T or PA-12,T monomer units, and do not form isomorphic structures. Instead, a eutectic melting point at 30 wt-% PA-6,T is observed for both copolymers. Contributions of each comonomer to the eutectic behavior were investigated.

Introduction

Semi-aromatic polyamides have the potential to combine the melt processability of aliphatic polyamides with the desirable mechanical and thermal properties of aromatic polyamides. Polyamides synthesized using aliphatic diamines and terephthalic acid have been studied extensively.[1] Aliphatic diamines containing two to seven methylene units yield materials with decomposition temperatures lower than their melting points. For example, the melting temperatures of PA-4,T and PA-6,T are 430 and 370 °C respectively[2], while their decomposition typically begins above 300 °C. Longer aliphatic

diamines produce polymers with melting points favorable for melt processing. For instance, the melting points of PA-9,T, PA-10,T, PA-12,T[3] and PA-18,T[4] are approximately 309, 325, 295 and 245 °C, respectively. The glass transition temperatures of these semi-aromatic polymers (100 – 140 °C) are greater than corresponding aliphatic polymers, rendering them useful for high temperature applications.

Comonomers are commonly used in semi-aromatic polyamides to alter properties such as melting temperature, processability, and optical clarity.[1] Copolymers which co-crystallize display different melting behavior than those which do not. A plot of copolymer melting temperature versus comonomer concentration is typically linear for co-crystalline (isomorphic) systems. Eutectic melting or completely amorphous behavior is observed for copolymers that are not isomorphic. Isomorphism of in PA-6,T-6,6 copolymers is well documented.[5,6,7] The distance between amide groups formed by adipic and terephthalic acid differ by only 0.3 angstroms.[5] Isomorphism in PA-6,T-6,6 is caused in part by the similar distances between and the orientations of amide groups for each comonomer, which allows each comonomer to occupy the same unit crystal. Comonomers displaying eutectic or amorphous behavior cannot share a crystalline lattice. In these cases, each comonomer can be though of as an impurity which introduces flaws into the crystalline structure of the other monomer. This decreases the size of crystalline domains and thus, overall degree of crystallinity. The extent to which this occurs depends on comonomer

structures and concentrations. Eutectic behavior has been reported previously for PA-6,T-6,I and Pa-6-6,T copolymers.

Research on copolymers containing PA-10,T has been limited to copolymerizations involving caprolactam[8] and adipic acid[6]. Adipic acid and terephthalic acid monomer units co-crystallized in PA-10,T-10,6 copolymers, with trends in melting point versus composition similar to those observed for PA-6,T-6,6 copolymers. Few publications are available that directly investigate copolymerization of PA-10,T or PA-12,T with other linear diamines. One article reported that PA-4,T and PA-6,T copolymerized with a series of linear aliphatic diamines yielded crystalline polymers with depressed melting temperatures.[9]

In the present study, PA-10,T-6,T and PA-12,T-6,T copolymers were synthesized by melt condensation polymerization. Polymers were characterized using high resolution ^{13}C nuclear magnetic resonance (NMR) spectroscopy, wide angle x-ray diffraction (WAXD), viscometry, and dynamic scanning calorimetry (DSC).

Experimental

Materials

Terephthalic acid, 1,10-diaminodecane, 1,12-diaminododecane, and 1,6-diaminohexane (HMDA) were purchased from Aldrich. Terephthalic acid and 1,6-diaminohexane were used as received. 1,10-Diaminodecane, and 1,12-diaminododecane were sublimed at 70 °C and dried at room temperature under vacuum before use. N,N-Dimethylacetamide (DMAc) and triethylamine were distilled from barium oxide onto molecular sieves before use. Concentrated

sulfuric acid (96%) for viscosity measurements was purchased from Aldrich and used as received. Solutia provided PA-6,T salt.

Synthesis

Monomer salt. Into a 2 L beaker, 1 L of deionized water, 1,10-diaminodecane (49.5 g, 0.287 mol) and terephthalic acid (42.3 g, 0.285 mol) were added, and the slurry was heated to a boil. Additional water was added and brought to boil to yield a supersaturated clear salt solution. The hot salt solution was transferred to a 2 L beaker containing 500 mL of reagent alcohol and cooled to room temperature, followed by cooling in a freezer. The precipitate was filtered and washed with reagent alcohol. The resulting 10,T salt was obtained in quantitative yield (95 %). The PA-12,T salt was prepared in a similar manner. All salts were precipitated from water into reagent alcohol and dried before use. PA 12,T, 10,T, and 6,T salt melting temperatures were 271.9, 271.6, and 281 ºC respectively, with melting enthalpies of between 430 and 450 J/g.

Melt condensation of polyamide (co)polymers. Synthesis of copolymers is depicted in Figure 4.1. Polyamide 10,T salt (or polyamide 12,T salt) and 0-60 wt-% polyamide 6,T salt were mixed with 3 mol-% excess diamine and 0.5 wt-% antioxidant using a mortar and pestle. The solid mixture was then added to a test tube and approximately 50 wt-% deionized water was added to create a slurry. Test tubes containing different comonomer ratios were loaded into a Parr reactor, which was then sealed and purged with nitrogen.

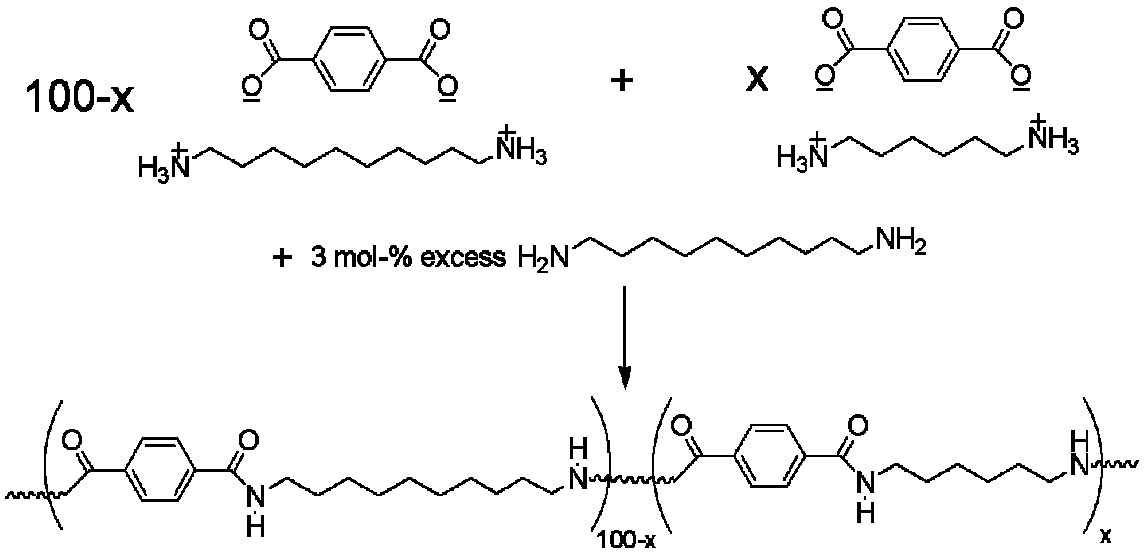

Figure 4.1. Synthetic scheme for PA-10,T-6,T copolymers, where x = 0-60 wt-%.

Temperature in the Parr reactor was monitored using a thermocouple located in one of the test tubes. Heater set points were programmed into the reactor controller. The reactor was surrounded by insulation to ensure precise heating control. Pressure was controlled manually with nitrogen and measured by a gauge on the reactor head. Temperature and pressure profiles of the melt condensation polymerization are plotted versus time in Figure 4.2. The reaction can be divided into three stages according to the pressure profile. In the first stage, pressure was maintained at 125 kPa with the heater set at 200 ℃. The temperature ramped up to a plateau at 126 ℃ as the water boiled. At approximately 110 minutes the temperature increased indicating that all the water had evaporated. In the second stage of the reaction, pressure was increased to 1724 kPa and the heater was set at 315 ℃. Here, the high pressure was used to minimize volatilization of monomer. After 145 minutes the

temperature had reached 276 ℃, at which point the pressure valve was opened. At 180 minutes the reactor reached atmospheric pressure. This marks the beginning of the reaction's third stage, with nitrogen gas purged through the reactor at zero gauge pressure and the heater turned off. Temperature decreased rapidly during the third stage. The maximum reaction temperature was 315 ℃.

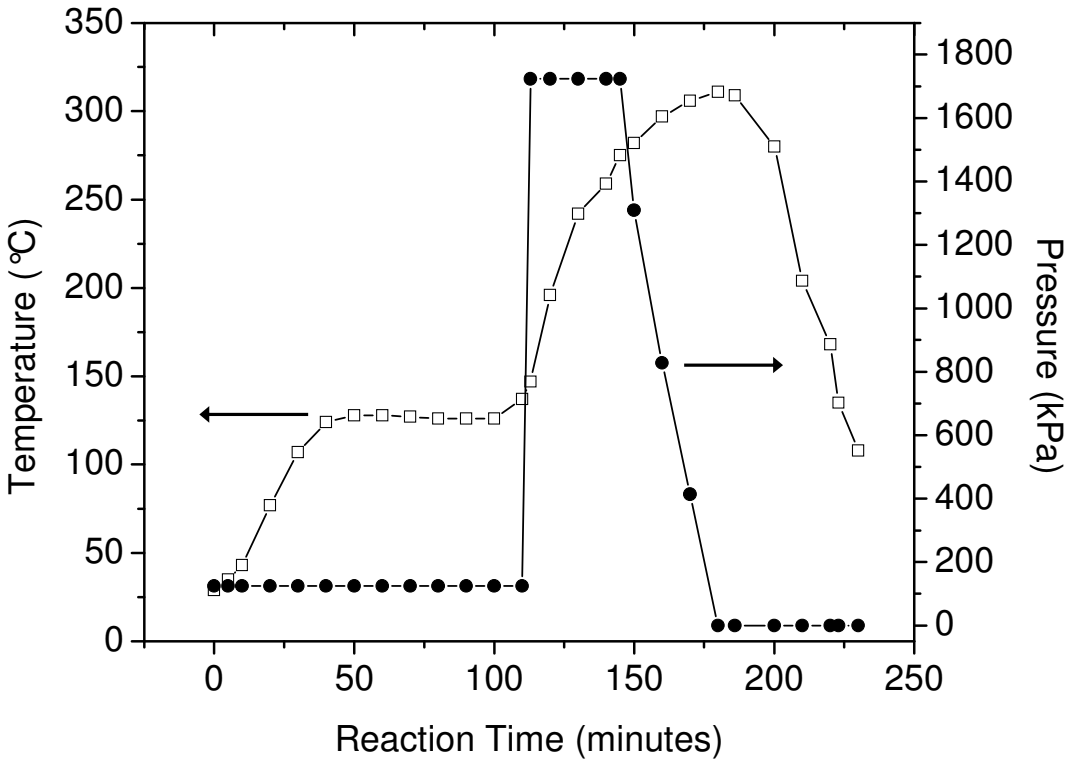

Figure 4.2. Temperature and pressure profiles for melt condensation polymerization of copolymers.

Solution polymerization of polyamide 6,T (PA-6,T). Hexamethylene diamine (10.98 g, 0.095 mol) and triethylamine (27 mL, 0.194 mol) were dissolved in 230 mL of DMAc and added to a glass Waring blender. The blender was turned on high, and 60 mL of DMAc with terephthaloyl chloride

(19 g, 0.094 mol) was quickly added. A white precipitate immediately formed with a corresponding increase in viscosity. After 5 minutes, the precipitate was filtered and washed with acetone and water. Yield for PA-6,T was 90%.

Sample Preparation

Solid polymers obtained from the test tubes immersed in liquid nitrogen for approximately 10 minutes were ground using a Waring blender with a stainless steel mixing jar. The pellets were then dried at 80 °C under vacuum for 24 hours and placed in a desiccator until further characterization.

Films were formed on a Carver 3851-0 melt press by placing pellets between two woven Teflon sheets sandwiched between two metal plates, with the metal plates preheated to 20 °C above polymer melting temperature. No external pressure was applied for three minutes. Then 2,700 kPa was applied to the plates for 2 minutes. Next, the plates, together with the Teflon sheets and polymer, were immersed in a water bath at ambient temperature for approximately 30 seconds. The polymer film was removed and cooled further between two room temperature steel plates. Films were dried at 80 °C under vacuum for 12 hours. Annealing was performed at 200 °C under vacuum for 12 hours.

Characterization

NMR spectroscopy. Samples contained 10 wt-% polymer dissolved in a 3:1 volume ratio of hexafluoroisopropanol (HFIP) and $CDCl_3$. Pellets were first dissolved in HFIP, followed by addition of $CDCl_3$. Solution ^{13}C spectra were collected on a Varian ^{UNITY}INOVA NMR spectrometer operating at a frequency of

125.7 MHz. Routine acquisitions were obtained using a 1.3 second acquisition time, a 45° pulse width of 2.9 µs, and a 1 second recycle delay. The number of transients accumulated ranged from 15,000 to 30,000, involving 12-24 hour collection times. Spectra were recorded at 25°C. Data was zero-filled up to 256k points and filtered with up to 1 Hz of line broadening prior to application of Fourier transformation. Baselines were corrected using a 10^{th} order polynomial.

Viscometry. Solutions were prepared by adding 0.25 grams of polymer to 25 mL of concentrated sulfuric acid in a 50 mL flask. Samples were stirred with a magnetic bar for 12 hours, diluted with an additional 25 mL of sulfuric acid, and stirred an additional 12 hours. Gel was detected by visual analysis in some samples and removed by filtering through a funnel packed with glass fibers. Measurements were obtained using a Cannon viscometer in a 25 °C controlled water bath. The viscometer was washed with sulfuric acid and a portion of the next sample to be tested before measurements were recorded. Flow times used for calculating specific and relative viscosities were averages of three testes within 0.2 seconds agreement. Single point intrinsic viscosities (IV) were determined using Solomon and Ciuta relationship:

$$[\eta] = [(2*(\eta_{sp} - \ln(\eta_{rel})]^{1/2})]/C$$

where, η_{sp} is specific viscosity, η_{rel} is relative viscosity, and C is concentration.[10]

Dynamic scanning calorimetry (DSC). Polymer melting temperatures were obtained using a TA Instruments 2920 DSC. Scans were taken at a heating rate of 10 ºC/min. Data were collected for the first and second heating scans. The first scan upper limit was approximately 10-20 °C above the melting temperature,

while the second scan's was 350 ℃. Samples were air cooled to room temperature between scans.

Wide-angle x-ray scattering (WAXD). WAXD measurements were performed on a Rigaku Ultima II x-ray diffractometer. Data was collected from 3-40º 2θ at a rate of 2 º/min. Melt pressed films were annealed at 200 ℃ for 12 hours prior to analysis.

Results and Discussion

High Resolution Nuclear Magnetic Resonance Spectroscopy

Solution-state ^{13}C NMR spectra for PA-12,T and PA-10,T homopolymers are shown in Figures 4.3 and 4.4. General peak assignments (Figure 4.3) for PA-12,T are as follows: carbonyl (1) – 170.8 ppm, substituted aromatic carbons (2) – 137.7 ppm, aromatic carbons (3) – 128.0 ppm, α-amide carbon (4) – 41.7 ppm, methylene carbons (5-9) – 30.0, 29.9, 29.7, 29.4, and 27.3 ppm. General peak assignments for PA-10,T (Figure 4.4) are as follows: carbonyl (1) – 170.8 ppm, substituted aromatic carbons (2) – 137.7 ppm, aromatic carbons (3) – 128.0 ppm, α-amide carbon (4) – 41.6 ppm, methylene carbons (5-8) – 29.8, 29.6, 29.4, and 27.2 ppm.

NMR analysis of PA-10,T-6,T and PA-12,T-6,T copolymers show characteristic homopolymer peaks as well as additional resonances for carbon atoms **1**, **2**, **3**, and **4**. Figure 4.5 shows expanded regions of NMR spectra exhibiting the additional resonances for carbon **2** (left spectra) and carbon **4** (right spectra) for PA-12,T-6,T copolymers at different comonomer concentrations. For the spectra on the right, the downfield peak corresponds to

PA-12,T segments, while the upfield peak corresponds to PA-6,T segments. Integrated areas of each peak match the comonomer feed ratios on a molar basis.

Spectra on the left hand side of Figure 4.5 show a single resonance for the substituted aromatic peak of PA-12,T and PA-6,T homopolymers. The peak for PA-12,T (137.74 ppm) is downfield of the peak for PA-6,T (137.62 ppm). Additionally, two unexpected peaks appear in the copolymer spectra.

To investigate the source of these peaks, a physical mixture containing 50 wt-% PA-12,T homopolymer and 50 wt-% PA-6,T homopolymer was prepared and analyzed under the same conditions. The NMR spectrum of the physical mixture is shown at the top of Figure 4.6. It contains only the two peaks (**a** and **b**) characteristic of the homopolymers.

Peak **a** is characteristic of a terephthalic acid monomer unit bonded through amide linkages to diaminododecane monomer units on both sides (a homo-linkage). Peak **b** is due to a terephthalic acid monomer unit bonded to diaminohexane monomer units on both sides (also a homo-linkage). Peaks **c** and **d**, represent a hetero-linkage whereby a terephthalic acid monomer unit is bonded to a diaminododecane monomer unit on one side and a diaminohexane monomer unit on the other. This concept is illustrated on the left hand side of Figure 4.6. Therefore, sequence information pertaining to the distribution of monomer units for these copolymers can be obtained by examining the relative intensities of peaks **a**, **b**, **c**, and **d**.

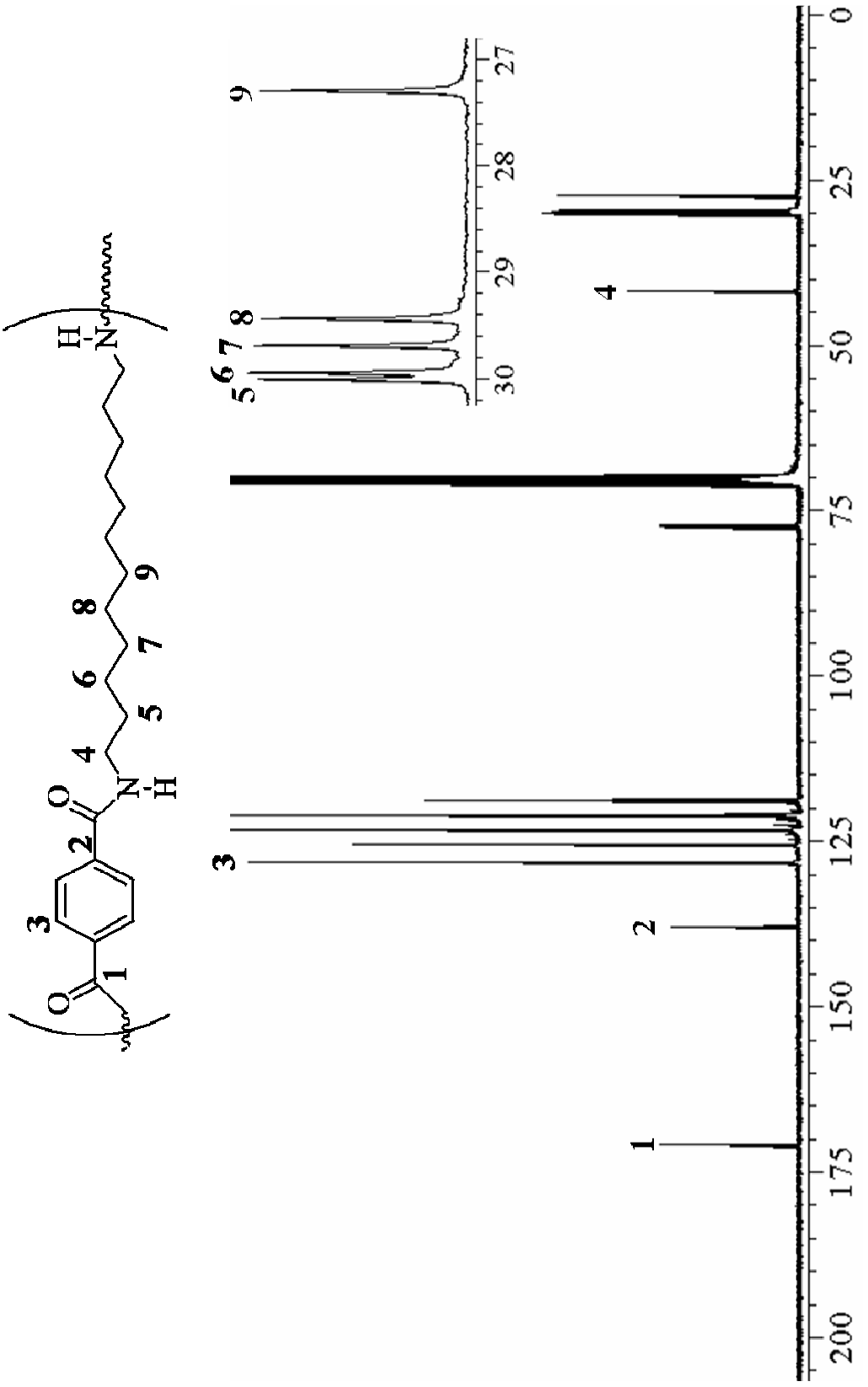

Figure 4.3. PA-12,T ^{13}C NMR spectra.

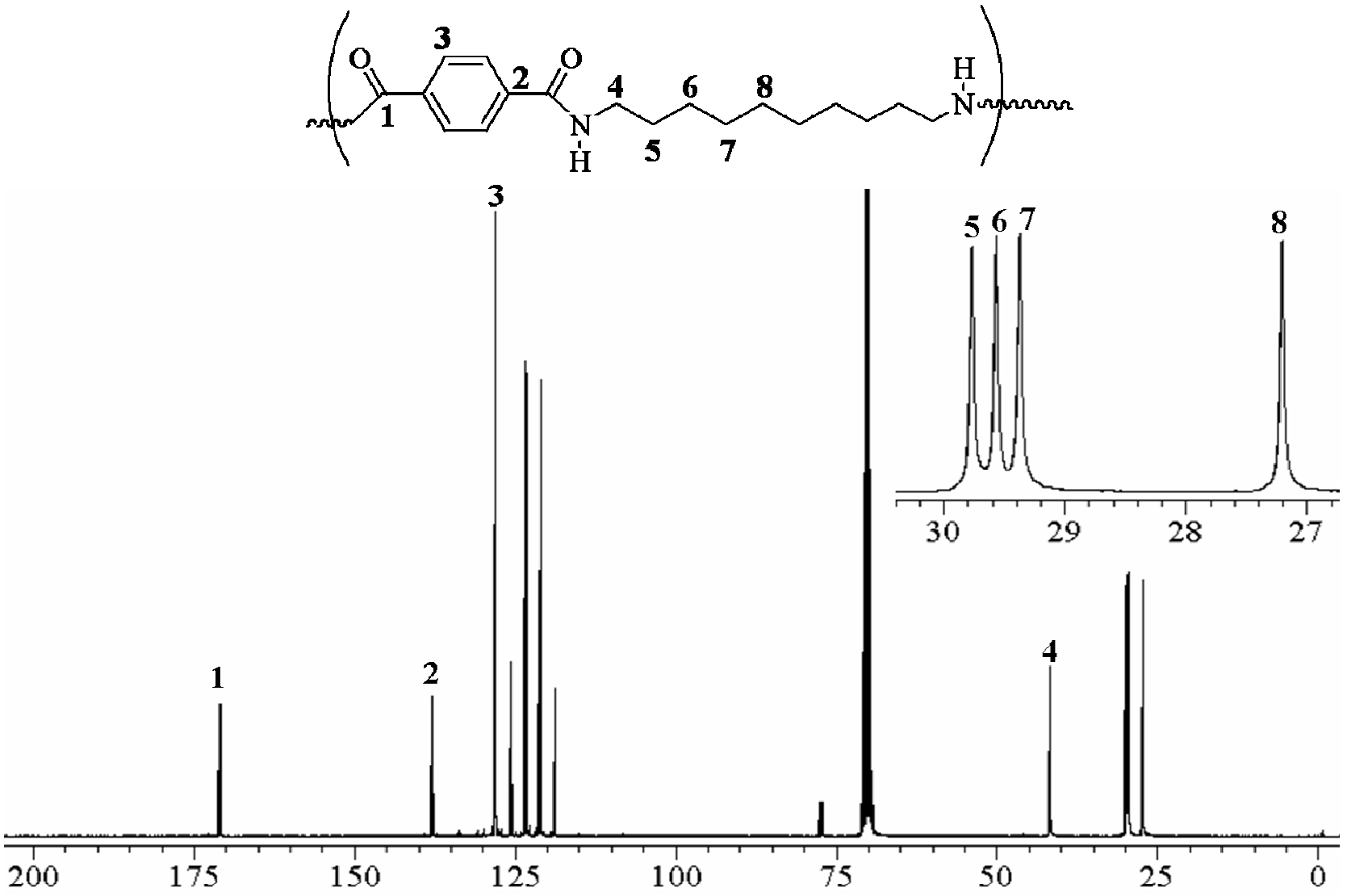

Figure 4.4. PA-10,T ^{13}C NMR spectra.

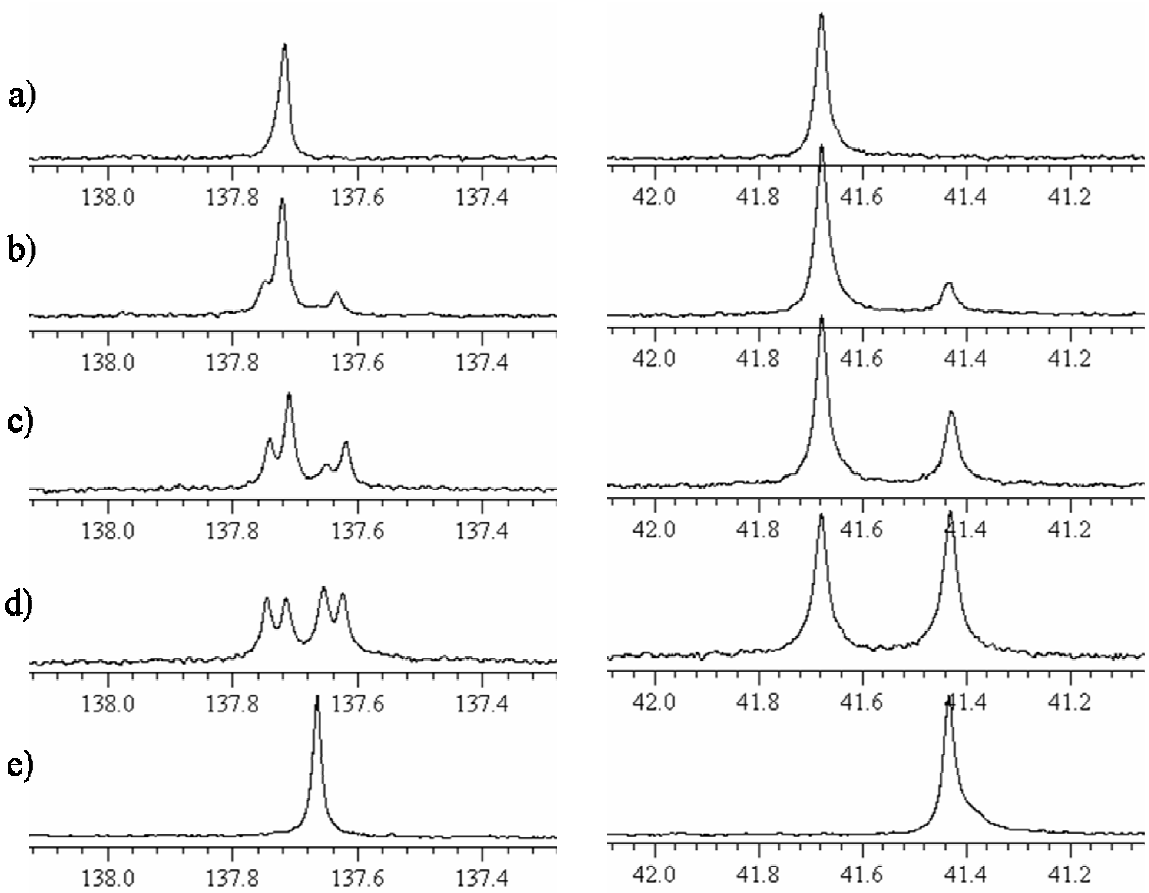

Figure 4.5. Expanded ^{13}C spectra of substituted aromatic and α-amide carbon of a) PA-12,T, b) 85:15 wt-% PA-12,T-6,T, c) 70:30 wt-% PA-12,T-6,T, d) 50:50 wt-% PA-12,T-6,T, and e) PA-6,T.

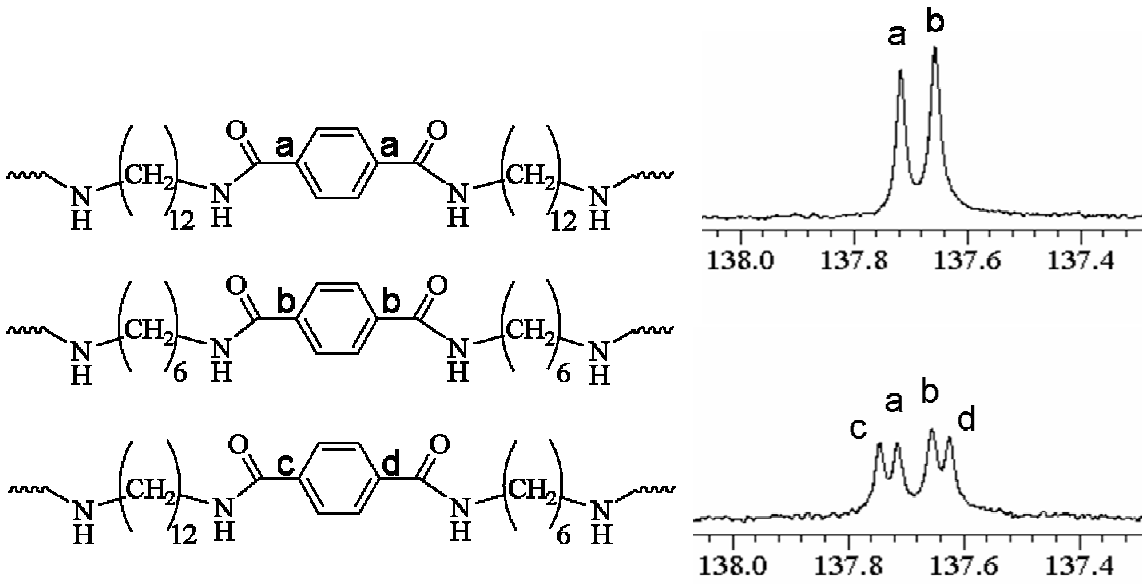

Figure 4.6. ^{13}C NMR peak assignments for substituted aromatic carbons. Top spectrum is of a physical mixture containing 50 wt-% PA-12,T homopolymer and 50 wt-% PA-6,T homopolymer. Bottom spectrum is of PA-12,T-6,T copolymer containing 50 wt-% PA-6,T comonomer.

As seen in Figure 4.6, at a concentration of 15 wt-% PA-6,T comonomer, 12,T-12,T homo-linkages (peak **a**) are dominant, while 6,T-6,T homo-linkages (peak **b**) are not observed. 12,T-6,T hetero-linkages (peaks **c** and **d**) are present at low concentrations. This indicates that individual PA-6,T comonomer units are isolated between longer PA-12,T comonomer segments. At a concentration of 30 wt-% PA-6,T comonomer, homo-linkages for 6,T-6,T segments are visible. At 50 wt-% PA-6,T, peaks **a**, **b**, **c**, and **d** are present in approximately equal proportions. This reveals that 12,T-12,T homo-linkages, 12,T-6,T hetero-linkages, and 6,T-6,T homo-linkages are present in a 1:2:1 ratio respectively. Therefore, this material is classified as a statistically distributed random copolymer.[11] If this material were a block copolymer, only peaks **a** and **b** would be present for all concentrations of comonomer. If this material were an

alternating copolymer, only peaks **c** and **d** would be present. This information is important for understanding crystalline behavior because it is influenced by the regularity of polymer structure.

Synthesis and Viscometry

Single point intrinsic viscosities were calculated for each sample. Number average molecular weights were estimated based on IV and Mark-Houwink constants developed for PA-12,T homopolymer in Chapter III: $K = 0.000558$ dL/g, $\alpha = 0.81$ (96% H_2SO_4, 25 °C). Results are summarized in Table 4.1.

Previous work has shown that diamine volatility can cause stoichiometric imbalances which affect molecular weight. For PA-12,T, it was observed that adding up to 3 mol-% excess diamine to the PA-12,T salt minimized end group concentration, balanced the concentration of acid and amine end groups, and maximized the molecular weight of the resulting polymer[12]. The excess diamine compensated for the diamine which volatilized during the reaction. Therefore, an excess of 3-mol% deca- or dodecamethylene diamine was added to each reaction mixture in the present work. One source of molecular weight variation in this system may be differences in volatility between hexa-, deca-, and dodecamethylene diamine.

Table 4.1. Intrinsic viscosities, estimated number average molecular weights, and 1st heating DSC melt temperatures of PA-10,T homopolymer, PA-12,T homopolymer, PA-10,T-6,T copolymer, and PA-12,T-6,T copolymer.

Feed Ratio (PA-n,T-6,T)	PA-10,T			PA-12,T		
	IV	M_n (g/mol)	T_m (°C)	IV	M_n (g/mol)	T_m (°C)
100:0	1.68	19700	327	1.14	12200	295
85:15	1.41	15900	316	1.21	13100	287
70:30	1.26	13800	283	1.24	13500	274
50:50	1.68	19700	324	2.17	27000	328

First heating DSC thermographs are presented in Figure 4.7. A comparison of first heating melting temperatures in Figure 4.7 with calculated molecular weights in Table 4.1 reveals a trend: all polymers with melting points below 315 °C had lower molecular weights than polymers with melting points above 315 °C. This could be attributed to annealing or solid-state polymerization. If this trend was caused by annealing it should not be reproducible on the second DSC heating scan. However Figure 4.8 shows that this trend is indeed reproducible.

At sufficiently high temperatures, polyamide end groups are reactive in both the solution and solid state. When heated to just below the melting temperature, the bulk of the chains are thermodynamically driven to crystallize. End groups do not participate in crystallization and thus will concentrate in the amorphous domain. Reaction of end groups to form higher molecular weight polymer is known as solid state polymerization[13] And explains the above mentioned trend observed in Table 4.1 and Figure 4.7.

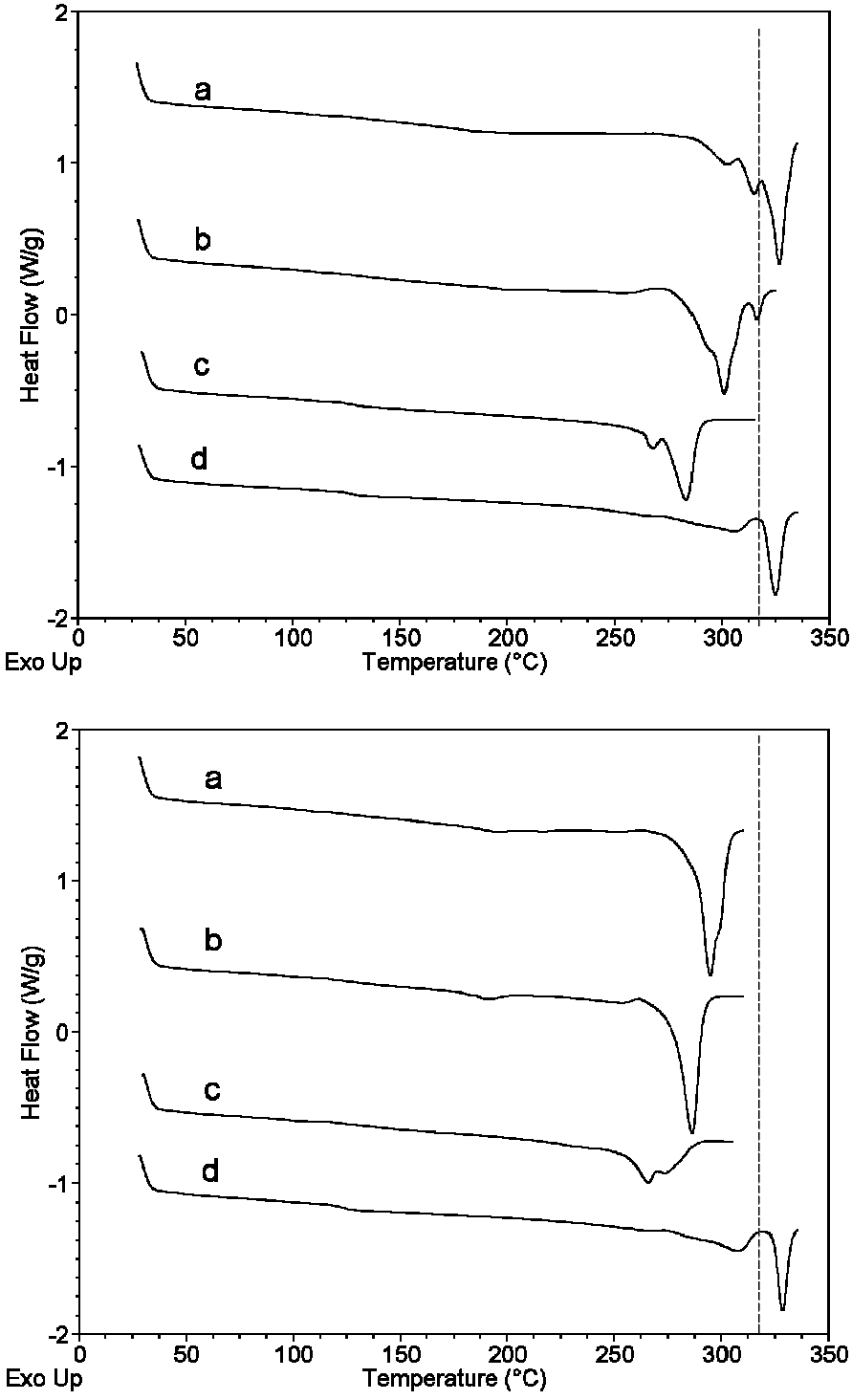

Figure 4.7. First heating DSC thermographs of PA-10,T (top) and PA-12,T (bottom) with (a) 0, (b) 15 wt-% (c) 30 wt-%, and (d) 50 wt-% PA-6,T (vertical line represents the maximum reaction temperature).

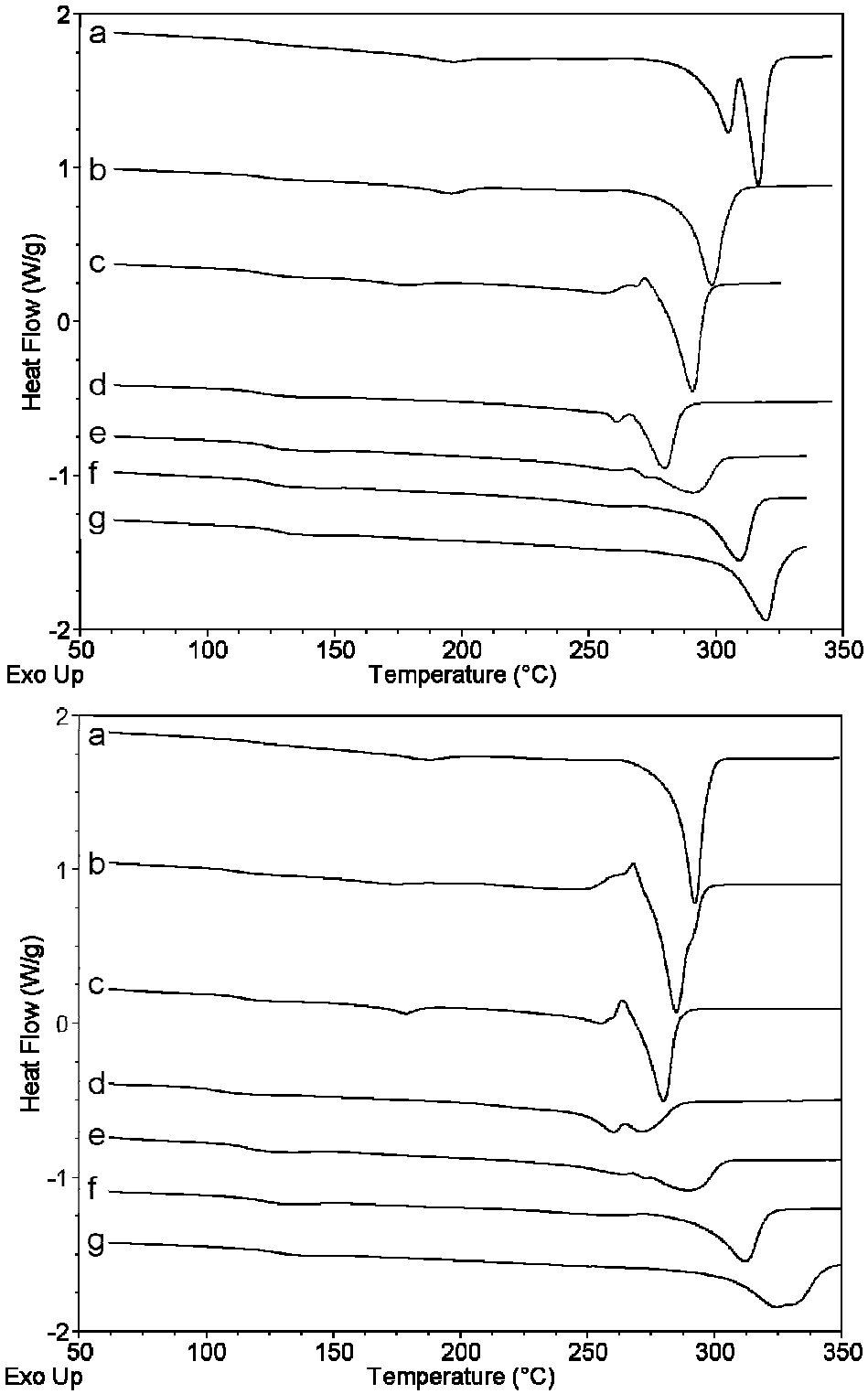

Figure 4.8. Second-heating DSC thermographs of PA-10,T (top) and PA- 12, T (bottom) containing 0 (a), 10 (b), 20 (c), 30 (d), 40 (e), 50 (f), and 60 (g) wt-% PA 6,T.

Thermal Characterization

Second heating melting temperatures and melting enthalpies of the copolymers are sensitive to comonomer content as seen in Figure 4.9. PA-10,T and PA-12,T homopolymers have melting temperatures of 315 and 292 °C, respectively. Copolymers initially show a linear decrease in melting temperature with increasing PA-6,T comonomer content. The lowest observed melting temperatures are 280 and 272 °C for PA-10,T, 6,T and 12,T, 6,T respectively. This eutectic point occurs at a concentration of 30 wt-% PA-6,T. Similarly, melting enthalpies of both sets of copolymers show a linear decrease with increasing PA-6,T comonomer. Melting enthalpies decrease from 70 to 24 J/g for PA-10,T-6,T and from 60 to 26 J/g for PA-12,T-6,T. Melting endotherms were also observed to broaden near the eutectic point. As the concentration of PA-6,T comonomer increased above 30 wt-%, melting temperatures and enthalpies increase for both copolymers. At 60 wt-% PA-6,T, melting temperatures were 320 °C for PA-10,T-6,T and 325 °C for PA-12,T-6,T. The crystalline melting temperature of high molecular weight PA-6,T homopolymer was 372 °C.

If co-crystallization had occurred between PA-6,T and the other comonomers, completely different behavior would have been observed in Figure 4.9. As PA-6,T comonomer concentration increased for PA-10,T-6,T, melting temperature would have increased in a linear manner from 315 to 372 °C. For PA-12,T-6,T melting temperature would have increased linearly from 292 to 372 °C. Instead, the observed eutectic behavior is strong evidence against isomorphism for these copolymers.

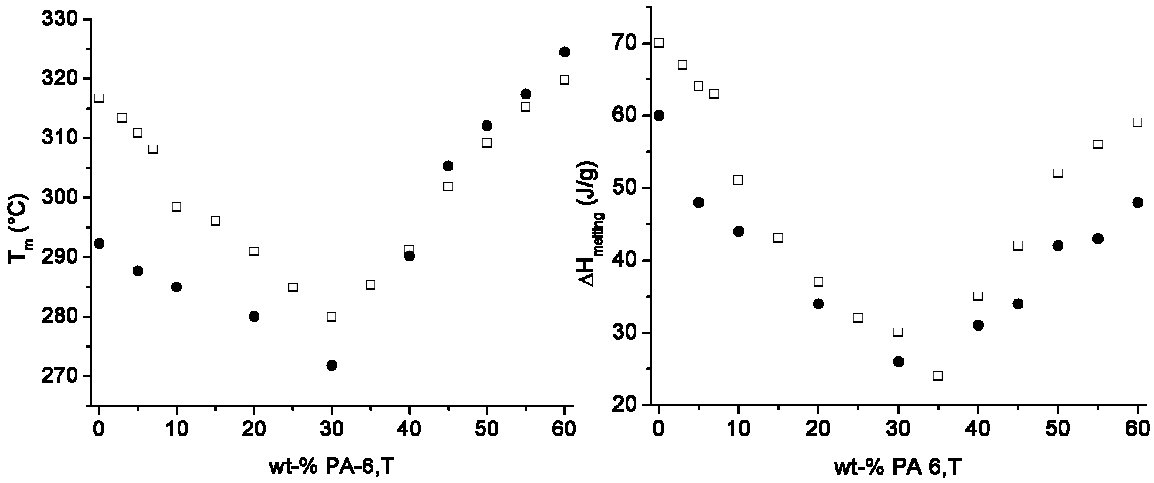

Figure 4.9. Second-heating DSC melting temperatures (left) and melting enthalpies (right) of PA-10,T-6,T copolymer (□) and PA-12,T-6,T copolymer (●) versus wt-% PA-6,T comonomer.

Melt Pressed Films

All polymers and copolymers were melt pressed, and resulting films were mechanically tough. Compared to the other samples, PA-12,T-6,T containing 50 wt-% PA-6,T, required higher pressure and temperature to melt press. Compression molded films at the eutectic concentration of 30 wt-% PA-6,T were the most transparent. Figure 4.10 illustrates this increased transparency compared to a film prepared from PA-12,T homopolymer.

Figure 4.10. Melt pressed films of PA-12,T homopolymer (left) and PA-12,T-6,T copolymer containing 30 wt-% PA-6,T comonomer (right).

WAXD Analysis

WAXD data were acquired for melt pressed films. Analyses of PA-10,T homopolymer, PA-6,T homopolymer, and PA-10,T-6,T copolymers are shown in Figure 4.11. Sharp peaks in the diffraction pattern of PA-10,T homopolymer represent crystalline domains. As PA-6,T comonomer content increased from 0-20 wt-%, the sharp diffraction peaks of PA-10,T broadened and decreased in intensity. At 25-45 wt-% PA-6,T, a broad amorphous halo dominated each spectrum. The eutectic point observed by DSC occurred in this range. WAXD data showed no indication of isomorphism between these different comonomers. As PA-6,T comonomer content increased from 50-60 wt-%, sharp diffraction peaks emerged with increasing intensity. Peak locations were consistent with crystalline domains of PA-6,T homopolymer. In summary, as PA-6,T concentration increased, WAXD patterns showed a gradual transition from characteristic PA-10,T peaks, to a broad amorphous halo, to characteristic PA-6,T peaks. This supports the argument that comonomers in this system form

independent crystalline domains and do not co-crystallize. WAXD trends of PA-12,T-6,T copolymers (not shown) display similar behavior.

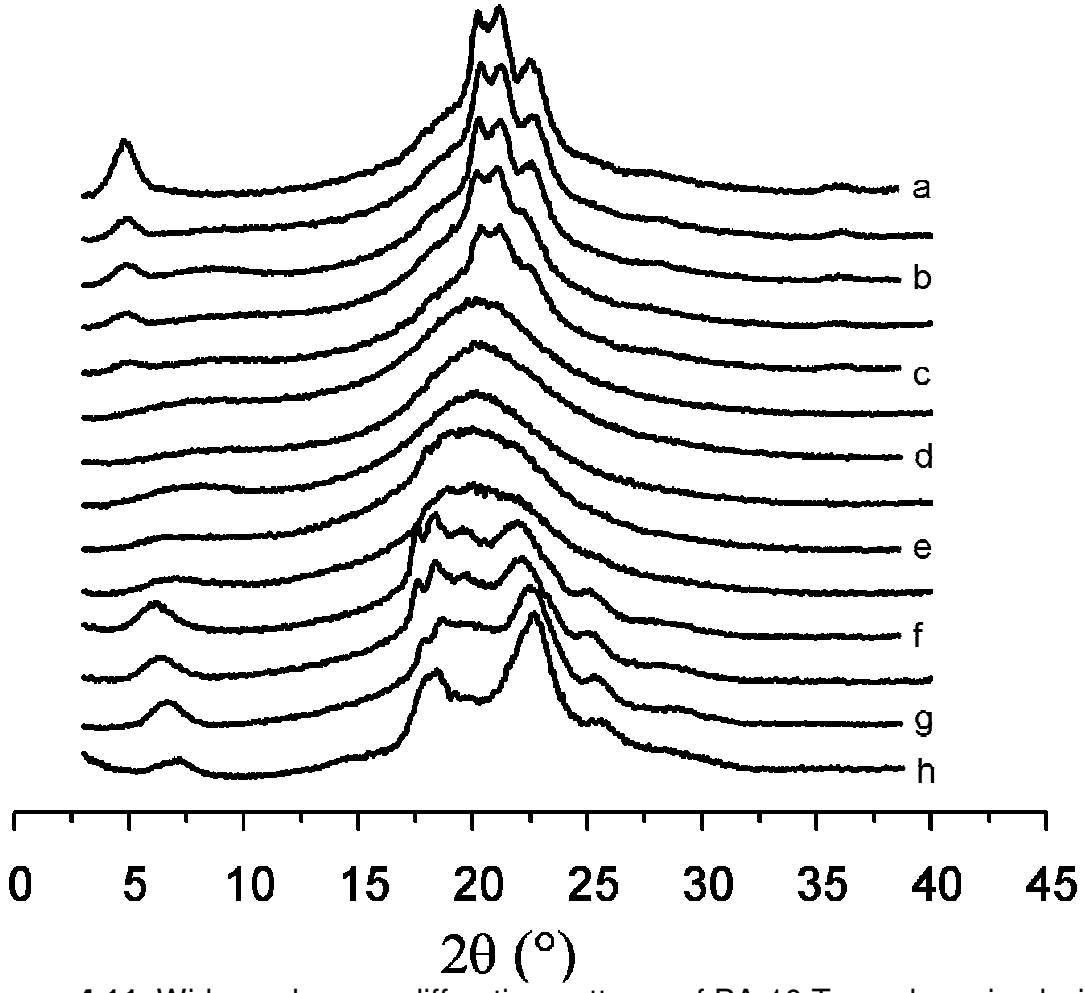

Figure 4.11. Wide angle x-ray diffraction patterns of PA-10,T copolymerized with PA-6,T at 5 wt-% increments. Labeled spectra are of PA-10,T homopolymer (a), PA-10,T-6,T copolymer containing 10 wt-% (b), 20 wt-% (c), 30 wt-% (d), 40 wt-% (e), 50 wt-% (f), and 60 wt-% (g) PA-6,T, and PA-6,T homopolymer (h).

Eutectic Behavior

Crystallization behavior of (co)polyamides is strongly influenced by the orientation of and the distance between amide groups. For example, the amide groups of PA-6,6-6,T comonomers have similar orientations and inter-distances,

allowing them to co-crystallize into isomorphic structures. Consequently, melting temperature increases linearly as a function of PA-6,T comonomer content as shown in Figure 4.12. The distance between amide bonds in comonomers of PA-4,T-6,T, PA-10,T-6,T, and PA-12,T-6,T are different enough to prevent isomorphism. Therefore, moderate melting temperature depressions are observed. At 34 mol-% PA-6,T comonomer content, the melting temperature of PA-12,T-6,T copolymer is depressed 20 °C relative to PA-12,T homopolymer. At 37 mol-% PA-6,T, a depression of 35 °C is observed in PA-10,T-6,T relative to PA-10,T.

For PA-6-6,T, the eutectic melting temperature is severely depressed relative to constituent homopolymers. The melting temperature of PA-6-6,T containing 16 mol-% PA-6,T is 88 °C less than the melting temperature of PA-6 homopolymer. Such pronounced eutectic behavior is caused by inherent differences in the orientation of amide bonds for each comonomer. PA-6 segments are composed of A-B-A-B monomer linkages, while PA-6,6 segments are composed of A-A-B-B monomer linkages. Although the distance between amide bonds is similar, differences in orientation exclude the possibility for isomorphism.

Differences in amide orientation are even more explicit when comparing terephthalic diacid with isophthalic diacid. Whereas repeat units containing terephthalic units can be considered linear, isophthalic units “kink” the polymer backbone. This causes PA-6,I homopolymer to be completely amorphous and PA-6,I-6,T copolymer to be amorphous up to approximately 40 mol-% PA-6,T.

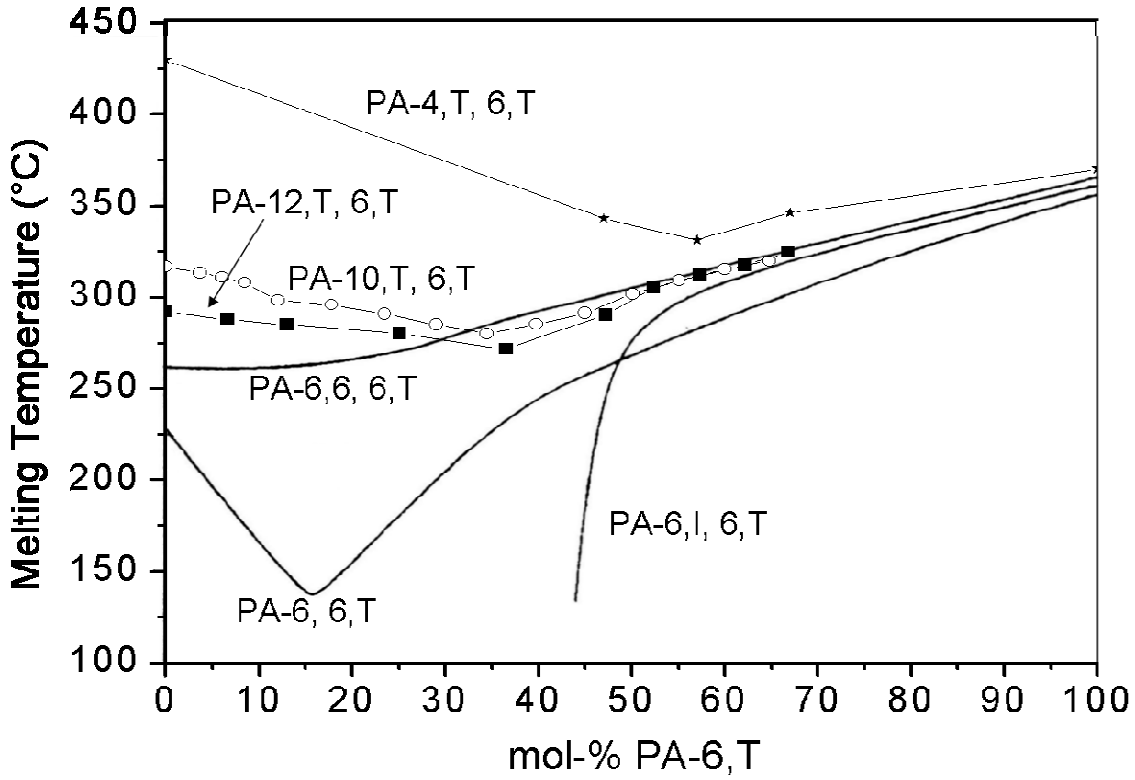

Figure 4.12. PA-10,T-6,T and PA12,T-6T melting behavior compared with other copolymers.

Melt pressed film transparency, NMR, DSC, and WAXD analysis are consistent with the PA-6,T monomer units not co-crystallizing with PA-10,T or PA-12,T monomer units and thus not forming isomorphic structures. Differences in length prevent different comonomer units from sharing a crystal lattice. Similarities in comonomer amide orientations result in a relatively moderate eutectic depression of 20-35 °C.

At 0 wt-% PA-6,T, the number of consecutive PA-10,T or PA-12,T homo-linkages is equal to the degree of polymerization, and ordered PA-10,T or PA-12,T homo-segments are the only possible crystal forms. As PA-6,T concentration increases up to 30 wt-%, ordered PA-10,T or PA-12,T domains remain the dominant crystal form. However, the length of PA-10,T or PA-12,T

homo-segments decreases, thereby lowering the melt temperatures. In this region, many of the statistically distributed PA-6,T homo-segments are not long enough to crystallize. This decreases copolymer melting enthalpy by diluting the segments capable of crystallization on a weight basis. PA-6,T units may also be considered as impurities which diminish the maximum attainable degree of order.

For copolymers with concentrations of PA-6,T greater than 30 wt-%, ordered PA-6,T homo-segments are the dominant crystal form. In this region, copolymer melting temperatures are approximately equal. This implies that the average length of PA-6,T homo-sequences that participate in crystallization are equal for both copolymers. Distribution of comonomer units in PA-10,T-6,T and PA-12,T-6,T copolymers appear to be similar. However, the lower melting enthalpy of PA-12,T-6,T indicates that the quantity of PA-6,T homo-segments which participate in crystallization is less for PA-12,T-6,T. This difference in enthalpy is amplified when considering the concentration of PA-6,T copolymer on a molar basis. Therefore, compared to PA-10,T comonomer, PA-12,T comonomer has a greater effect on disrupting the crystallization of PA-6,T homo-segments.

Conclusions

PA-10,T-6,T and PA-12,T-6,T copolymers have been synthesized by melt condensation polymerization. High resolution ^{13}C solution-state NMR analysis revealed that substituted phenyl carbons are sensitive to comonomer connectivity. NMR spectra showed that comonomer sequences were distributed statistically to give random copolymers. Melt pressed film behavior, NMR, DSC,

and WAXD analysis agree that PA-6,T monomer units do not co-crystallize with PA-10,T or PA-12,T monomer units, and do not form isomorphic structures in the copolymers studied. Instead, a eutectic melting point at 30 wt-% PA-6,T is observed for both copolymers. Ordered PA-6,T homo-segments were the major crystalline form above the eutectic point, while the ordered homo-segments of the other comonomer were the major crystalline form below the eutectic point. Compared to PA-10,T comonomer, PA-12,T comonomer has a greater effect on disrupting the crystallization of PA-6,T homo-segments above the eutectic point. Melt pressed films of copolymers show the highest optical clarity at the eutectic point. Comonomer concentrations are shown to predictably impact melting temperature, degree of crystallinity, and optical clarity.

Acknowledgments

Theodore Novitsky synthesized all materials and conducted IV, DSC, and WAXD analysis for this study. Dr. Scott Osborne, Dr. Steven Manning, Dr. Roger Ayotte and Solutia Nylon Plastics and Fiber division provided funding, access to their facilities, starting materials, and expertise throughout this project.

References

[1] Kohan, M.I. *Nylon Plastics Handboook*. 1995 Carl Hanser Verlag, Munich Vienna NewYork. Pages 372-374 and 594-599.

[2] Shashoua, V.E.; Eareckson, W.M. *J. Poly. Sci*., **1959**, 40, 343-358.

[3] Morgan, P. W.; Kwolek, S. L. *Macromolecules*. **1975**, 8, 2, 104-111.

[4] Kaitian X.; Jarrett, W.; Mathias L. J. *Polymer Preprints* **2005**, 46, 1, 789.

[5] Edgar, O. B.; Hill R. *J. Polymer Sci.* **1952**, 8, 1.

[6] Yu, A.J.; Evans, R.D. *J. Poly Sci.* **1960**, 42, 249-257.

[7] Harveym E. D.; Hybart, F. J. *Polymer* **1971**, 12, 711-716.

[8] Liu, H.; Yang, G.; He, A.; Wu, M. *J. Apl. Poly Sci*. **2004**, 94, 819–826.

[9] Rulkens, R.; Crombach R.C.B. (DSM). U.S. Patent 6,747,120, June 8, **2004**.

[10] Solomon, O. F.; Ciuta, I.Z. *J. Appl. Polym. Sci*. **1962**, 6, 683.

[11] Aerdts, A. M.;. Eersels, K. L. L; Groeninckx, G. *Macromolecules.* **1996**, *29,* 1041-1045.

[12] Novitsky, T.; Lange, C. A.; Mathias, L.J.; Osborn, S.; Manning, S.; Ayotte, R. *J. Apl. Poly. Sci.* **2009**, Article in Press.

[13] Vouyiouka, S.N.; Karakatsani, E.K.; Papaspyrides, C.D. *Prog. Polym. Sci.* **2005**, 30, 10–37.

CHAPTER V

THERMALLY RESPONSIVE SUPRAMOLECULAR ASSEMBLIES OF LOW MOLECULAR WEIGHT BISCAPROLACTAM DERIVATIVES AND STEREOISOMERS

Abstract

A new family of hydrogen-bonded supramolecular polymers based on biscaprolactams was synthesized. DSC and solid-state NMR spectroscopy were used to characterize these materials. Properties were investigated with regard to distance between caprolactam units, amide versus urea linkages, enantiomeric identity of caprolactam, and sample preparation. Different bislactams were blended to form supramolecular copolymers. Urea linkages and copolymers showed glassy polymeric behavior.

Introduction

The defining characteristic of supramolecular polymers is that monomer connectivity arises through non-covalent interactions such as hydrogen-bonding, electrostatic forces, or metal/ion coordination. Supramolecular assemblies with adequate interactions have been demonstrated to exhibit glass transition temperatures, viscoelasticity, and mechanical properties sufficient to draw fibers.[1] In 1997, Meijer et al. described a supramolecular assembly which formed highly viscous dilute solutions.[2] Bouteiller et al. mixed bisphenol A with tetrapyridine at a 2:1 molar ratio to yield a stable glassy material with a T_g of 31 °C.[3] Supramolecular polymers consisting of a tetraphenylmethyl core grafted with alkyl functional triaminotriazine groups exhibited T_gs which varied according to

alkyl chain length.[4] Low molecular weight nucleoside and alkylsilylyated guanosine derivatives have been shown to form fibers by melt spinning.[5,6]

Hydrogen-bonding groups have also been incorporated on the chain ends of low molecular weight oligomers in order to prepare thermo-reversible networks. Liquid siloxane oligomers have displayed rubbery behavior when end-functionalized with ureidopyrimidinone.[7] This approach has been extended to telechelic poly(ethylene/butylene), polyether, polyester and polycarbonate oligomers.[8]

Reversibility of supramolecular interactions offers potential for designing materials with improved processability, stimuli responsiveness, and self healing capabilities.[9,10] Thermal, mechanical, and electrical properties, for example, can be drastically altered in supramolecular polymers by external stimuli that change the nature of the interactions. Temperature is a simple external stimulus which can "trigger" changes in hydrogen-bonded systems. Hydrogen bonding between phenyl-urazole end groups were used in the thermo-reversible chain extension of telechelic polyisobuylenes[11] and crosslinking of polybutadienes.[12] Other examples of supramolecular polymers and their properties can be found in the recent literature.[13-17]

One challenge in developing applications for supramolecular polymers is finding monomers that are inexpensive and commercially available or that can be easily synthesized on a large scale.[18] The present work reports supramolecular polymers prepared via a one-step, high-yield synthesis using

α-amino-ε-caprolactam, a renewable resource which can be synthesized by closure of ε-lysine.

Experimental

Materials

A mixture of D-α-amino-ε-caprolactam and L-α-amino-ε-caprolactam was purchased from TCI Chemical Company (>97%). L-α-amino-ε-caprolactam, succinoyl chloride, adipoyl chloride, azeloyl chloride, hexamethylene diisocyanate, thionyl chloride and triethyl amine were purchased from Aldrich Chemical Company. Octadecanedioic acid (C18 diacid) was donated by Cognis. All solvents were purchased from Fischer Scientific.

Synthesis of C18 Diacid Chloride

The C18 diacid chloride was synthesized from the reaction of C18 diacid (0.02 mol) and thionyl chloride (0.10 mol) with a drop of DMF (N,N-dimethylformamide). The reaction mixture was allowed to reflux for 3 h with excess thionyl chloride removed by vacuum distillation. Essentially 100% conversion of acid to acid chloride was obtained based on the purity of the crude product as determined by ^{13}C NMR spectroscopy in $CDCl_3$ solution.

Synthesis of Biscaprolactams

Chloroform was used as a reaction solvent except for the synthesis of C18-biscaprolactam (DL-C18ABC), which used *N*-methyl pyrolidone. In a typical experiment, a solution of DL-α-amino-ε-caprolactam (0.02 mol) and triethylamine (0.022 mol) in 50 ml $CHCl_3$ was placed into an ice bath. Acid chloride (0.01 mol) was added drop-wise under nitrogen purge. The ice bath was removed and

purging with N_2 stopped after 15 min. The reaction was allowed to proceed overnight. A solid product precipitated from the reaction mixture and was filtered and washed with $CHCl_3$. After drying, the product was dispersed in 50 ml of a CH_3OH:H_2O (4:1) mixture, stirred for 30 min, filtered and dried under vacuum overnight. Reaction yields were 90-95%. As-synthesized materials were in the form of fine powders or flakes.

Synthesis of Enantiomerically Pure Biscaprolactams

Synthesis was performed under Schotten-Baumann conditions. In a typical experiment, L-α-amino-ε-caprolactam hydrochloride (0.01 mol) was dissolved in 10 ml H_2O and 5 ml 4N NaOH (aq) was added. The diacid chloride (0.005 mol) was dissolved in 15 ml $CHCl_3$ and added into the aqueous solution with vigorous stirring. The product precipitated from the reaction mixture, and was filtered and washed with water. After drying, the product was dispersed in a methanol:water (80:20) mixture, stirred 30 min, filtered, and dried under vacuum overnight.

The numbers and letters in the abbreviations indicate the number of carbon atoms in the spacer (diacid or diisocyanate) and the type of linkage between the spacer and the end groups. For example: DL-C6ABC was synthesized using a mixture of D- and L-α-amino-ε-caprolactam, “C6” signifies six carbon atoms in the di-acid chloride, “A” refers to the amide linkage, and “BC” refers to biscaprolactam. L-C6ABC was synthesized using enantiomerically pure L-α-amino-ε-caprolactam. For DL-C6UBC, “U” refers to the urea linkage formed between hexamethylene diisocyanate and DL-α-amino-ε-caprolactam.

Differential Scanning Calorimetry (DSC)

DSC data were obtained using a TA Instruments DSC 2920, a heating rate of 10 ºC/min, and a nitrogen purge. Data were collected for up to six heating scans. Samples were cooled to room temperature between scans via air cooling or controlled cooling at 10 ºC/min using liquid nitrogen. Additional experimental details are provided in the Results and Discussion section.

NMR Spectroscopy

Proton and ^{13}C solution spectra were obtained on Varian 300 spectrometer using TFE:$CDCl_3$ (70:30; v:v) solvent mixture. **DL-C4ABC:** ^{1}H NMR (300 MHz, TFE:$CDCl_3$) δ 7.3 (O=C-N<u>H</u>-CH-,1H), 6.7 (O=C-N<u>H</u>-CH_2,1H), 4.5 (-NH-C<u>H</u>-,1H), 3.2 (-NH-C<u>H_2</u>,2H), 2.5 (O=C-C<u>H_2</u>-,4H), 1.8 (>CH-C<u>H_2</u>-,2H), 1.4 (>CH-CH_2-C<u>H_2</u>-C<u>H_2</u>-CH_2-NH-,4H) ^{13}C NMR (75 MHz, TFE:$CDCl_3$) δ 176.5, 172.4, 52.3, 41.9, 30.9 (2C), 27.9, 27.5 ppm. **DL-C6ABC**: ^{1}H NMR (300 MHz, TFE:$CDCl_3$) δ 7.1 (O=C-N<u>H</u>-CH-,1H), 6.7 (O=C-N<u>H</u>-CH_2,1H), 4.5 (-NH-C<u>H</u>-,1H), 3.2 (-NH-C<u>H_2</u>,2H), 2.2 (O=C-C<u>H_2</u>-,4H), 1.8 (>CH-C<u>H_2</u>-,2H), 1.6 (-C<u>H_2</u>-CH_2-C=O, 4H), 1.4 (>CH-CH_2-C<u>H_2</u>-C<u>H_2</u>-CH_2-NH-,4H) ^{13}C NMR (75 MHz, TFE:$CDCl_3$) δ 176.7, 173.9, 52.2, 41.9, 35.7, 31.0, 27.9, 27.5, 24.8 ppm. **DL-C9ABC:** ^{1}H NMR (300 MHz, TFE:$CDCl_3$) δ 7.1 (O=C-N<u>H</u>-CH-,1H), 6.7 (O=C-N<u>H</u>-CH_2,1H), 4.5 (-NH-C<u>H</u>-,1H), 3.2 (-NH-C<u>H_2</u>,2H), 2.2 (O=C-C<u>H_2</u>-,4H), 1.9 (>CH-C<u>H_2</u>-,2H), 1.7 (>CH-CH_2-C<u>H_2</u>-C<u>H_2</u>-CH_2-NH-,4H), 1.5 (-C<u>H_2</u>-CH_2-C=O, 4H), 1.2 (-C<u>H_2</u>-CH_2-CH_2-C=O, 8H) ^{13}C NMR (75 MHz, TFE:$CDCl_3$) δ 176.6 174.5, 52.1, 41.9, 36.2, 31.0, 28.7 (2C), 27.9, 27.5, 25.4 ppm. **DL-C18ABC:** ^{1}H NMR (300 MHz, TFE:$CDCl_3$) δ 7.1 (O=C-N<u>H</u>-CH-,1H), 6.7 (O=C-N<u>H</u>-CH_2,1H), 4.5 (-NH-C<u>H</u>-,1H), 3.2 (-NH-

C$\underline{H}_2$,2H), 2.2 (O=C-C$\underline{H}_2$-,4H), 1.9 (>CH-C$\underline{H}_2$-,2H), 1.7 (>CH-CH$_2$-C$\underline{H}_2$-C$\underline{H}_2$-CH$_2$-NH-,4H), 1.5 (-C$\underline{H}_2$-CH$_2$-C=O, 4H), 1.2 (-C$\underline{H}_2$-CH$_2$-CH$_2$-C=O, 24H) ^{13}C NMR (75 MHz, TFE:$CDCl_3$) δ 176.6, 174.5, 52.2, 42.0, 36.4, 31.1, 29.6, 29.5, 29.4, 29.2, 29.0, 27.9, 27.5, 25.6 ppm. **DL-C6UBC:** ^{1}H NMR (300 MHz, TFE:$CDCl_3$) δ 6.7 (O=C-N$\underline{H}$-CH-,1H), 5.9 (-N$\underline{H}$-O=C-N$\underline{H}$-,2H), 4.4 (-NH-C$\underline{H}$-,1H), 3.2 (-NH-C$\underline{H}_2$,2H), 3.0 (-C$\underline{H}_2$-NH-C=O-NH-,2H), 2.2 (O=C-C$\underline{H}_2$-,4H), 1.8 (>CH-C$\underline{H}_2$-,2H), 1.7 (>CH-CH$_2$-C$\underline{H}_2$-C$\underline{H}_2$-CH$_2$-NH-,4H), 1.4 (-C$\underline{H}_2$-CH$_2$-NH-C=O-NH-,2H), 1.2 (-C$\underline{H}_2$-CH$_2$-CH$_2$-NH-C=O-NH-,2H) ^{13}C NMR (75 MHz, TFE:$CDCl_3$) δ 177.9, 158.8, 52.8, 41.9, 40.2, 31.9, 29.4, 27.9, 27.5, 26.1 ppm.

Solid-state NMR spectroscopy was performed on a Varian ^{UNITY}INOVA 400 spectrometer using a standard Chemagnetics 7.5 mm PENCIL™-style probe. Samples were loaded into zirconia rotor sleeves, sealed with Teflon™ caps, and spun at a rate of 4.0 kHz. The standard cross-polarization/magic angle spinning (CPMAS) technique[19] was used with high-power proton decoupling implemented during data acquisition. The acquisition parameters were as follows: the ^{1}H 90° pulse width was 5.5 μs, the cross-polarization contact time was 1 ms, the dead time delay was 5.2 μs, and the acquisition time was 45 ms. A recycle delay of 3 seconds between scans was utilized, and a ^{1}H decoupling field of 65 kHz was implemented during acquisition.

Bloch decay spectra were acquired using a modified version of the DEPTH sequence[20] to suppress background signals due to the probe. The acquisition parameters were as follows: The ^{13}C pulse width was 5.5 μs, the

dead time delay was 6.4 μs, and the acquisition time was 45 ms. A recycle delay of 60-100 seconds between scans was utilized.

For variable temperature (VT) analysis, samples were heated to the specified temperature using the standard Chemagnetics apparatus, whereby heated VT gas is directed onto the spinning rotor. Each sample was tuned at temperature prior to analysis.

The number of accumulated transients ranged from 512 to 2048 for CPMAS spectra and 128 to 512 for DEPTH spectra involving 1-24 hour collection times. Data was zero-filled up to 128k points and an exponential broadening of 11 Hz applied prior to application of Fourier transformation. Baselines were corrected when necessary using a 10^{th} order polynomial.

Thermogravimetric Analysis (TGA)

TGA were performed on a TA instruments SDT 2960 TGA-DTA at 10 °C/min under nitrogen from ambient temperature to 700 °C.

Wide Angle X-ray Diffraction (WAXD)

WAXD patterns were obtained using a Rigaku Ultima III X-ray diffractometer with Ni-filtered CuKα radiation (wavelength λ= 1.54 Å) operating at 40 kV and 44 mA. WAXD data were recorded between 2 and 90° at a rate of 2°/min.

Fiber Drawing

Approximately 0.25 grams of as-synthesized material was inserted into a test tube and heated in an oil bath preset to 300 °C. Upon melting, material was a low viscosity liquid. The test tube was removed from the oil bath and partially

submerged in water. A spatula was repeatedly dipped into and removed from the liquid until a fiber formed.

Results and Discussion

Succinic acid chloride (C4ABC), adipic acid chloride (C6ABC), azelaic acid chloride (C9ABC) and octadecanedioic acid chloride (C18ABC) were reacted with α-amino-ε-caprolactam to form biscaprolactams of varying length (Figure 5.1). The L-C6ABC and L-C9ABC materials were synthesized using enantiomerically pure L-α-amino-ε-caprolactam to investigate the effects of stereo configuration and diastereomeric mixtures on properties. Hexamethylene diisocyanate was reacted with DL-α-amino-ε-caprolactam (DL-C6UBC) to form a bisurea analog for comparing effects of urea and amide linkages. Solution ^{1}H and ^{13}C NMR analysis verified structural composition and purity of all samples as seen in Figures 5.2-5.7.

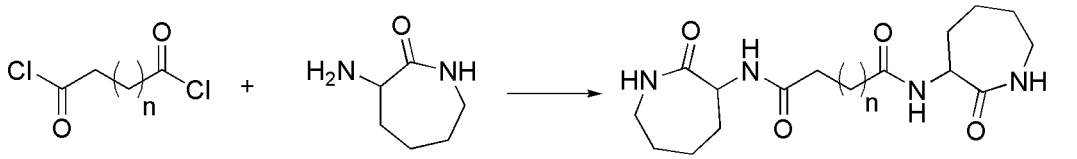

Figure 5.1. Synthesis of biscaprolactams.

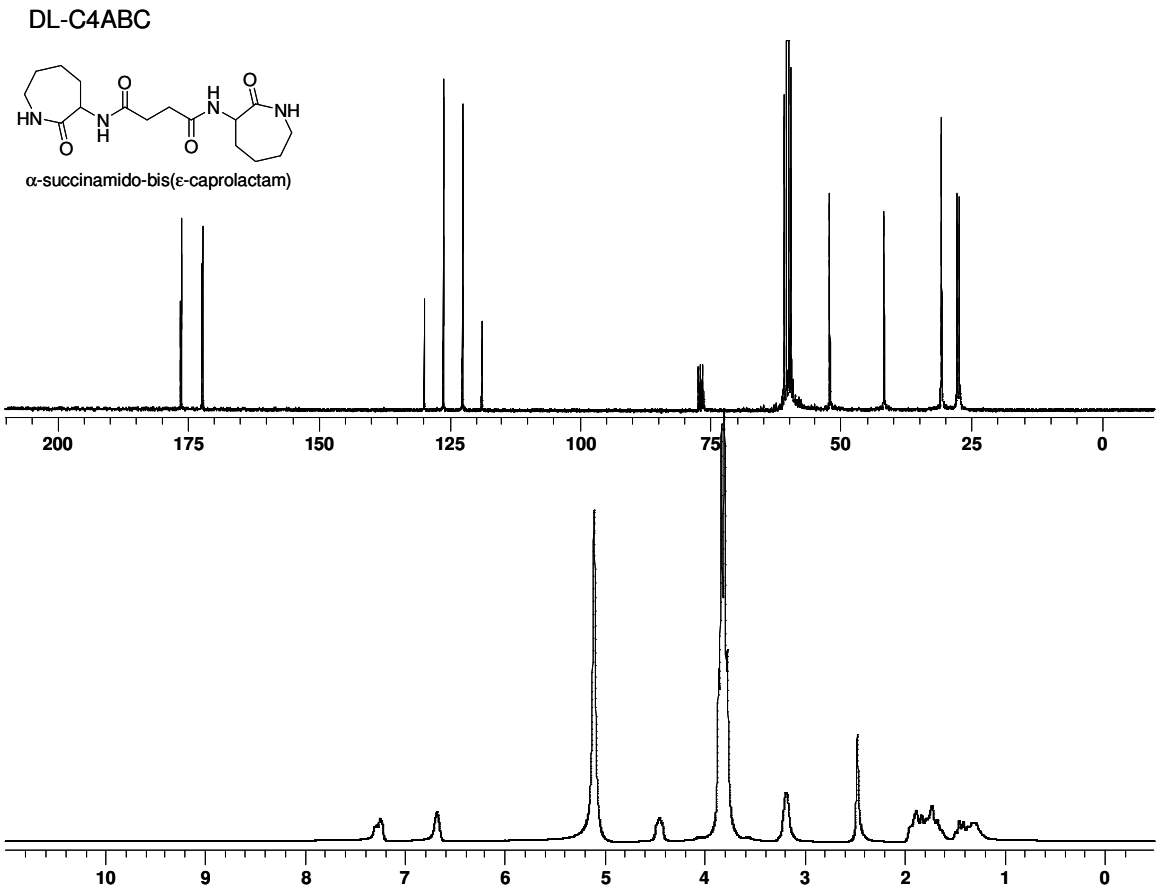

Figure 5.2. Solution-state ^{13}C (top) and ^{1}H (bottom) NMR spectra of DL-C4ABC.

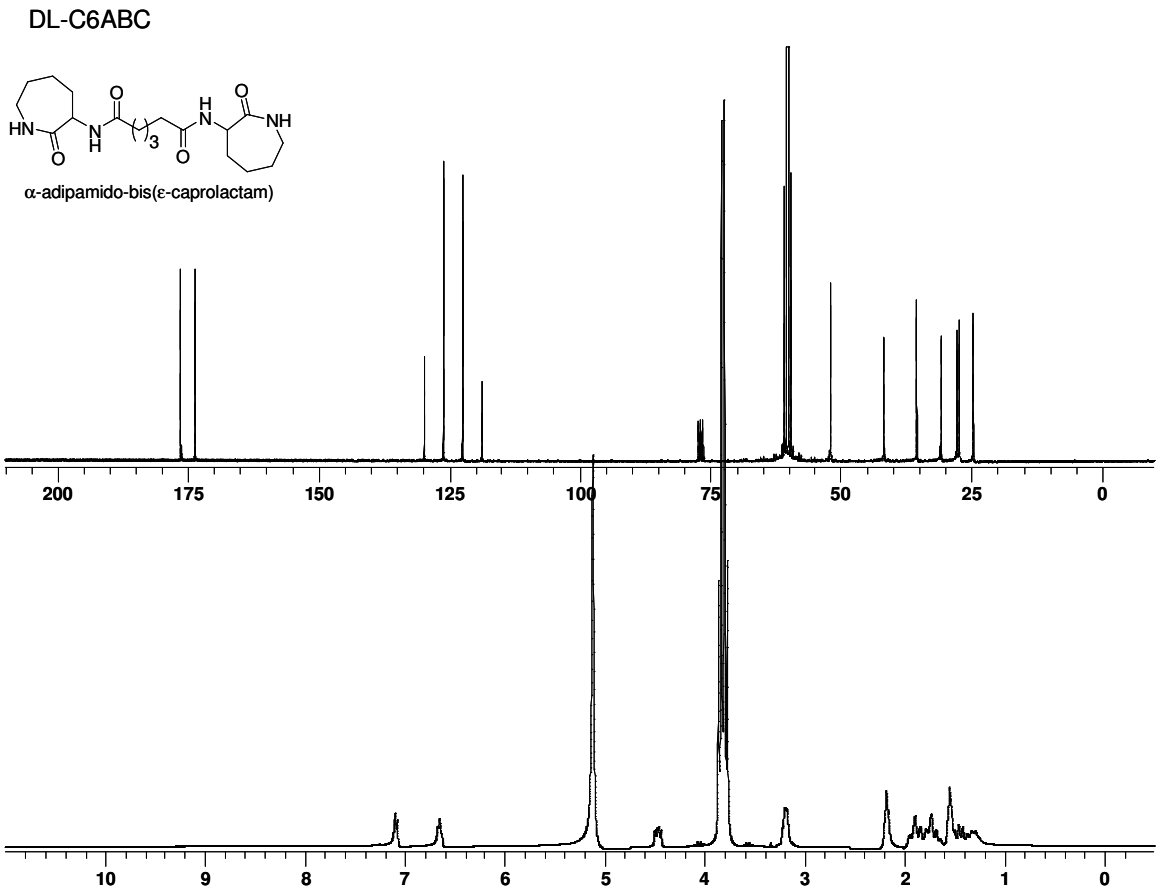

Figure 5.3. Solution-state ^{13}C (top) and ^{1}H (bottom) NMR spectra of DL-C6ABC.

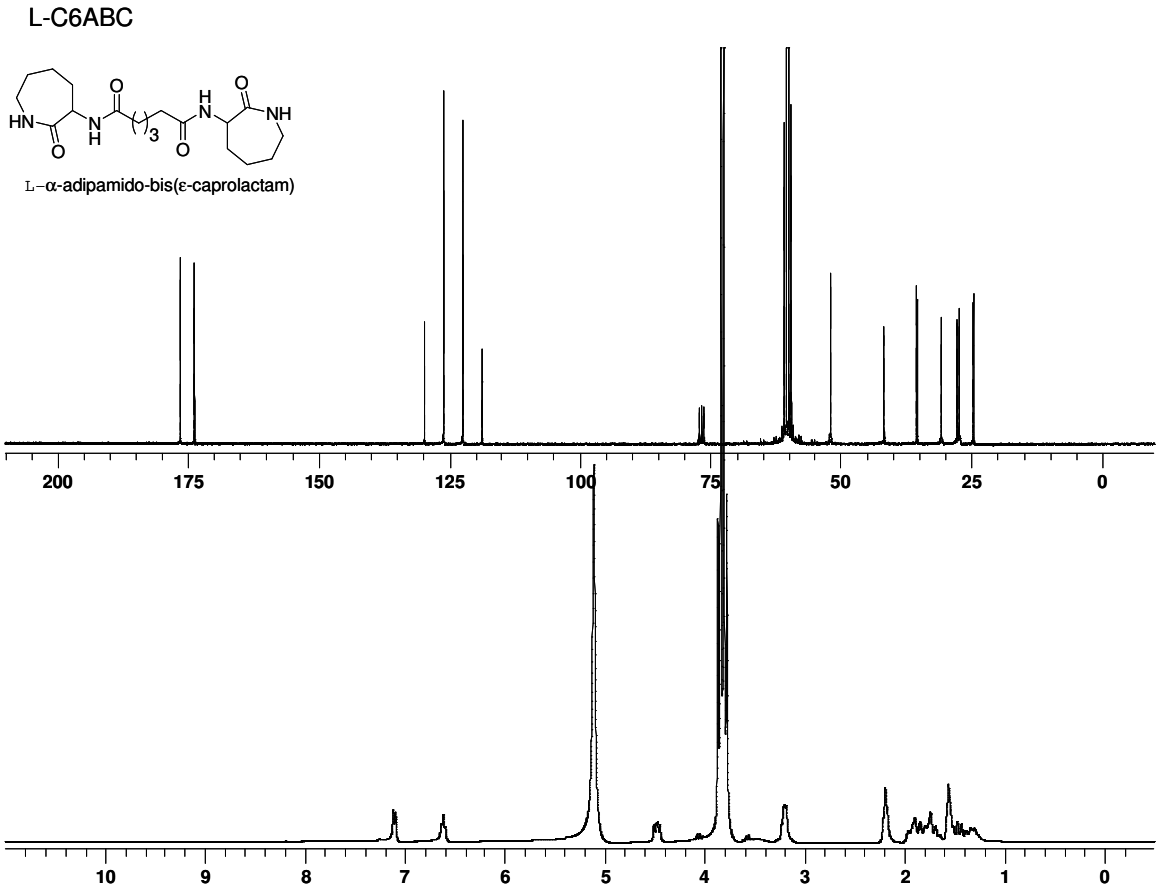

Figure 5.4. Solution-state ^{13}C (top) and ^{1}H (bottom) NMR spectra of L-C6ABC.

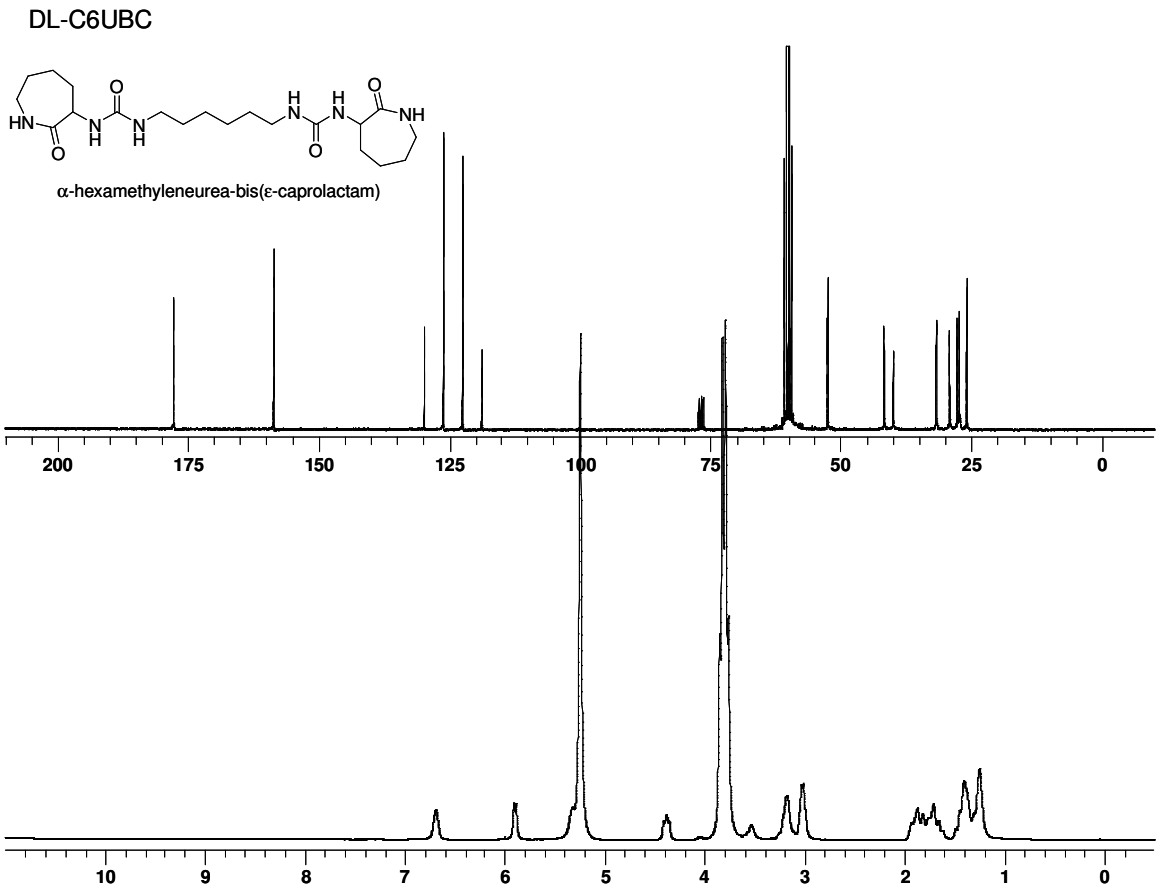

Figure 5.5. Solution-state ^{13}C (top) and ^{1}H (bottom) NMR spectra of DL-C6UBC.

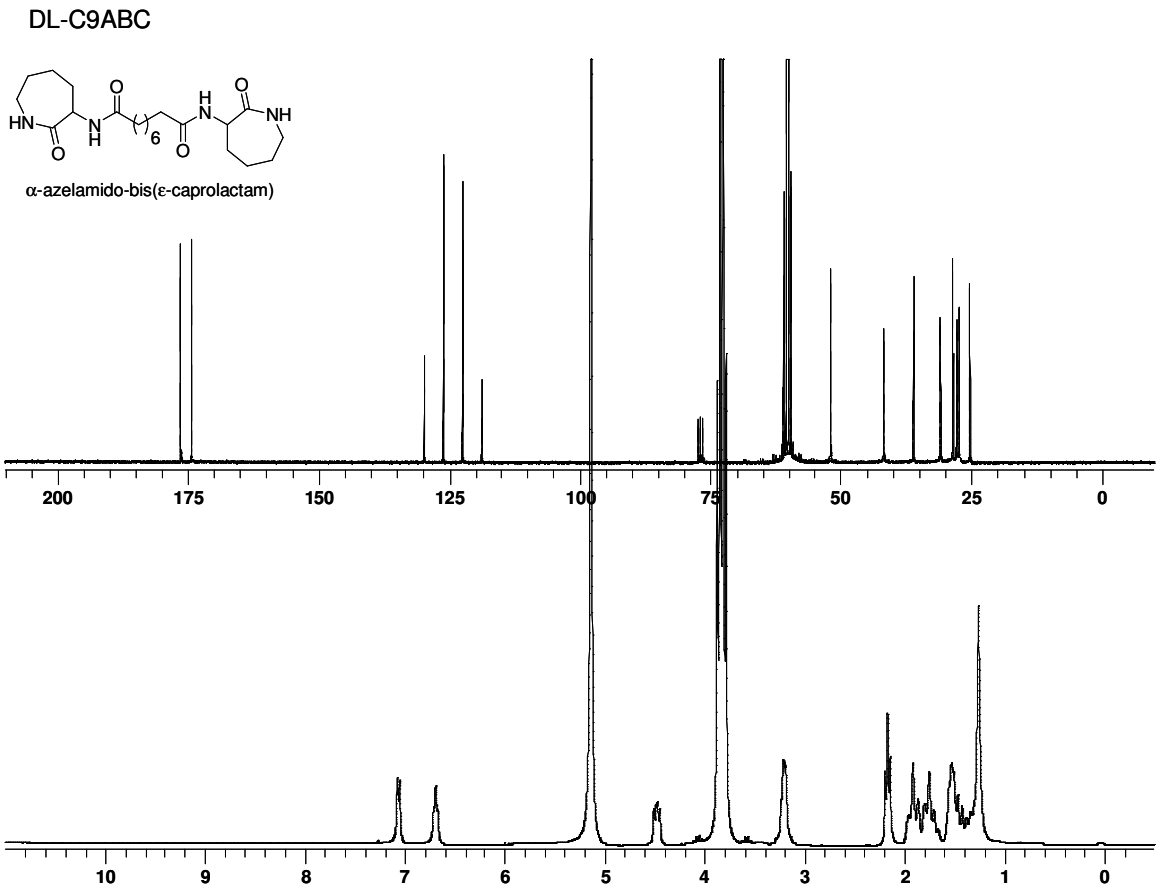

Figure 5.6. Solution-state ^{13}C (top) and ^{1}H (bottom) NMR spectra of DL-C9ABC.

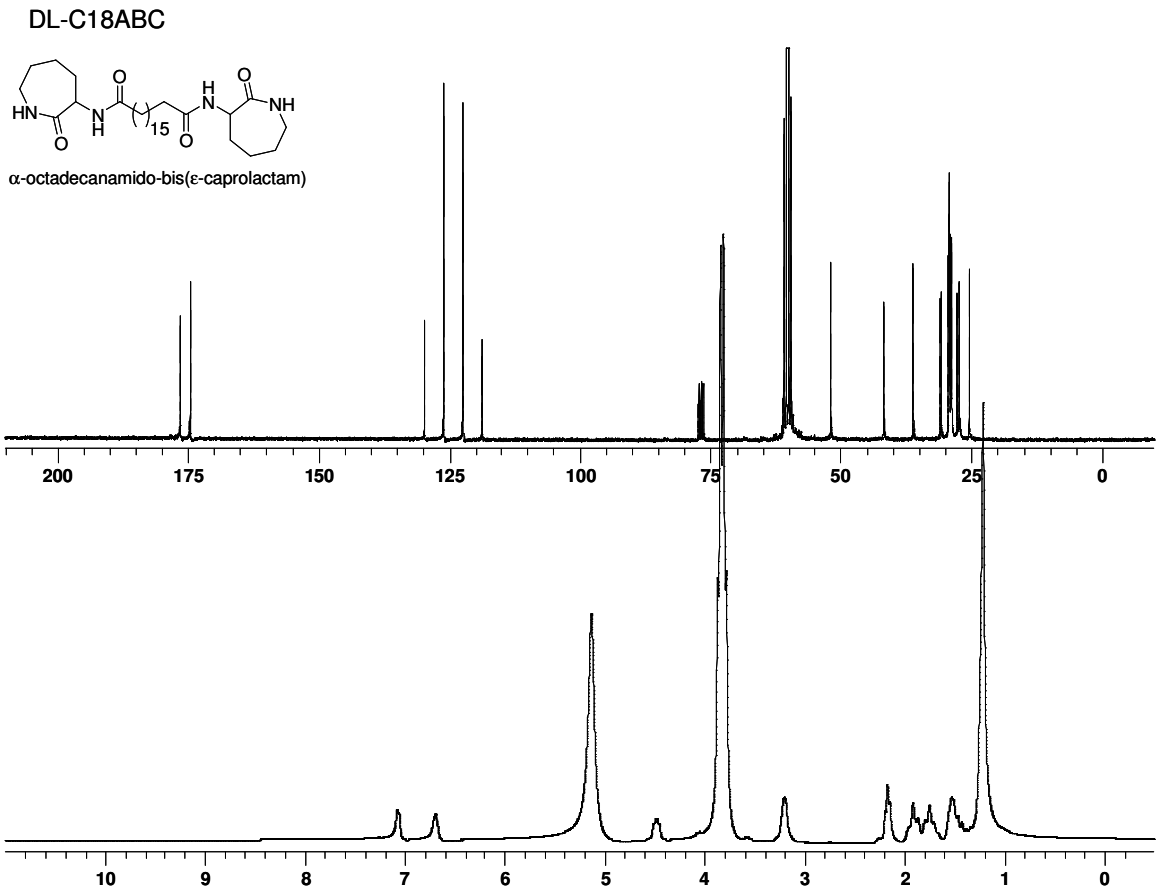

Figure 5.7. Solution-state ^{13}C (top) and ^{1}H (bottom) NMR spectra of DL-C18ABC.

Thermal properties are summarized in Table 5.1. Data from the first DSC heating scan indicates all compounds crystallized upon precipitation from the reaction mixture. No glass transitions (T_g) or crystallization exotherms (T_c) were present. Data from the second scan showed drastically different behavior. Glass transitions were observed for all samples except DL-C18ABC, and a T_c was present in all samples except for DL-C18ABC and DL-C6UBC. It is possible that the T_g for DL-C18ABC was not detected because it occurs at a temperature lower than those probed by DSC. Four additional DSC scans showed behavior

identical to the second scan within experimental error for all samples. Observation of T_g and T_c by DSC is typical of polymer samples. However, solution state ^{13}C NMR spectroscopy (not shown) showed no difference between materials before and after heating, eliminating the possibility of ring opening chain extension or conventional polymerization. A supramolecular assembly connected by reversible hydrogen-bonds, however, is consistent with these data. Apparently, the supramolecular assembly does not form in the "as-synthesized" materials until after they have been melted and cooled. Surprisingly, any crystallization that may have occurred during controlled cooling experiments in the DSC was not detected.

The DL-C6UBC sample exhibits interesting behavior in that it has a high T_g with no T_c or T_m between 25 and 275 °C. Typically, small molecules are thermodynamically driven to crystallize in bulk. In supramolecular assemblies, excessive crystallization is a common cause of diminished polymer-like properties.[13] Thus, retention of amorphous character for DL-C6UBC gives it potential for application development.

Table 5.1. Summary of DSC and TGA analyses of biscaprolactams. All first scan data are for samples as-synthesized, without thermal treatment prior to analysis.

Sample	DSC 1st scan		DSC 2nd scan					TGA
	T_m (°C)	ΔH_m (J/g)	T_g (°C)	T_c (°C)	ΔH_c (J/g)	T_m (°C)	ΔH_m (J/g)	T_d (°C)
DL-C4ABC	261 297	40.1 74.0	73	130	28.1	248	58.3	269
L-C6ABC	247	108.5	76	135	51.0	229	93.5	-
DL-C6ABC	255	168.1	75	162	99.6	253	133.4	281
DL-C6UBC	244	125.4	92	-	-	-	-	242
L-C9ABC	205	154.7	59.5	103	63.6	204	130.1	-
DL-C9ABC	217	209.8	58	106 145	57.5 37.6	216	120.5	297
DL-C18ABC	170	147.1	-	-	-	155 177	35.1 32.6	313

The most unexpected result was the observation of two distinct T_cs in the second DSC scan of DL-C9ABC. These results are reproducible as observed in the third DSC scan in Figure 5.8, and by repeated synthesis and analysis. Figure 5.9 shows additional DSC analysis probing this phenomenon. As-synthesized DL-C9ABC was heated to 250 °C in the first scan, then rapidly cooled (cooling curve not shown). Without removing the sample, the second scan heated the sample to 125 °C followed by rapid cooling. The T_g appeared at 58 °C and the first crystallization event appeared at 106 °C with a melting enthalpy of 55.2 J/g. These temperatures and enthalpies are identical within experimental error to those seen in Figure 5.8.b. Without removing the sample, the third scan heated

the sample to 250 ℃ followed by rapid cooling. The second crystallization event and T_m were identical to those seen in Figure 5.8.b. Thus, manipulating thermal history in this way does not appear to alter the nature of these crystallization or melting events. However, the disappearance of T_g in the third scan (Figure 5.9.c) indicates that the first crystallization event suppresses cooperative movements and may decrease or eliminate polymer-like properties. Without removing the sample, the fourth scan (Figure 5.9.d) heated the sample to 250 ℃ again. This scan appears identical to the second scan in Figure 5.8.b. Upon melting, the thermal history of the sample was erased. This behavior provides further evidence these compounds form a supramolecular polymer system connected by thermo-reversible hydrogen-bonds.

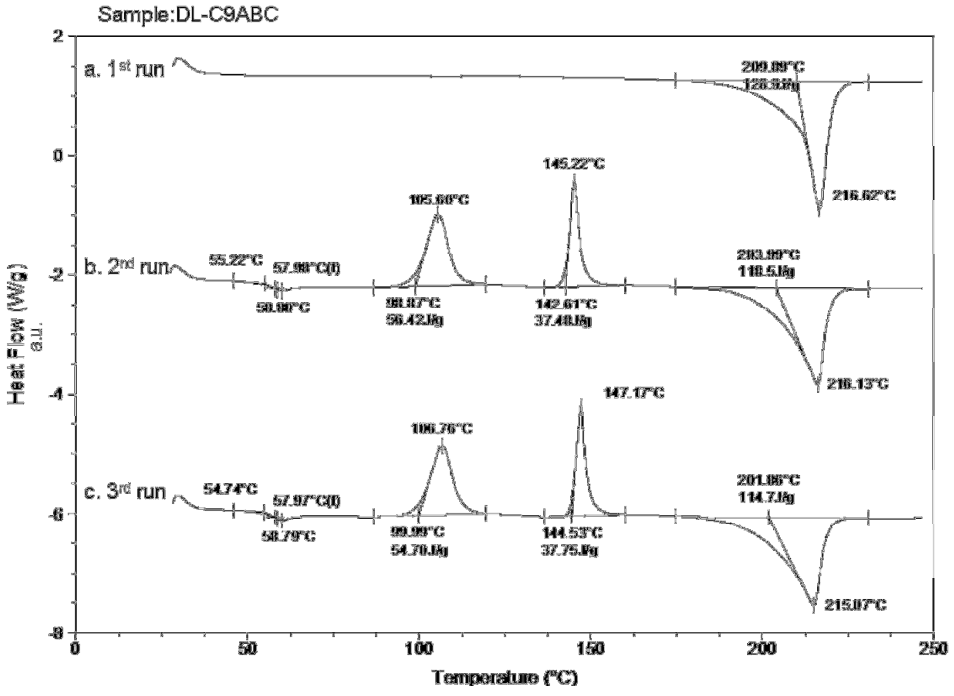

Figure 5.8. DSC heating curves of DL-C9ABC
a) 1st scan, b) 2nd scan and c) 3rd scan.

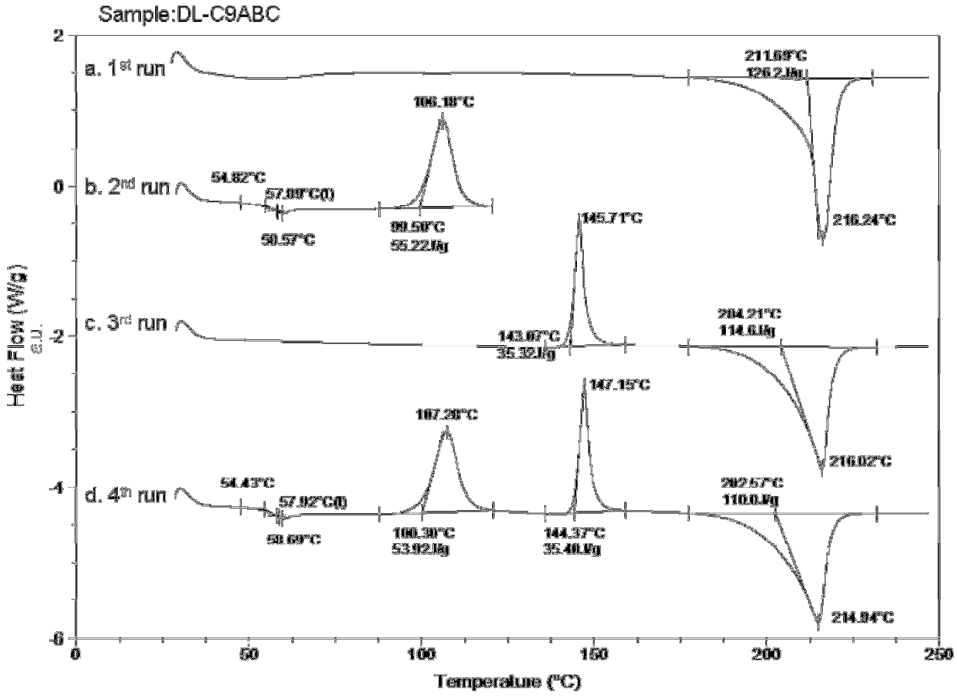

Figure 5.9. DSC heating curves of DL-C9ABC heated to: a) 250 °C b) 125 °C c) 250 °C d) 250 °C.

Figure 5.10 shows additional DSC analyses using a similar methodology as described for Figure 5.9. The primary difference is that the second scan reaches 165 °C, a temperature where both crystallization events had occurred. In Figure 5.10.c, disappearance of both T_cs indicates that the crystalline domains are stable, while the disappearance of T_g confirms that crystallization prevents segmental motion.

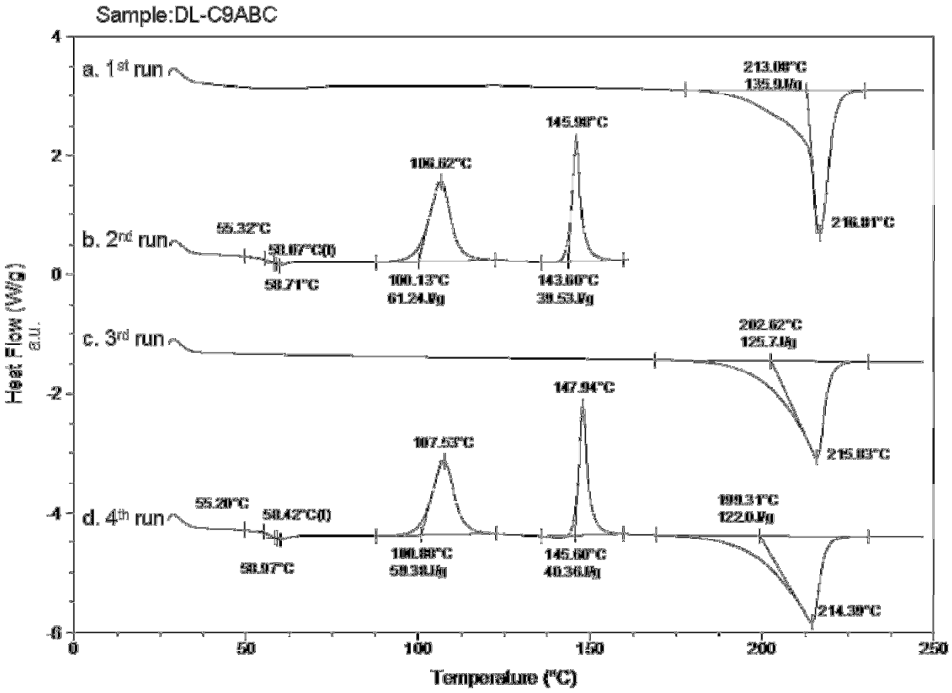

Figure 5.10. DSC heating curves of DL-C9ABC heated to: a) 250 °C b) 165 °C c) 250 °C d) 250 °C.

Figure 5.11 shows DSC analysis of enantiomerically pure L-C9ABC. Polymer-like behavior is not present in the first scan. The second and third scans showed a T_g at 59 °C, a single T_c at 103 °C, and T_m at 203 °C. The second DSC scans of L-C9ABC and DL-C9ABC are compared in Figure 5.12. The single exotherm for L-C9ABC is similar to the first exotherm for DL-C9ABC. One explanation is that different enantiomers form two distinct crystal forms. Another possibility is that reorganization of the first crystal structure into a new crystal structure is possible in an enantiomeric mixture.

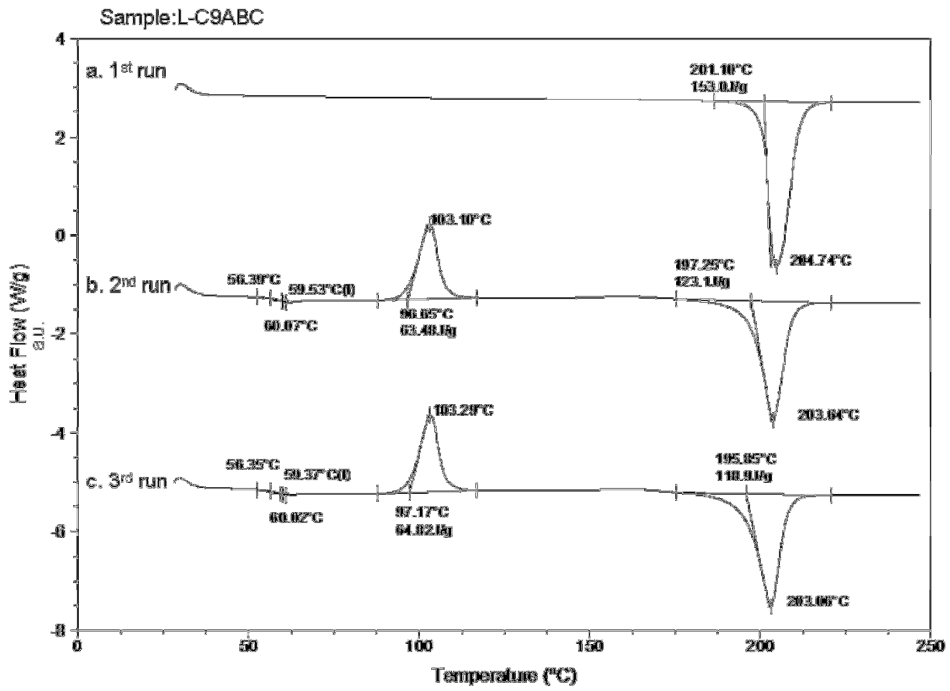

Figure 5.11. DSC heating curves of L-C9ABC
a) 1st scan, b) 2nd scan and c) 3rd scan.

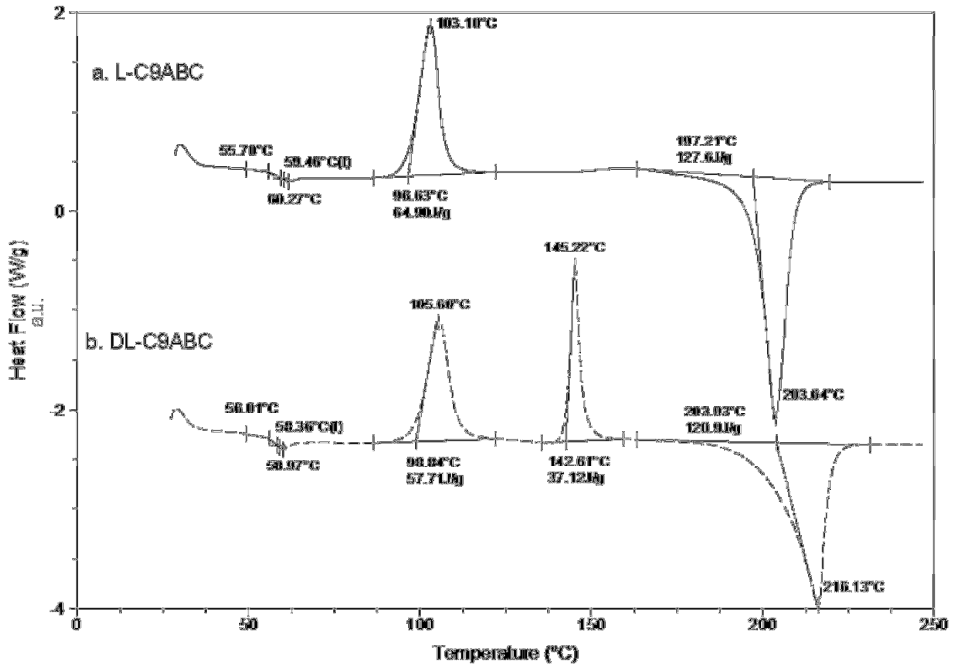

Figure 5.12. DSC 2nd heating curves of a) L-C9ABC and b) DL-C9ABC.

A physical mixture (50:50, w:w) of DL-C6ABC and DL-C9ABC was prepared by dissolving materials in trifluoroethanol, then allowing the solvent to evaporate. The second scan in Figure 5.13 showed a T_g, but no T_c or T_m. This demonstrates the ability to create completely amorphous, supramolecular copolymers by blending different monomers.

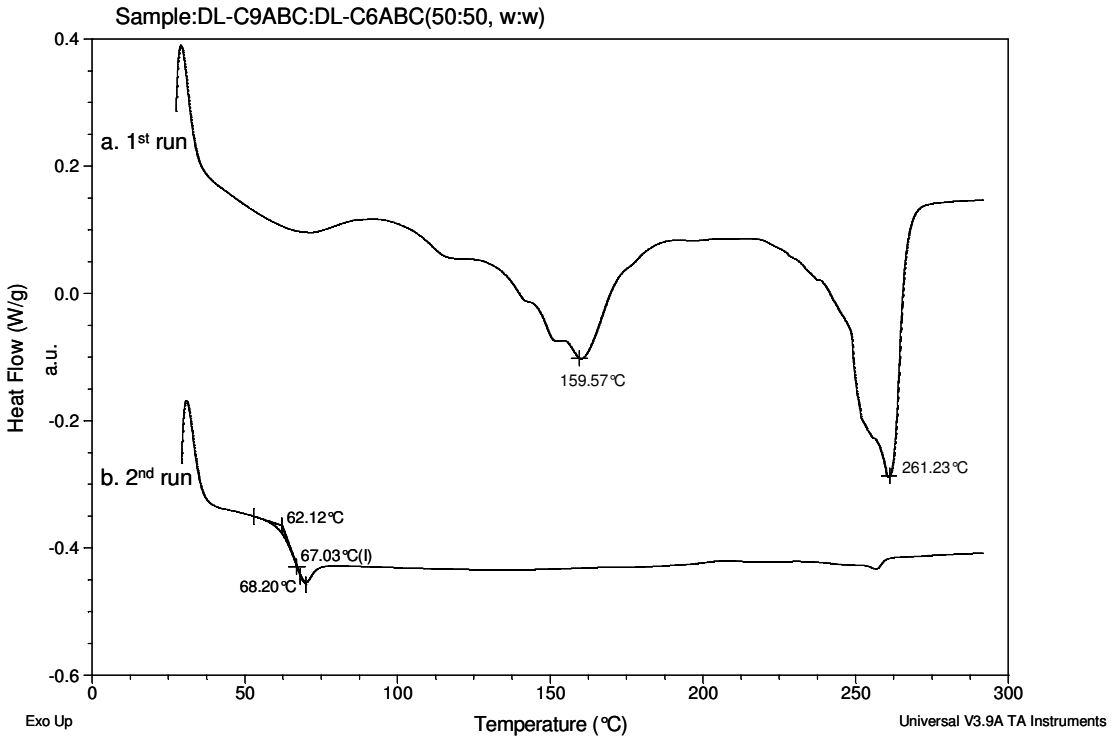

Figure 5.13. DSC heating curves of a physical mixture (50:50, w:w) of DL-C6ABC and DL-C9ABC.

In Figure 5.14, sharp peaks typical of highly crystalline materials are present for as-synthesized DL-C9ABC. After melting and cooling, broad amorphous peaks dominate the spectrum, suggesting the material has an amorphous morphology.

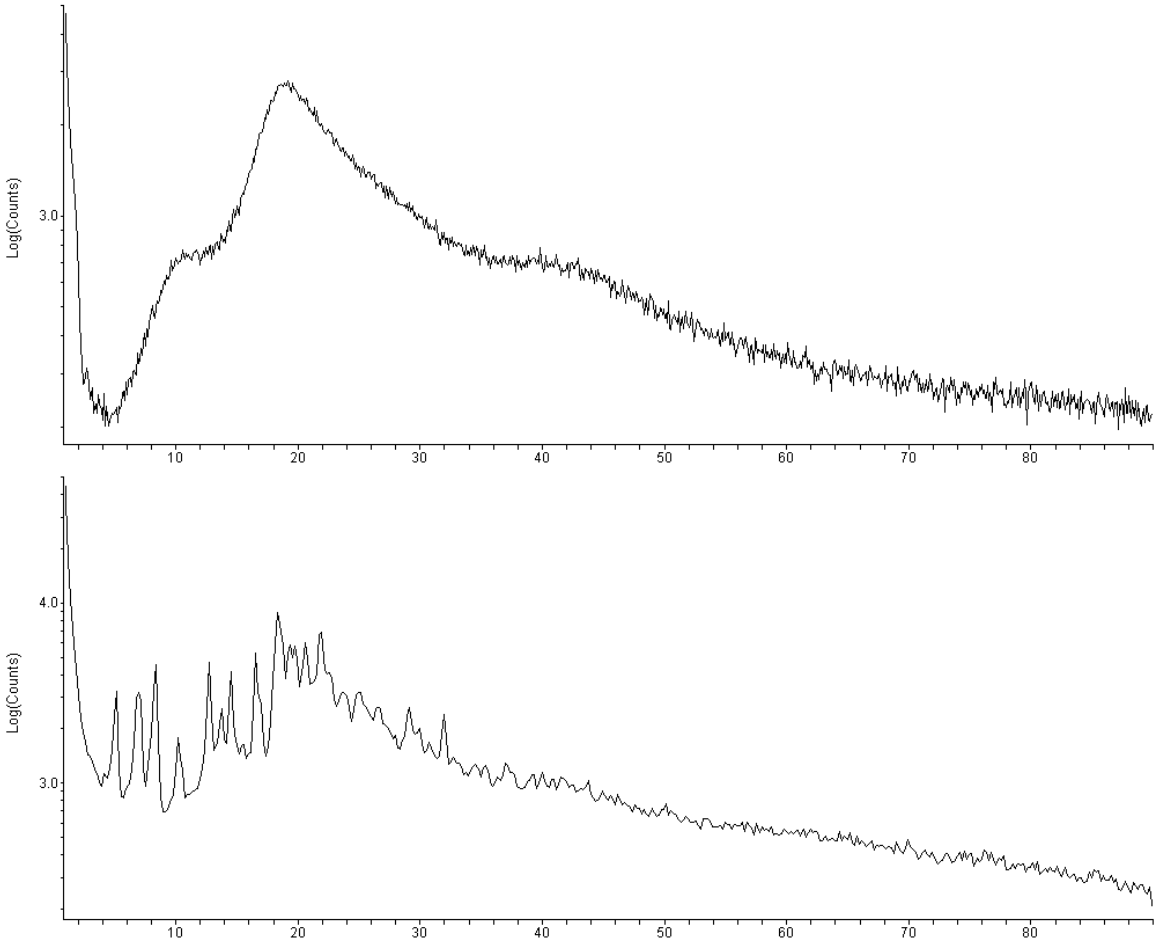

Figure 5.14. Wide angle x-ray diffraction patterns of as-synthesized DL-C9ABC (bottom) and after heating to 250 °C and cooling (top).

Fibers approximately 5-30 cm long were drawn from molten DL-C6ABC, DL-C9ABC, DL-C6UBC, and a physical mixture (50:50, w:w) of DL-C6ABC and DL-C9UBC. Fiber lengths were in the range of 5-30 cm. Each fiber was strong enough to support the weight of it's test tube, with brittle fracture occurring when they were bent sharply at 180°. This is strong qualitative evidence of

intermolecular associations and polymer-like behavior. Fibers could not be drawn for L-C9ABC and DL-C18ABC, due to the materials crystallizing rapidly.

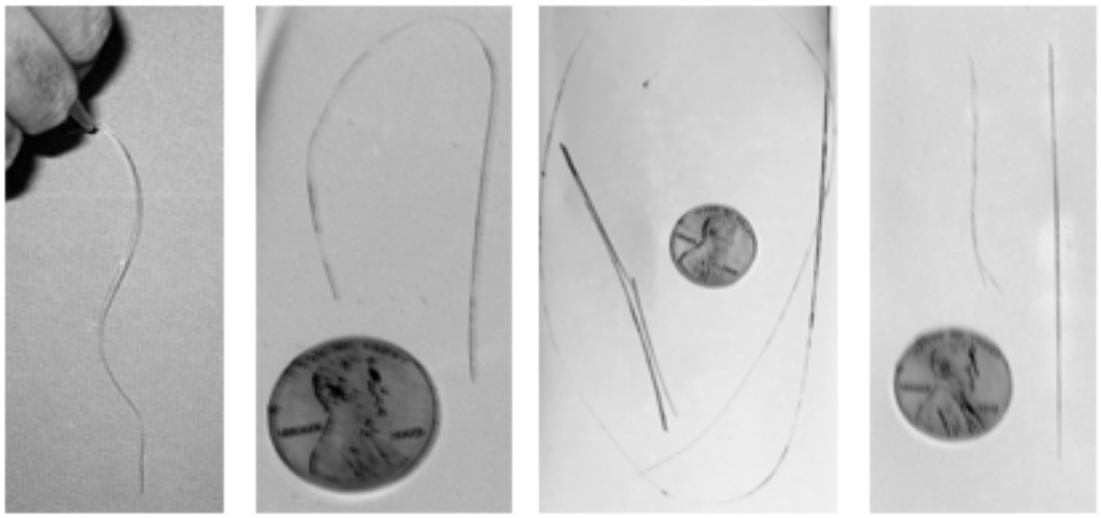

Figure 5.15. Images of fibers drawn from DL-C6ABC (left), DL-C9ABC (middle-left), DL-C6UBC (middle-right) and a physical mixture (50:50, w:w) of DL-C6ABC and DL-C9ABC.

On the left side of Figure 5.16, the L-C6ABC-As-Synthesized sample was heated in staged increments up to 170 °C with no apparent changes in NMR spectra. After the L-C6ABC had been melted (right side of Figure 5.16), the spectra exhibited much broader peaks in both the aliphatic and carbonyl regions. However, solution state ^{13}C NMR spectroscopy showed no difference between the two materials. This is expected, since the hydrogen-bonds which connect monomers in the solid-state are disrupted by solvent in the solution state. On the right side of Figure 5.16, as temperature increased above T_g, the carbonyl region became more resolved, with the peaks for carbons **8** and **3** becoming clearly discernable. After cooling the sample, these spectral changes remained. These

data suggest a thermally induced organization had occurred, but not to the extent that was present in the as-synthesized sample precipitated from solution. This is in agreement with the lower DSC melting enthalpy of thermally crystallized samples (Figure 5.1 DSC 2nd scan) as compared to solvent precipitated samples (Figure 5.1 DSC 1st scan).

Significant differences between DL-C6ABC-As-Synthesized (Figure 5.17) and L-C6ABC-As-Synthesized (Figure 5.16) are detected in their solid-state NMR spectra. For the DL materials, additional resonances appear for carbons **1** and **2,** while the peak for carbon **9** vanishes under the intense resonances of carbons **4** and **5**. Thus, chiral centers are shown to influence the extent and/or nature of crystalline or ordered organization in both as-synthesized and thermally treated materials.

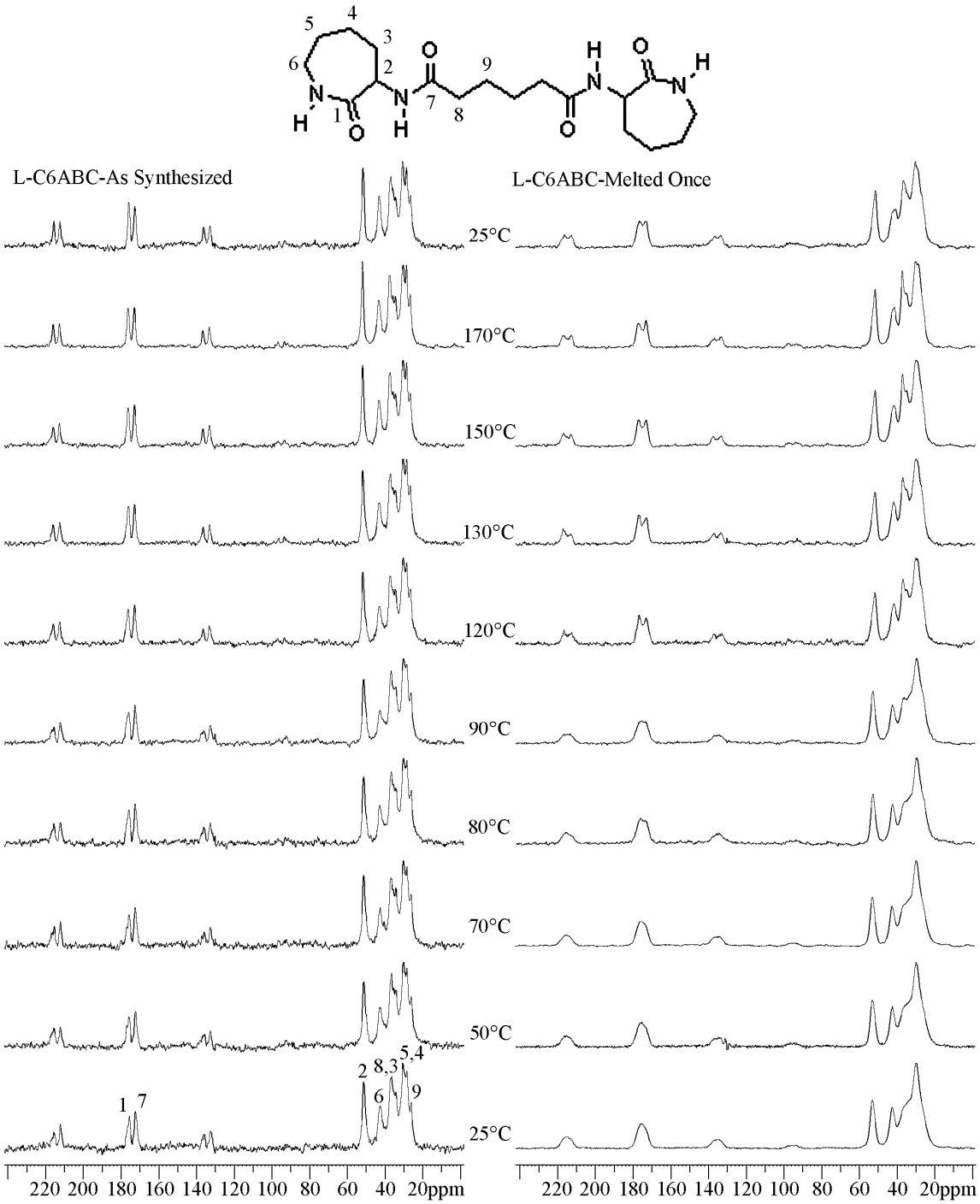

Figure 5.16. Solid state ^{13}C NMR spectra of L-C6ABC recorded at increments from 25 ℃ to 170 ℃ and again at 25 ℃ after cooling. The sample on the left was as-synthesized material which precipitated from the reaction solvent. The sample on the right was prepared by melting the as-synthesized material at 250 ℃ and cooling prior to analysis.

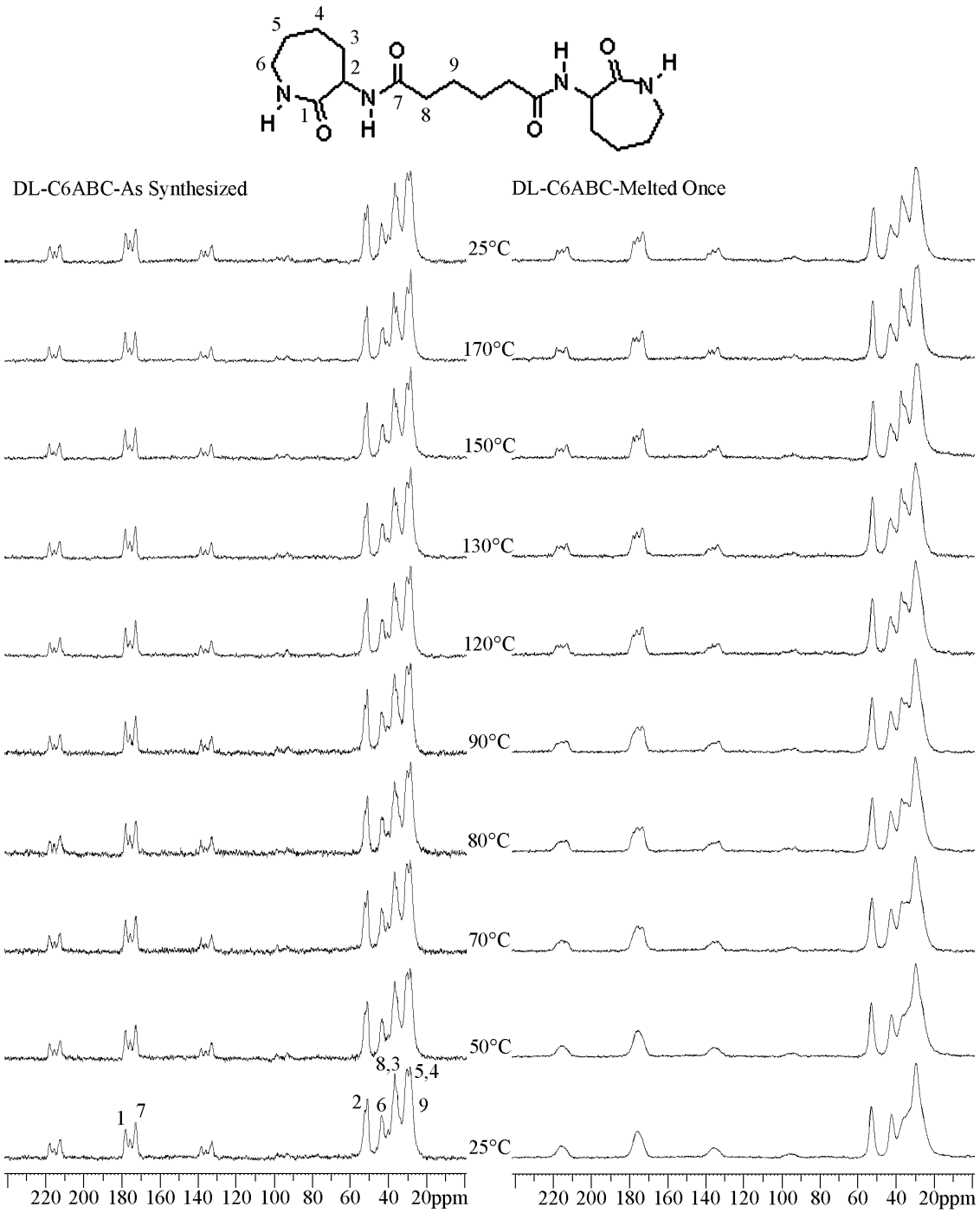

Figure 5.17. Solid-state ^{13}C NMR spectra of DL-C6ABC recorded at increments from 25 ℃ to 170 ℃ and again at 25 ℃ after cooling. The sample on the left was as-synthesized material which precipitated from the reaction solvent. The sample on the right was prepared by melting the as-synthesized material at 250 ℃ and cooling prior to analysis.

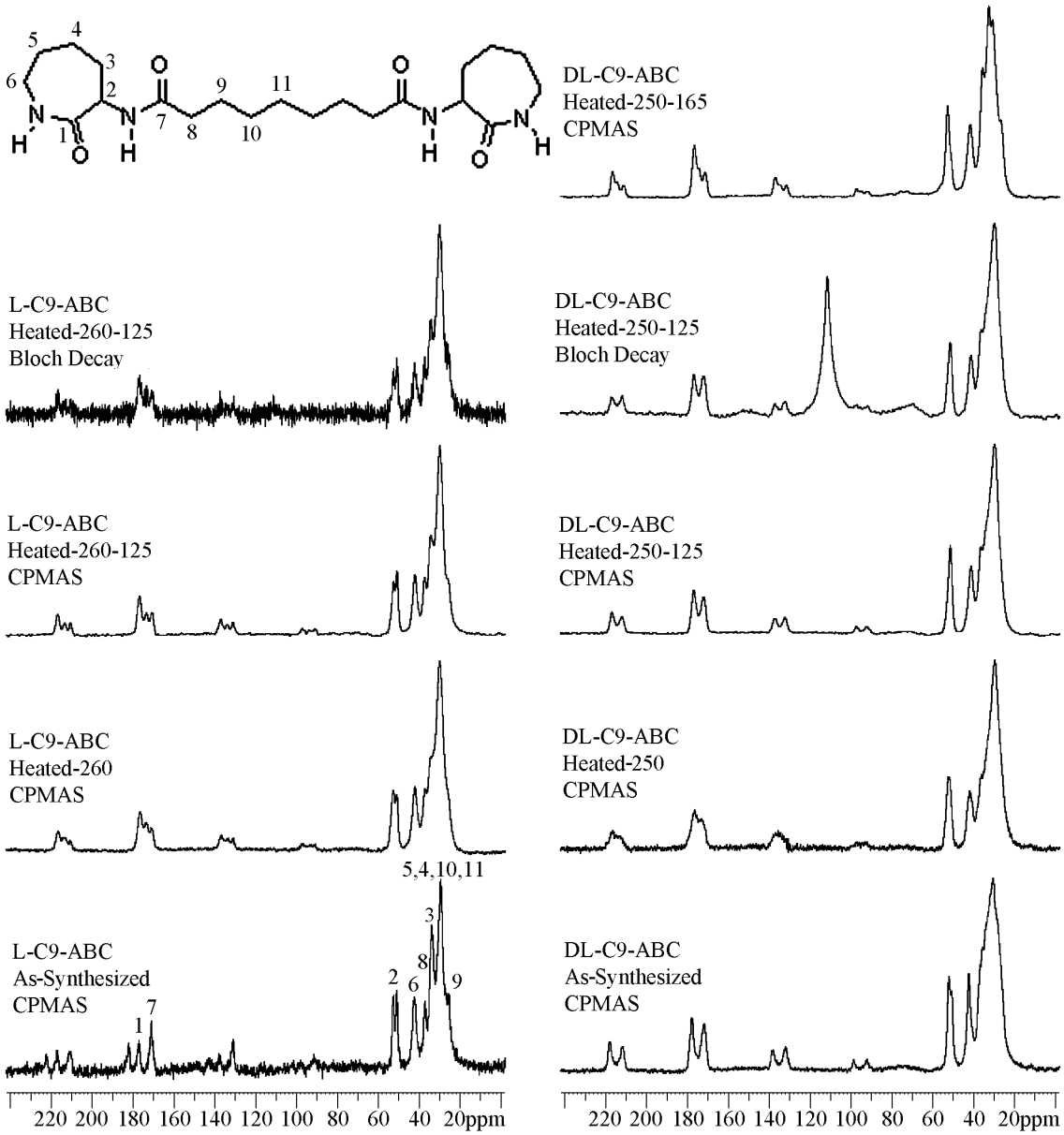

Figure 5.18. Solid-state 13C NMR spectra of L-C9-ABC (left) and DL-C9-ABC (right). The spectra on bottom are of as-synthesized materials which precipitated from the reaction solvent. The other spectra show samples thermally treated as indicated prior to NMR analysis. For example, "Heated-250-125" indicates that as-synthesized material was heated to 250 °C, cooled, then heated to 125 °C prior to analysis. CPMAS and Bloch Decay specify the pulse sequence used to obtain each spectrum.

Figure 5.18 shows solid-state NMR spectra of L-C9ABC and DL-C9ABC as-synthesized and with thermal treatments similar to those described in Figures 5.9 and 5.10. The downfield carbonyl in L-C9ABC-As-Synthesized shifts upfield 8.6 ppm after melting and cooling the sample. Furthermore, the most intense carbonyl peak before thermal treatment was the upfield carbonyl at 170.9 ppm, whereas the most intense carbonyl peak after thermal treatment was the downfield carbonyl at 176.9 ppm. This suggests different ordered forms between thermally treated and solvent precipitated L-C9ABC. The carbonyl present at 181.9 ppm in L-C9ABC-As-Synthesized does not appear in DL-C9ABC-As-Synthesized. This indicates differences in crystalline or ordered domain structures. Crystalline materials typically have sharp, well defined peaks compared to the broad peaks observed in polymers. A higher degree of order for L-C9ABC-As-Synthesized is suggested by the narrow line widths relative to DL-C9ABC-As-Synthesized.

Conclusions

A new family of compounds has been synthesized and observed to form supramolecular assemblies connected by hydrogen-bonding. Thermal treatment and solvent precipitation produced differently organized structures and extents of crystallinity. As-synthesized materials did not assemble into supramolecular polymers until after they had been melted and cooled. Thermally induced crystallization diminished polymer-like behavior. Chiral centers played an important role in ordered domain behavior. Urea linkages suppressed

crystallinity. Crystallinity was also suppressed in supramolecular copolymer blends of compounds containing amide linkages.

Acknowledgements

Eylem Tarkin-Tas synthesized all materials and performed DSC, TGA, and solution-state NMR analysis. Draths Coorporation is gratefully acknowledged for financial support of this project.

References

[1] Lee, C-M.; Griffin, A.C. Macromol. Symp. **1997**, 117, 281.

[2] Sijbesma R.P.; Beijer, F.H.; Brunsveld, L.; Folmer, B.J.B.; Hirschberg, J.H.K.K.; Lange, R.F.M.; Lowe, J.K.L, Meijer, E.W. Science **1997**, 278, 1601-1604.

[3] Boileau, S.; Bouteiller, L.; Foucat, E.; Lacoudre, N. J. Mater. Chem. **2002**, 12, 195-199.

[4] Boils, D.; Perron, M-E.; Monchamp, F.; Duval, H. ; Maris, T. ; Wuest, J.D. Macromolecules **2004**, 37, 7351-7357.

[5] Araki, K.; Takasawa, R.; Yoshikawa, I. Chem. Commun. **2001**, 1826-1827.

[6] Takasawa, R.; Murato, K.; Yoshikawa, I.; Araki, K. Macromol. Rapid. Commun. **2003**, 24, 335-339.

[7] Hirschberg, J.H.K.K.; Beijer, F.H.; van Aert, H.A.; Magusin, P.C.M.M.; Sijbesma, R.P.; Meijer, E.W. Macromolecules **1999**, 32, 2696-2705.

[8] Folmer, B.J.B.; Sijbesma, R.P.; Versteegen, R.M.; van der Rijt J.A.J.; Meijer, E.W. Adv. Mater. **2000**, 12, 874-878.

[9] Brinke, G.; Ruokolainen, J.; Ikkala, O. Adv. Poly. Sci. **2007**, 207, 113-177.

[10] Cordier, P.; Tournilhac, F.; Soulie-Ziakovic, C.; Leibler, L. Nature **2008**, 451, 977-980.

[11] Muller, M. ; Dardin, A. ; Seidel, Ul. ; Balsamo, V.; Ivan, B.; Spiess, H. W.; Stadler, R. Macromolecules **1996**, 29, 2577-2583.

[12] de Lucca Freitas, L.L.; Stadler, R. Macromolecules **1987**, 20, 24-2485.

[13] Bouteiller, L. Adv. Poly. Sci. **2007**, 207, 79-112.

[14] Binder, W.H.; Zirbs, R. Adv. Poly. Sci. **2007**, 207, 1-78.

[15] Wilson, A.J. Soft Matter. **2007**, 3, 409-425.

[16] Shimizu, L. S. Polym. Int. **2007**, 56, 444-452.

[17] Fox, J.D. ; Rowan, S.J. Macromolecules **2009**, 42, 6823-6835.

[18] Serpe, M.J.; Craig, S.L. Langmuir **2007**, 23, 1626-1634.

[19] Schaefer, J.; Stejskal, E. O.; Buchdahl, R. Macromolecules **1977**, 10, 384.

[20] Cory, D. G.; Ritchey, W. M. J. Magn. Reson., **1988**, 80, 128.

CHAPTER VI

CONCLUSIONS

The synthesis, characterization, and deuterium labeling of polyamides and polyamide derivatives have been investigated. A facile, solvent-free, catalyst-free method for selective deuterium labeling of various polyamides is described in Chapter II. Deuterium incorporation at the carbon alpha to the carbonyl ranged from 20-75%. Incorporation in ε-caprolactam increased with repeated treatments. This method reduces the amount of time, the amount of raw materials consumed, and the costs associated with generating selectively deuterium labeled polyamides. Future investigations include optimization of variables such as: reaction time, reaction temperature, deuterium oxide purity, ratio of deuterium oxide to monomer, and the number of modifications. Data concerning compound isotopic shift effects have been collected and tabulated. The isotopic shift effects were additive for all sites within experimental error. This data may be useful for developing a comprehensive theory for understanding and predicting isotopic shift effects.

In Chapter III, PA-12,T of varying molecular weight was synthesized by melt condensation polymerization of 12,T salt with 0-10 mol-% excess 1,12-diaminododecane, terephthalic acid, or benzoic acid. Intrinsic viscosity measurements were directly related with molecular weights calculated by NMR analysis. Addition of 1 and 3 mol-% excess diamine increased the number average molecular weight of products compared to pure salt. It is believed that excess diamine balances stoichiometry by compensating for its greater volatility.

On a molar basis, excess terephthalic acid and benzoic acid both decreased molecular weights to a similar degree. Molecular weights of all polymers calculated using ^{13}C NMR spectroscopy showed a linear trend on a log (Mn) - log (IV) plot with Mark-Houwink constants of $K=55.8*10^{-5}$ dL/g and $\alpha=0.81$. Since these values are based on the single-point IV measurements used to a great extent in semi-aromatic polymer patent literature, they are useful for evaluating data in existing literature and future investigations. Such investigations may include optimization of other semi-aromatic polyamides and applying this method of characterization to understanding other industrially relevant problems.

Eutectic melting behavior of PA-10,T-6,T and PA-12,T-6,T copolymers are described in Chapter IV. High resolution ^{13}C solution-state NMR analysis revealed that substituted phenyl carbons are sensitive to comonomer connectivity. Nuclear magnetic resonance spectra showed that comonomer sequences were distributed statistically to give random copolymers. Melt pressed film behavior, NMR, DSC, and WAXD analysis agree that PA-6,T monomer units do not co-crystallize with PA-10,T or PA-12,T monomer units, and do not form isomorphic structures in the copolymers studied. Instead, a eutectic melting point at 30 wt-% PA-6,T is observed for both copolymers. Ordered PA-6,T homo-segments were the major crystalline form above the eutectic point, while the ordered homo-segments of the other comonomer were the major crystalline form below the eutectic point. Compared to PA-10,T comonomer, PA-12,T comonomer has a greater effect on disrupting the crystallization of PA-6,T homo-segments above the eutectic point. Melt pressed films of copolymers

show the highest optical clarity at the eutectic point. Comonomer concentrations are shown to predictably impact melting temperature, degree of crystallinity, and optical clarity. Copolymers containing odd-numbered amine and A-B type aromatic comonomers have received little attention and merit further investigations for better understanding the melting behavior of polyamides.

Chapter V investigated a new family of hydrogen-bonded supramolecular assemblies. As-synthesized materials behaved as typical small molecules and only formed assemblies after melting and cooling. Additional heating above T_g restored crystalline behavior, but with different organization and extent of crystallinity compared to as-synthesized materials. Chiral centers also influenced ordered domain behavior. Glassy materials formed for compounds containing urea linkages and copolymers of compounds containing amide linkages. Macroscopic assembly was demonstrated by fiber formation. The ability to systematically vary the composition of biscaprolactam based compounds shows promise for understanding their structure-property relationships.